1967

Hydromagnetic Waves in the Ionosphere: Propagation through Inhomogeneous and Current Carrying Regions

Muhammad Abbas
University of Rhode Island

HYDROMAGNETIC WAVES IN THE IONOSPHERE: PROPAGATION THROUGH INHOMOGENEOUS AND CURRENT CARRYING REGIONS

BY

MUHAMMAD ABBAS

A THESIS SUBMITTED IN PARTIAL FULFILLMENT OF THE

REQUIREMENTS FOR THE DEGREE OF

DOCTOR OF PHILOSOPHY

IN

ELECTRICAL ENGINEERING

UNIVERSITY OF RHODE ISLAND

1967

DOCTOR OF PHILOSOPHY THESIS

OF

MUHAMMAD ABBAS

Approved:

Thesis Committee:

Chairman _____

_____

_____

_____

Dean of the Graduate School _____

UNIVERSITY OF RHODE ISLAND

1967

ABSTRACT

This dissertation is concerned with the analysis of hydromagnetic waves which are generated in various regions of the magnetosphere and propagated to the earth in the extremely low frequency spectrum. Two different aspects of the problem are investigated, namely, propagation through inhomogeneous regions of the ionosphere and propagation and excitation of waves in current carrying regions of the ionosphere and the magnetosphere.

Propagation through inhomogeneous regions is studied by two different methods. With the first method, transmission coefficients for hydromagnetic waves are obtained in terms of Airy integral functions by assuming a linearly varying inhomogeneous region. Simplified expressions are obtained by using series and asymptotic approximations. Numerical results are given for typical ionospheric parameters.

The second approach to propagation through inhomogeneous regions employs "Epstein's theory". In this method, the wave equation is transformed into the hypergeometric equation to obtain more tractable solutions for the types of inhomogeneities which are characteristic of the ionosphere. Assuming a hydromagnetic wave incident from above and propagating parallel to the earth's magnetic field, power transmission coefficients are calculated. Complex refractive index profiles are employed in the calculations. These profiles approximate those which are obtained from the dispersion relations for a partially ionized plasma and available ionospheric data. The transmission coefficients are calculated for various times of day and show that maximum transmission occurs at about local midnight and minimum transmission at about local noon.

The various mechanisms which may be responsible for the generation and amplification of hydromagnetic waves are examined. The expected characteristics of electromagnetic noise in the earth-ionosphere cavity due to excitation by hydromagnetic waves are compared with experimentally observed data and with characteristics deduced from excitation by world-wide thunderstorm activity.

Propagation of hydromagnetic waves through a current carrying plasma is investigated on the basis of macroscopic equations involving additional terms due to the existence of a constant current density. These equations are derived from the basic plasma equations in which streaming velocities for both electron and ion fluids are allowed. A general dispersion relation for small amplitude waves is derived from these equations. Approximate solutions of the dispersion relation for certain special cases are obtained.

For transverse propagation (propagation normal to the steady magnetic field), when the currents are also transverse to both, the direction of propagation and the static magnetic field, it is found that amplification takes place. For longitudinal propagation with currents in the transverse plane, the propagation constant remains unaffected. In this case, however, an electric field component along the wave normal is introduced which changes the direction of the ray path. For longitudinal propagation, with currents also along the direction of propagation and the static magnetic field, the propagation constant has a resonance at the ion-cyclotron frequency for both right and left hand polarizations. A nonconvective instability is found to exist in the neighborhood of this frequency for certain values of currents. Numerical results are presented for longitudinal propagation, for data corresponding to the ionospheric and magnetospheric conditions.

ACKNOWLEDGEMENT

The author wishes to express his sincere gratitude and appreciation to his thesis advisor, Dr. Charles Polk, for his help and guidance throughout the course of this work, The author is also indebted to Dr. H. Poeverlein for many helpful discussions, advice, and many suggestions which have been embodied in this work. He is grateful to both for having introduced him to this exciting field of research. The author would also like to thank Messrs. James J. Beville, John J. Dooley, Richard A. Sundberg, and Daniel M. Viccione for their help in computer programming and obtaining the numerical results presented in various parts of this work.

The work reported in this dissertation has been sponsored by the Air Force Cambridge Research Laboratories under contract AF 19 (604) 7252.

TABLE OF CONTENTS

LIST OF FIGURES

FIGURES PAGE

FIGURES PAGE

LIST OF SYMBOLS

A_j, B_j (j=1,n)	Coefficients of algebraic equations
$\vec{B}$	Magnetic induction
D, D_1	Denominators of the dispersion relations
$\vec{E}$	Electric field intensity
$\vec{J}$	Electric current density
M	Magnetic moment of the earth
N_j	Total particle density of the jth species
Q	Power coupling coefficient
R	Earth's radius
R	3x3 matrix
R_{ij}	Elements of matrix R
T	Transmission coefficient
T	Temperature
V_a	Alfvén velocity
$\vec{V}_j$	Total velocity of the jth species of particles
W	Molecular weight
X	$\frac{\omega}{\Omega_i}$
a	Arbitrary constant
a_j, b_j (j=1,n)	Coefficients of algebraic equation
	Also used with other meanings
b	Arbitrary constant
	Also used with other meanings

c	Velocity of light
e	Electronic Charge
j	$\sqrt{-1}$
k	Propagation constant
m_j	Mass of the jth species of particles
$m_{e,i}$	Electron or ion mass
n	Refractive index
n	Electron or ion number density
n	An integer
n_n	Neutral particle density
q	Refractive index
	Also used with other meanings
q_j	Charge of the jth species of particles
t	Time
$\vec{u}$	Particle velocity
	Also used to denote other functions
$\vec{v}$	Center of mass perturbed fluid velocity
$\vec{v}_o$	Center of mass streaming (zero order) fluid velocity
$\vec{v}_{oe,oi}$	Electron or ion streaming velocity
x, y, z	Cartesian coordinates
x	$\left(\frac{\Omega_i^2}{\omega_i^2} - \frac{\omega^2}{\omega_e^2}\right)$
	Also used to denote other functions
x_1	$\frac{\Omega_e \omega_e}{\omega_i^2}$

x_2	$\frac{\Omega_e \Omega_i}{\omega_i^2}$
x_3	$\frac{\Omega_e}{\omega_i}$
x_4	$\frac{\omega_i^2}{c^2}$
y	$\frac{J_o k}{\omega_e^2 (\rho_o \epsilon_o)^{\frac{1}{2}}}$
z	$\frac{y}{k}$
Γ	Gamma function
Γ	Locus of ω in the complex ω plane for real k
Λ	Locus of k in the complex k plane for real ω
$\Omega_{e,i}$	Electron or ion cyclotron frequency
α	Constant of the hypergeometric equation
α_j (j=1,n)	Coefficients of equation (6.26)
	Roots of the denominator of the dispersion (6.51)
β	Constant of the hypergeometric equation
β	$\frac{\Omega_i}{\omega_i}$
γ	Constant of the hypergeometric equation
ϵ	$\frac{m_e}{m_i}$
μ_o	Permeability of free space
θ	Angle
ϵ_o	Permittivity of free space

ξ	Variable of Stoke's equation (2.4)
ρ	Mass density
σ_E	Earth's conductivity
ϕ	Azimuthal angle
ω	Angular frequency
$\omega_{e,i}$	Electron or ion plasma frequency

I. INTRODUCTION

The relation of extremely low frequency electromagnetic fields of natural origin, detected on the surface of the earth, to hydromagnetic waves in the ionosphere is now well established. These low frequency waves are generated in the various regions of the magnetosphere due to a variety of phenomena related to the solar plasma wind which is incident on the outer boundary of the magnetosphere. They are propagated through the ionosphere in various modes under appropriate conditions and are detected on the surface of the earth as electromagnetic waves in the VLF, ELF and micropulsations spectrum (Piddington, 1964).

In an ionized gaseous medium, in the presence of a magnetic field, a variety of complex wave types may propagate. In the simplified macroscopic treatment of a "cold" plasma model, however, there are only two modes of propagation. At frequencies below the ion cyclotron frequency these two modes are usually called hydromagnetic waves, and are variously identified as: the Alfvén and modified Alfvén waves, ordinary and extraordinary waves, or for propagation along the magnetic field, as left hand and right hand polarized waves. In an inhomogeneous medium, these modes are, in general, described by two coupled second order differential equations. In certain special cases, however, such as for propagation along the magnetic field, the two modes are uncoupled and may be described by a simple wave equation.

The problem of propagation of hydromagnetic waves in the ionosphere is complex due to the complicated nature of the ionosphere. At extremely

low frequencies, the various parameters characterizing the ionosphere, such as particle densities and interparticle collision frequencies, vary rapidly in a distance comparable to one wavelength. Due to rapid spatial variation, it is difficult to obtain analytical solutions for hydromagnetic waves in the ionosphere. The approach to the problem has been basically twofold. In the first approach, some simple idealized model for the ionosphere is assumed to make the problem mathematically tractable in a way which permits solutions in terms of known mathematical functions.

Kahalas (1960), and Ullah and Kahalas (1963) have studied the coupling of hydromagnetic waves in a collisionless homogeneous plasma to electromagnetic waves in vacuum. They calculated coupling coefficients for a discontineous transition between plasma and vacuum. Greifinger and Greifinger (1965) and Field and Greifinger (1965) investigated the propagation of hydromagnetic waves in the ionosphere (80-500 km) and the lower exosphere (500-2000 km.). In the first of the Greifinger studies the ionosphere was assumed to have a constant electron density and Alfvén velocity, while the collision frequencies were assumed to vary exponentially with height. The ionosphere was assumed to be terminated abruptly by vacuum at a height of 80 km. Analytical expressions for transmission coefficients were obtained in terms of Bessel functions. In the second paper applicable to the lower exosphere, interparticle collisions were neglected, and the electron density and Alfvén velocity were assumed to vary exponentially with height. The solutions for transmission coefficients in that case were obtained in terms of gamma functions.

In the second approach, relatively few approximations are made in the formulation of the physical model. The solutions for various desired

quantities such as transmission and reflection coefficients, power dissipation etc., are obtained, however, either by numerical solution of differential equations or by stratifying the ionosphere into a sufficiently large number of homogeneous regions.

Dungey (1954) studied the propagation of Alfvén waves through the ionosphere travelling parallel to the magnetic field by solving a second order differential equation by numerical methods. In his study he assumed a partially ionized plasma in which the collisions between charged particles, usually ignored in earlier studies, were included. Francis and Karplus (1960) and Karplus et al., (1962) studied the attenuation of hydromagnetic waves in the ionosphere by numerical integration of coupled differential equations and calculated the power absorption, and transmission and reflection coefficients of the ionosphere.

Extensive numerical studies of hydromagnetic wave propagation in the ionosphere have been carried out by Prince, Bostick, Ti-Shu Li and others (1964) at the University of Texas. They considered realistic models corresponding to the actual ionospheric parameters, and included the effect of motion of neutral particles and collisions between charged particles. Their analysis, however, was based on stratifying the ionosphere into a sufficiently large number of homogeneous regions and considering the interlayer reflections on the usual basis. Akasofu (1965) has studied, by numerical methods, the diurnal variations in the attenuation of hydromagnetic waves due to variations in electron density. The attenuation in his study was, however, assumed to be only due to the imaginary part of the propagation constant (equivalent to neglecting reflections).

A problem of particular interest in connection with the propagation of hydromagnetic waves in the ionosphere, is the possible excitation of the earth-ionosphere cavity by hydromagnetic waves. This cavity, formed by the concentric spherical shells of the earth and the lower boundary of the ionosphere, has its fundamental resonant frequency at about 8 c/s. It is generally believed that the worldwide thunderstorm activity is mainly responsible for the excitation of this cavity. Some of the experimentally observed properties of the cavity noise are, however, not clearly explained in terms of thunderstorm activity. An alternative mechanism for the excitation of the cavity is by hydromagnetic waves.

In the present study we wish to investigate the propagation of hydromagnetic waves in the ionosphere by analytical methods. Our first objective in this study is to investigate the propagation of hydromagnetic waves through inhomogeneous regions of the ionosphere. We consider, in particular, extremely low frequency (ELF) waves which could propagate through the ionosphere and reach the earth as electromagnetic waves. Waves at these frequencies may be generated and amplified in the magnetosphere due to a variety of phenomena originating from the solar corpuscular radiation, such as gyroresonances and plasma-beam interactions. Excitation of the earth-ionosphere cavity could thus result from these waves as they propagate to the earth guided by the field lines of the earth's magnetic field.

Our second objective in this study is to investigate the propagation of hydromagnetic waves through current carrying regions of the ionosphere and the magnetosphere. The existence of constant currents in the medium is usually ignored in analyzing the propagation of hydromagnetic waves, mainly to simplify the problem, and also because data describing these

currents is not accurately known. The effect of constant currents may, however, be important at certain frequencies and for certain current densities.

The existence of electrostatic fields and a system of currents in the ionosphere is now well established. These "dynamo" induced electrostatic fields, arise due to the motion of air in the earth's magnetic field in the E-region of the ionosphere. It has been suggested (Dewitt and Akasofu, 1965) that these currents extend beyond the ionosphere and cause large scale wind motions in the magnetosphere. A similar system of currents is produced by the solar plasma wind incident on the outer boundary of the magnetosphere. It has been suggested that these currents also penetrate deep into the magnetosphere and have an important role in the structure of the magnetosphere (Alfvén et al., 1964). Although the quantitative description of these currents, either in the ionosphere or in the magnetosphere is not yet precise, their existence is now well established both, on theoretical grounds as well as through experimental observations. In the second part of this study, we investigate the effect of such currents on hydromagnetic waves as they propagate through regions carrying a constant current density $\vec{J}_o$.

In chapter 2, we consider the propagation of hydromagnetic waves in inhomogeneous media and study the special case when the propagation constant is assumed to vary linearly with distance. Curves are given for coupling coefficients of hydromagnetic waves in a homogeneous plasma to electromagnetic waves in vacuum when the two media are separated by a linearly varying transition region.

In chapter 3, we consider more realistic situations and apply Epstein's theory (Epstein, 1930) to the propagation of hydromagnetic waves through the ionosphere. This theory provides the most general method by which propagation through inhomogeneous media may be studied. We assume propagation parallel to the magnetic field for which the two circularly polarized waves are uncoupled and are described by the simple wave equation. The Epstein's method, which consists of transforming the wave equation into the hypergeometric differential equation may thus be applied to this problem. We use a transformation which provides rather general types of profiles through which propagation may be studied. Analytical expressions for transmission coefficients for these transformations are given. These expressions are then used for calculating the transmission coefficients of hydromagnetic waves through the ionosphere.

In chapter 4, we review some of the experimentally observed data on ELF noise in the earth-ionosphere cavity as reported by various investigators. These experimental results are compared with the theoretical noise characteristics deduced from excitation by worldwide thunderstorm activity. Some of the expected differences in characteristics due to excitation by hydromagnetic waves and worldwide thunderstorm activity are discussed.

In chapter 5, we examine the various generation mechanisms which may excite ELF waves in the magnetosphere. In particular, we look for processes and regions in the magnetosphere where signals close to the resonant frequencies of the first few modes of the earth-ionosphere cavity may be generated.

In chapter 6, we investigate the propagation of hydromagnetic waves in current carrying media. We derive macroscopic equations for a fully

ionized plasma in which the effects of streaming velocities of electrons and ions are expressed explicitly in terms of a constant current density $\vec{J}_o$. A general dispersion equation for small amplitude waves is then derived from these equations. Simplified forms of the dispersion equation are investigated by considering the following special cases:

(1) Transverse propagation with constant currents transverse to both, the direction of propagation and the static magnetic field.

(2) Longitudinal propagation with constant currents in the transverse plane (i.e. normal to the direction of propagation which is also the direction of the static magnetic field).

(3) Longitudinal propagation with constant currents also along the direction of the magnetic field.

The modifications in the propagation constants due to the existence of constant currents in the above three cases are studied and the existence of instabilities introduced by the currents is investigated. Numerical results are presented for data corresponding to altitudes of 500 km. and 50,000 km., representing, respectively, the conditions in the upper ionosphere and the magnetosphere.

II. PROPAGATION OF HYDROMAGNETIC WAVES THROUGH A LINEARLY VARYING MEDIUM

The propagation of hydromagnetic waves along the direction of the static magnetic field is described by the simple wave equation, which for a particular mode may be written for the electric field as

$$E''(z) + k^2(z)\, E = 0 \qquad (2.1)$$

where it is assumed that the static magnetic field is along the z-axis, and the propagation constant k varies along the z-axis only.

For $k^2(z)$ varying in an arbitrary manner, there are no known general solutions of the above equation. Solutions for special cases may, however, be obtained. They involve transforming the wave equation into some equation for which the solutions are known.

A hydromagnetic wave may be considered simply as an electromagnetic wave in which the hydromagnetic effects of the medium are coupled to the electromagnetic fields. If a homogeneous collisionless plasma were to merge into vacuum through a slowly varying transition region such that the reflections at each infinitesimal layer were negligibly small, then to the same approximation a hydromagnetic wave would smoothly transform into a pure electromagnetic wave in vacuum without any reflections. This is the well known WKB approximation (Budden, 1964). If the medium is rapidly varying, however, the wave is continuously reflected as it propagates through the transition region. In the limiting case of an

infinitesimally thin region, the reflection is the same as at a sharp boundary between a homogeneous plasma and vacuum.

2.1 Coupling through a linearly varying transition region

In this chapter, we consider the coupling of hydromagnetic waves in a cold, homogeneous collisionless plasma to electromagnetic waves in vacuum, for the special case when the plasma and vacuum are separated by a transition region in which the square of the propagation constant of the wave varies linearly with distance. The general solution for this case is in terms of Airy functions. Simplified solutions for this case may, however, be obtained by using approximate expressions for the Airy functions.

We consider a hydromagnetic wave propagating parallel to the direction of the static magnetic field B_o, which is assumed to be along the z-axis. An anlysis based on the macroscopic equations of a plasma in which the pressure gradient and Hall terms are neglected shows that in this special case the Alfvén and modified Alfvén modes become identical. The effect of pressure gradient and Hall terms is negligible for the sufficiently low frequencies which are considered here. The transition region is assumed to be stratified along the y-axis, with the plane of incidence being the (y-z) plane. The wave equation for the electric field of a hydromagnetic wave is given by equation (2.1), where the propagation constant k(z) is given by (Ullah and Kahalas, 1963).

$$k^2(z) = \frac{\frac{\omega^2}{c^2}\left(\frac{V_a^2}{c^2} - \frac{\omega^2}{\omega_e^2} + 1\right)}{\left(\frac{V_a^2}{c^2} - \frac{\omega^2}{\omega_e^2}\right)} \qquad (2.2)$$

where ω is the radian frequency of the wave, V_a is the Alfvén velocity

given by $V_a^2 = B_o^2/\mu_o\rho_o$, and ω_e^2 is the plasma frequency defined by $\omega_e^2 = ne^2/m_e\varepsilon_o$. The mass density ρ_o is equal to $n(m_e+m_i)$, where n is the electron or ion particle density and m_e and m_i are the electron and ion masses respectively. The rationalized MKS system of units is used. A time dependence of the form $e^{j\omega t}$ has been assumed.

In the transition region, the propagation constant is a function of z due to the variations of electron density, average ion mass and static magnetic field. When $k^2(z)$ is a rapidly varying function of distance, equation (2.1) can be solved exactly only for a few special cases. If it is assumed that $k^2(z)$ varies linearly with z, one of the well known methods is to transform equation (2.1) into Stoke's equation which has solutions in terms of Airy functions (Budden, 1961). Let k_p and k_o represent the propagation constants for the plasma and vacuum, separated by the transition region between z_1 and z_2 above the origin. Using the following transformation

$$k^2(z) = k_o^2 + \frac{(z-z_2)}{(z_1-z_2)} \quad (k_p^2 - k_o^2). \tag{2.3}$$

The differential equation (2.1) can be transformed into Stoke's equation.

$$\frac{d^2E(\xi)}{d\xi^2} = \xi E(\xi) \tag{2.4}$$

where

$$\xi = \left(\frac{k_p^2-k_o^2}{z_1-z_2}\right)^{1/3} \left[(z_2-z) - k_o^2 \quad \frac{(z_1-z_2)}{(k_p^2-k_o^2)} \right] \tag{2.5}$$

We consider a hydromagnetic wave incident on the transition region at z_1 and propagating towards the origin. In the homogeneous plasma and vacuum

the wave solutions of the form $e^{jk_p z}$, $e^{jk_o z}$ may be assumed. In the transition region, the fields must be given by the solutions to equation (2.4). The Airy integral functions $A_i(\xi)$, $B_i(\xi)$ may be taken as the two linearly independent solutions to Stoke's equation. The transmission coefficient expressing the ratio of transmitted to incident electric fields may be determined by the usual procedure which is indicated below. The fields in the plasma, transition region and vacuum can be written as follows:

In the plasma

$$E_x = e^{jk_p z} + Re^{-jk_p z} \tag{2.6}$$

In the transition region

$$E_x = C_1 A_i(\xi) + C_2 B_i(\xi) \tag{2.7}$$

In vacuum

$$E_x = T\, e^{jk_o z} \tag{2.8}$$

The only magnetic field component H_y in the three regions is obtained by using Maxwell's equation, which under the present assumptions reduces to

$$H_y = \frac{1}{j\omega\mu_o} \frac{\partial E_x}{\partial z}$$

Use of the boundary conditions for the continuity of the tangential electric and magnetic fields at z_1 and z_2 yields four equations from which the constants R, C_1 and C_2 may be eliminated to obtain the expression for T:

$$T = \frac{E_x^t}{E_x^i} = \frac{2}{\pi\xi_2^{\frac{1}{2}}} \exp.\left[jk_p(z_1 - z_2)\right] / \text{Det.} \tag{2.9}$$

where the determinant is given by

$$\text{Det.} = \begin{vmatrix} A_1(\xi_2) + \xi_2^{-\frac{1}{2}} A_1'(\xi_2) & B_1(\xi_2) + \xi_2^{-\frac{1}{2}} B_1'(\xi_2) \\ A_1(\xi_1) - \xi_1^{-\frac{1}{2}} A_1'(\xi_1) & B_1(\xi_1) - \xi_1^{-\frac{1}{2}} B_1'(\xi_1) \end{vmatrix} \tag{2.10}$$

In equations (2.9) and (2.10) ξ_1 and ξ_2 represent the values of ξ at z_1 and z_2; the prime indicates differentiation with respect to ξ. In deriving equation (2.9) the Wronskian $[A_1(\xi)\, B_1'(\xi) - A_1'(\xi) B_1(\xi)\,] = \pi^{-1}$ has been used, and the reference level for the transmission coefficient has been chosen as z_2.

The power transmission coefficient is determined by taking the ratio of the Poynting vectors in vacuum and plasma. With our present assumptions this is given by (Ullah and Kahalas, 1963)

$$Q = \frac{k_o}{k_p} \mid T \mid^2 . \tag{2.11}$$

2.2 Approximate expressions

The expression for T involves Airy integral functions which are tabulated for a limited range of values of ξ (Abramowitz and Stegun, 1964). For small values of ξ simplified expressions for T may be obtained, however, by using series representations for the Airy integrals. For large values of ξ asymptotic expansions for the Airy integrals are useful. The following asymptotic expansions for $A_1(\xi)$ and $B_1(\xi)$ may be employed (Budden, 1961), if ξ is large:

$$A_1(\xi) \simeq \frac{1}{2} \pi^{-\frac{1}{2}} \xi^{-1/4} [\exp(-\tfrac{2}{3} \xi^{3/2}) + j \exp(\tfrac{2}{3} \xi^{3/2})] \tag{2.12}$$

$$\text{for } \tfrac{2}{3}\pi \leq \arg\xi \leq \tfrac{4}{3}\pi$$

$$B_1(\xi) \simeq \frac{1}{2}\pi^{-\frac{1}{2}}\,\xi^{-1/4}\left[j\exp(-\frac{2}{3}\xi^{3/2}) + \exp(\frac{2}{3}\xi^{3/2})\right] \qquad (2.13)$$

$$\text{for } \frac{2}{3}\pi \leq \arg\xi \leq \frac{4}{3}\pi$$

The series representation for the Airy integrals is given by (Abramowitz and Stegun, 1964)

$$A_1(\xi) = c_1 f(\xi) - c_2\, g(\xi) \qquad (2.14)$$

and

$$B_1(\xi) = \sqrt{3}\ [c_1 f(\xi) + c_2\, g(\xi)] \qquad (2.15)$$

where

$$f(\xi) = 1 + \frac{1}{3!}\xi^3 + \frac{1\cdot 4}{6!}\xi^6 + \cdots$$

$$g(\xi) = \xi + \frac{2}{4!}\xi^4 + \frac{2\cdot 5}{7!}\xi^7 + \cdots$$

and

$$c_1 = A_1(0) = B_1(0)/\sqrt{3} \simeq .3550,\quad c_2 = -A_1'(0) = B_1'(0)/\sqrt{3} \simeq .2588$$

The series of $f(\xi)$ and $g(\xi)$ are also two linearly independent solutions of Stoke's equation and are convergent for all ξ. For small values of ξ, the series solutions $f(\xi)$ and $g(\xi)$ may therefore be used in place of $A_1(\xi)$ and $B_1(\xi)$. Substituting $f(\xi)$ and $g(\xi)$ for $A_1(\xi)$ and $B_1(\xi)$ and their respective derivatives in equation (2.9) and (2.10) we obtain

$$T = \frac{2\exp\{jk_p(z_1-z_2)\}}{\left\{(1+\xi_1^{-\frac{1}{2}}\xi_2^{\frac{1}{2}})-(\frac{\xi_1^{3/2}}{2}-\frac{\xi_1^3}{3\cdot 2}+\frac{\xi_1^{9/2}}{5\cdot 3\cdot 2}-\cdots)-\xi_2^{\frac{1}{2}}(\xi_1-\frac{\xi_1^{5/2}}{3}+\frac{\xi_1^4}{4\cdot 3}-\cdots)-\xi_2^{3/2}(-1+\frac{\xi_1^{3/2}}{2}-\frac{\xi_1^3}{3\cdot 2}+\cdots)\right.}$$

$$\left.-\xi_2^2(-\xi_1^{-\frac{1}{2}}+\frac{\xi_1}{2}-\frac{\xi_1^{5/2}}{3\cdot 2}+\cdots)-\cdots\right\} \qquad (2.16)$$

where

$$\xi_1 = -\left(\frac{z_1-z_2}{k_p^2-k_o^2}\right)^{2/3} k_p^2, \quad \xi_2 = -\left(\frac{z_1-z_2}{k_p^2-k_o^2}\right)^{2/3} k_o^2 \quad .$$

Equation (2.16) is valid for small values of ξ, and for $|\xi_2| \ll |\xi_1|$. Small values of ξ_1 occur when the transition region (z_1-z_2) is very small as compared to a wavelength. It is interesting to note that in the limiting case when the transition length is zero, equation (2.16) simply reduces to

$$T = \frac{2k_p}{k_p+k_o} \tag{2.17}$$

which, together with Eq.(2.11), is the same as equation (20) of Ullah and Kahalas (1963), for the coupling coefficient of hydromagnetic to electromagnetic waves at the interface between a homogeneous plasma and vacuum.

To obtain a simplified expression for T for large values of ξ_1, we assume that $|\xi_2|$ is always $\ll 1$, so that $f(\xi)$ and $g(\xi)$ may be approximated by the first terms in the series. Using asymptotic expressions (2.12) and (2.13) for $A_i(\xi_1)$ and $B_i(\xi_1)$ and their respective derivatives, and series representations (2.14) and (2.15) for $A_i(\xi_1)$ and $B_i(\xi_1)$, we obtain an expression for T, valid for large values of ξ_1

$$T = \frac{2\xi_1^{1/4}\, e^{u}\, \exp.\{jk_p(z_1-z_2)\}}{(\alpha_2 + \alpha_1\, \xi_2^{\frac{1}{2}})} \tag{2.18}$$

where

$$\alpha_1 = c_1\, (\sqrt{3} - j)\, \pi^{\frac{1}{2}}\ , \quad \alpha_2 = c_2\, (\sqrt{3} + j)\, \pi^{\frac{1}{2}}$$

and

$$u = 2/3\ \xi_1^{3/2}$$

Using equations (2.18) and (2.11) for large values of ξ_1 and equations (2.16) and (2.11) for small values of ξ_1, the power coupling coefficients

Q have been calculated. Figures (2.1) to (2.3) show the variation of Q versus the length of the transition region, for various values of ω/ω_e, and V_a/c. The parameters chosen are representative of the ionosphere. The coupling coefficients for the plasma-vacuum interface for each value of V_a/c converge to a constant value of Q, which is independent of frequency in the present approximation. With finite transition lengths, however, a considerable variation in Q takes place as the frequency is changed.

2.3 Discussion

It may be noted that the regions close to the left hand side of Figs.(2.1)-(2.3) represent the cases which approach the coupling of hydromagnetic to electromagnetic waves at a sharp plasma-vacuum interface while those to the right approach the WKB approximation when the transition takes place over a relatively long distance. Under the present approximations the coupling coefficient is independent of frequency if the plasma-vacuum transition is abrupt; but if the transition region between the plasma and the vacuum has dimensions of the order of a wavelength (in the plasma), the coupling coefficient depends upon frequency and the thickness of the transition layer. Hydromagnetic waves at higher frequencies are coupled more efficiently than at lower frequencies.

III. PROPAGATION OF HYDROMAGNETIC WAVES THROUGH AN ARBITRARILY VARYING MEDIUM (APPLICATION OF EPSTEIN'S METHOD)

The variation of the propagation constants of hydromagnetic waves corresponding to the actual variation of the ionospheric parameters, is such that it may not be described accurately by any of the simple mathematical functions. If the interparticle collisions which have a predominant effect in the lower ionosphere are considered, the problem is even more complicated; the real and imaginary parts of the propagation constant in this case follow completely different forms of variation.

3.1 Introduction to Epstein's theory

The most general profile for the propagation constant of an inhomogeneous medium for which the problem of wave propagation may be studied analytically, results from a method originally due to Epstein (Epstein, 1930). Significant contributions have been made by subsequent authors (Rawer, 1939; Burman and Gould, 1965). The method consists of transforming the wave equation into a hypergeometric differential equation which has solutions in terms of hypergeometric functions. By using various transformations, and by choosing proper constants involved in the transformation, it is possible to study a wide range of profiles. The hypergeometric equation has been studied extensively and its properties are very well known. The circuit relations, i.e., the relations between solutions valid in different regions of convergence are completely known for this equation. This fact makes it possible to determine the transmission and reflection coefficients for propagation through a large variety of

ionospheric models.

In transforming the wave equation into a hypergeometric differential equation, various transformations may be used. We shall use a slightly modified form of the transformation studied by Burman and Gould (1965), which provides rather general types of profiles for the refractive index for which transmission coefficients may be obtained.

3.2 Hypergeometric differential equation

The hypergeometric differential equation can be written as

$$x(1-x)\,u''(x) + [\gamma-(\alpha+\beta+1)x]\,u'(x)-\alpha\beta u(x) = 0 \qquad (3.1)$$

where α, β and γ are arbitrary constants. The two solutions of the hypergeometric differential equation which are convergent for $|x|<1$ can be written in terms of hypergeometric function as (Budden, 1961)

$$u_1 = F(\alpha,\beta;\gamma;x) \qquad (3.2)$$

$$u_2 = (-x)^{1-\gamma}F(\alpha-\gamma+1,\beta-\gamma+1;2-\gamma;x) \qquad (3.3)$$

where the hypergeometric function F is defined by the series

$$F(\alpha,\beta;\gamma;x) = 1+\frac{\alpha\beta}{\gamma\cdot 1}x + \frac{\alpha(\alpha+1)\beta(\beta+1)}{\gamma(\gamma+1)2!}x^2 + \cdots\cdots \qquad (3.4)$$

The two solutions u_1 and u_2 are linearly independent.

For the region of convergence $|x|>1$, the two linearly independent solutions are given by

$$u_3 = (-x)^{-\alpha}F(\alpha,\alpha-\gamma+1;\alpha-\beta+1;x^{-1}) \qquad (3.5)$$

$$u_4 = (-x)^{-\beta}F(\beta,\beta-\gamma+1;\beta-\alpha+1;x^{-1}) \qquad (3.6)$$

3.3 Circuit Relations

In the above equations, u_1 and u_2 are solutions of the hypergeometric

differential equation valid for the region $|x|>1$, and are not valid for $|x|<1$. Similarly u_3 and u_4 are solutions of equation (3.1) only for region $|x|<1$. By the process of analytic continuation (Whitaker and Watson, 1935) it is possible, however, to express solutions valid in the inner region of convergence as a linear combination of the solutions valid outside the circle of convergence of unit radius. These linear combinations are called circuit relations.

The circuit relation connecting the solution u_1, which is valid for $|x|<1$, and (u_3,u_4) which are valid for $|x|>1$ is given by (Budden, 1961)

$$u_1 = A_3u_3 + A_4u_4 \tag{3.7}$$

where

$$A_3 = \frac{\Gamma(\gamma)\Gamma(\beta-\alpha)}{\Gamma(\beta)\Gamma(\gamma-\alpha)}$$

$$A_4 = \frac{\Gamma(\gamma)\Gamma(\alpha-\beta)}{\Gamma(\alpha)\Gamma(\gamma-\beta)}$$

Similarly, the circuit relation connecting solutions u_2 and (u_3,u_4) is given by

$$u_2 = B_3u_3 + B_4u_4 \tag{3.8}$$

where

$$B_3 = \frac{\Gamma(\beta-\alpha)\Gamma(2-\gamma)}{\Gamma(1-\alpha)\Gamma(\beta-\gamma+1)}$$

$$B_4 = \frac{\Gamma(\alpha-\beta)\Gamma(2-\gamma)}{\Gamma(1-\beta)\Gamma(\alpha-\gamma+1)} \quad .$$

In the above equations, Γ represents the gamma function.

3.4 Transformation of the hypergeometric equation into wave equation

The hypergeometric differential equation (3.1) can be transformed into the wave equation by the following transformation

$$u = r(z)E(z) \tag{3.9}$$

where
$$r(z) = x^{-\gamma/2}(1-x)^{(\gamma-\alpha-\beta-1)/2}\left(\frac{dx}{dz}\right)^{\frac{1}{2}} \tag{3.10}$$

and
$$x = P(z)$$

where P(z) is some arbitrary function which determines the refractive index profile. Various functions for P(z) have been used. Following Burman and Gould (1965) with slight modifications, we shall use the transformation.

$$x = P(z) = -\frac{1}{2}\left(e^{akz+c} + e^{bkz+d}\right) \tag{3.11}$$

where k is the propagation constant for free space, a, b are real constants such that $a \geq b$; c and d are arbitrary constants. This transformation (Eq.3.11) introduces additional constants as compared to that used in the well known Epstein profiles (Epstein, 1930). As a result, the range of profiles which may be studied is greatly increased. If a and b are equal, and c, d are both zero, this transformation reduces to the one which provides the symmetrical Epstein profiles.

If the above transformations are carried out, we obtain the wave equation for electric fields travelling in the z-directions:

$$E''(z) + k^2 n^2(z) E(z) = 0 \tag{3.12}$$

where the refractive index as a function of z is given by

$$n^2(z) = \frac{(a-b)^2 e^{(a+b)kz+(c+d)}}{\left(e^{akz+c}+be^{bkz+d}\right)^2} - \frac{1}{4}\left(\frac{a^2 e^{akz+c}+b^2 e^{bkz+d}}{ae^{akz+c}+be^{bkz+d}}\right)^2 - \left(\frac{ae^{akz+c}+be^{bkz+d}}{e^{akz+c}+e^{bkz+d}}\right)^2$$
$$\cdot\left[K_1 - K_2\left(\frac{e^{akz+c}+e^{bkz+d}}{2+e^{akz+c}+e^{bkz+d}}\right) - \frac{2K_3\left(e^{akz+c}+e^{bkz+d}\right)}{\left(2+e^{akz+c}+e^{bkz+d}\right)^2}\right] \tag{3.13}$$

The constants K_1, K_2, K_3 are given by

$$4K_1 = \gamma(\gamma-2)$$

$$4K_2 = 1-(\alpha-\beta)^2+\gamma(\gamma-2)$$

$$4K_3 = (\alpha+\beta-\gamma)^2-1$$

From these constants the parameters of the hypergeometric functions are obtained:

$$\begin{aligned} 2\alpha &= 1+\sqrt{(1+4K_1)} + \sqrt{(1+4K_3)} - \sqrt{1+4(K_1-K_2)} \\ 2\beta &= 1+\sqrt{(1+4K_1)} + \sqrt{(1+4K_3)} + \sqrt{1+4(K_1-K_2)} \\ \gamma &= 1+\sqrt{(1+4K_1)} \end{aligned} \tag{3.14}$$

We assume that the origin of the coordinate system is chosen to be somewhere within the ionosphere. If we now assume that the refractive index tends to some constant value q for large positive values of z, and to the free space value of unity for large negative values of z, then from equation (3.13) the constants K_1 and K_2 are given by

$$K_1 = -\frac{1}{4} - \frac{1}{b^2} \tag{3.15}$$

$$K_2 = \frac{q^2}{a^2} - \frac{1}{b^2} \tag{3.16}$$

If the constants a and b are chosen, then K_1 and K_2 are fixed by equations (3.15) and (3.16). The three constants of the hypergeometric function are thus given by

$$\begin{aligned} 2\alpha &= 1+2j\left(\frac{1}{b} - \frac{q}{a}\right) + \sqrt{(1+4K_3)} \\ 2\beta &= 1+2j\left(\frac{1}{b} + \frac{q}{a}\right) + \sqrt{(1+4K_3)} \\ \gamma &= \left(1+\frac{2j}{b}\right) \end{aligned} \tag{3.17}$$

3.5 Solutions for Electric Fields

The solutions for the fields in the general case are complicated.

With the origin in the ionosphere, approximations can, however, be made which give simplified expressions for the electric field for large positive and negative values of z, or above and below the region of interest in the ionosphere.

From equation (3.11) it can be seen that as $z \to \infty$, $x \to -\infty$, and as $z \to -\infty$, $x \to 0$. For large positive values of x the hypergeometric functions in equations (3.5) and (3.6) can be approximated by the first term in the series of equation (3.4), namely unity. Similarly for small x the hypergeometric functions in equation (3.2) and (3.3) can be approximated by unity. The approximate expressions for electric fields for large negative values of z are obtained from equations (3.9) and (3.10) corresponding to the solutions u_1 and u_2 respectively:

$$E_1(z) = (-1)^{(\gamma-1)/2}\,(2)^{(1-\gamma)/2}\,(bk)^{-\frac{1}{2}}e^{d(\gamma-1)/2}\,(1+e^{\delta kz+\delta'})^{\gamma/2}\,(1+\frac{a}{b}e^{\delta kz+\delta'})^{-\frac{1}{2}}e^{bkz(\gamma-1)/}$$

and (3.18)

$$E_2(z) = (-1)^{3/2(1-\gamma)}\,(2)^{(\gamma-1)/2}\,(bk)^{-\frac{1}{2}}e^{d(1-\gamma)/2}\,(1+e^{\delta kz+\delta'})^{(1-\frac{\gamma}{2})}\,(1+\frac{a}{b}e^{\delta kz+\delta'})^{-\frac{1}{2}}e^{bkz(1-\gamma)/2}$$

(3.19)

where $\delta = a-b$, and $\delta' = c-d$. Equation (3.18) represents the electric field due to a wave incident from "below" (large negative value of z) and equation (3.19) represents the field due to a wave reflected from "below". Similarly for large positive values of z, corresponding to solutions u_3 and u_4, we obtain from equations (3.5) and (3.6):

$$E_3(z) = (-1)^{\frac{1}{2}(2\beta-2\alpha-\gamma+1)}\,(2)^{(\alpha-\beta)/2}\,(ak)^{-\frac{1}{2}}e^{c(\beta-\alpha)/2}\,(1+e^{-\delta kz-\delta'})^{(\beta-\alpha+1)/2}$$

$$(1+\frac{b}{a}e^{-\delta kz-\delta'})^{-\frac{1}{2}}\,e^{akz(\beta-\alpha)/2} \qquad (3.20)$$

and

$$E_4(z) = (-1)^{\frac{1}{2}(2\alpha-2\beta-\gamma+1)}(2)^{(\beta-\alpha)/2}(ak)^{-\frac{1}{2}}e^{c(\alpha-\beta)/2}(1+e^{-\delta kz-\delta'})^{(\alpha-\beta+1)/2}$$

$$(1+\frac{b}{a}e^{-\delta kz-\delta'})^{-\frac{1}{2}}e^{akz(\alpha-\beta)/2} \qquad (3.21)$$

Equations (3.20) and (3.21) represent electric fields due to incident and reflected waves from above the ionosphere (positive values of z). A time dependence of the form $e^{j\omega t}$ is assumed. The parameters α, β, and γ of the hypergeometric functions are to be chosen such that $\frac{\beta-\alpha}{j}$ and $\frac{\gamma-1}{j}$ are real and positive for waves propagating along the z-axis. This requirement is satisfied if a and b are chosen to be real and positive.

3.6 Transmission Coefficient

We shall assume first that there is no ground conductor at the "bottom" (below the ionosphere) so that the reflected wave u_1 below the ionosphere does not exist. The transmission coefficient may then be found by using the circuit relation (3.8) which connects the field in the wave transmitted through the ionosphere, to the fields above the ionosphere which are due to the incident and reflected waves. By taking the ratio of equation (3.19) to the first term in (3.8), and assuming the incident field at z_1, and transmitted at $-z_2$, we obtain:

$$T = (-1)^{(\alpha-\beta-\gamma+1)}(2)^{(\beta-\alpha+\gamma-1)/2}(\frac{a}{b})^{\frac{1}{2}}(1+e^{-\delta kz_2+\delta'})^{(1-\gamma/2)}(1+e^{-\delta kz_1+\delta'})^{(\alpha-\beta-1)/2} \qquad (3.22)$$

$$\cdot C(1+\frac{a}{b}e^{-\delta kz_2+\delta'})^{-\frac{1}{2}}(1+\frac{b}{a}e^{-\delta kz_1-\delta'})^{\frac{1}{2}}\exp\left[(-bkz_2+d)(1-\gamma)/2-(akz_1+c)(\beta-\alpha)/2\right]$$

where

$$C = \frac{\Gamma(1-\alpha)\Gamma(\beta-\gamma+1)}{\Gamma(\beta-\alpha)\Gamma(2-\gamma)}$$

The constants α, β and γ in the above expressions are given by equation (3.17), while a, b, c and d are constants chosen to represent a given ionospheric profile. The values of z_1 and z_2 must be large enough so

that the conditions used in deriving the expressions for electric fields are satisfied. The power transmission coefficient Q is calculated from the relation (Ullah and Kahalas, 1963)

$$Q = \frac{1}{q} |T|^2 \tag{3.23}$$

where q is the index of refraction of the ionosphere at $z=z_1$.

3.7 Numerical Calculations

For calculating the transmission coefficients from the expressions given in the last section, the constants in equation (3.13) have to be chosen to provide variations of the refractive index corresponding to the desired profiles. For the refractive index to be unity for large negative values of z (below the ionosphere) and to some constant complex value q for large positive values of z (above the ionosphere) the constants K_1 and K_2 are given by equations (3.15) and (3.16). The constant K_3 may be conveniently chosen to give the value of $n^2(z)$ at the origin. This gives K_3 as

$$K_3 = \frac{(2+e^c+e^d)^2}{2a^2(e^c+e^d)} (n^2(0)-1) - \frac{K_2}{2} (2+e^c+e^d) \tag{3.24}$$

In the above expression for K_3, the known value of the square of refractive index at the origin, $n^2(0)$, is calculated from the dispersion relation.

An approximate choice for the constants can thus be made readily with the help of equations (3.15-3.16) and (3.24). With such a choice, the assumed values for the real and imaginary part of $n^2(z)$, below, above and at some region within the ionosphere would correspond exactly to the calculated values from the dispersion relation. The proper slope for the profiles is then mainly determined by the constants a and b, which may be

chosen arbitrarily. For more accurate correspondence between the assumed profiles and those calculated from the dispersion relation, a readjustment of the constants may be required.

The expression for the transmission coefficient (3.23) involves gamma functions of complex arguments. These functions are tabulated for a limited range of the complex arguments (Abramowitz and Stegun, 1964). For computer calculations, the gamma functions may, however, be evaluated more conveniently by using asymptotic expressions or series representations. For large values of the argument z of the gamma function, Stirling's formula (Abramowitz and Stegun, 1964) may be used:

$$\Gamma(z) \simeq (2\pi)^{\frac{1}{2}} e^{-z} z^{z-\frac{1}{2}} \left[1+ \frac{1}{12z} +\ldots.\right] \qquad (3.25)$$

$$\text{for } |z| \to \infty, \ |\arg z| < \pi$$

For smaller values of the arguments, the following series representation (Erdelyi, 1953) may be used:

$$\Gamma(z) = \lim_{n\to\infty} \frac{n^z}{z(1+\frac{z}{2})(1+\frac{z}{3})\ldots.(1+\frac{z}{n})} \qquad (3.26)$$

The above two expressions for gamma functions were used for calculating the power transmission coefficients of hydromagnetic waves through the ionoshpere discussed in the next section. For the transition values of the arguments of the gamma function, enough terms were used in the series (3.25) and (3.26) such that the results from the two expressions agreed up to at least the first two decimal places.

3.8 Power Transmission Coefficients for the Ionosphere

The power transmission coefficients, for which expressions have been given in section (3.6) may be calculated for hydromagnetic waves in the

ionosphere which arrive as electromagnetic waves in the lower atmosphere. The refractive index profiles for these waves may be calculated from the known dispersion relations for the hydromagnetic waves in a partially ionized plasma. The basic equations on which the analysis of hydromagnetic waves is usually based, are the linearized macroscopic plasma equations (Spitzer, 1963) in addition to Maxwell's equations. The effect of collisions in such a description is introduced by defining interparticle collision frequencies which are assumed to be independent of the velocity perturbations. The pressure tensor term is usually replaced by an isotropic pressure term.

In a partially ionized plasma, in which the neutral particles are allowed to be in motion, there are in general, five modes of propagation (Bostick, et al., 1964). Two of these are essentially transverse waves, while the other three are acoustic waves. The dispersion relation for this general case is difficult to solve, and the roots for the individual modes can only be evaluated numerically from a fifth degree polynomial in the square of the propagation constant. For the frequency range of interest it has been shown (Bostick, et al., 1964), however, that the pressure gradient terms have very little effect on the two transverse waves. These two waves thus propagate almost independently of the acoustic waves. If the pressure gradient terms are then neglected, all the acoustic modes vanish and the only two remaining modes are the transverse waves. The dispersion relations for this case are relatively simple, particularly if it is further assumed that the magnetic field is along the direction of propagation. The dispersion relations thus obtained by Bostick et al., include the effect of all interparticle collisions and the motion of neutral particles. One or both of these effects were usually neglected in relatively more simple

dispersion relations which were given by Hines (1953), Dungey (1954), and Fejer (1960). The refractive indices for the two modes are given by

$$n^2 = -\frac{1}{k^2}(y_{11} \pm jy_{21}) \tag{3.27}$$

where

$$y_{11} = j\omega\mu_o(\sigma_{11} + j\omega\epsilon_o)$$

$$y_{21} = j\omega\mu_o(\sigma_{21})$$

The "conductivities" σ_{11} and σ_{22} are defined in the Appendix. Field variations of the form $e^{j(\omega t - nk\, z)}$ have been assumed.

In equation (3.27) the upper sign gives the right hand circularly polarized wave (also called extraordinary mode or whistler mode) while the lower sign gives the left hand circularly polarized wave (ordinary mode). These two modes have different propagation characteristics depending upon the frequency and the parameters of the plasma. Both modes have "zones" in which they are "allowed" or "forbidden" to propagate (Booker, 1962). For longitudinal propagation (i.e. along the direction of $\vec{B}_o$), the right hand polarized wave (R wave) can propagate at all frequencies from zero to the electron gyrofrequency, at which it has a resonance. For the left hand polarized wave (L wave) the upper frequency for the allowed zone is the ion-gyrofrequency. Beyond the electron and ion gyrofrequencies for the R and L modes respectively, propagation cannot take place in a wide frequency band which extends up into the megacycle region. On the basis of the assumed electron density and the earth's magnetic field, Booker (1962) has plotted allowed and forbidden zones in the magnetosphere for a large range of frequencies. This is shown in Fig. (3.1). At frequencies close to 10 c/s and above, the L wave cannot propagate in the magnetosphere, except at heights

less than about 2 earth radii. The L wave, therefore, cannot propagate to the earth unless it is generated below this height.

In addition to the above considerations, it is known that at frequencies close to 10 c/s and above, the dissipation of the L mode in the lower regions of the ionosphere, even for longitudinal propagation is many of orders of magnitude more than that for the R mode (Akasofu, 1965). Therefore at the frequencies of interest it is more likely that the right hand polarized wave reaches the earth.

There is some experimental evidence for a field aligned structure of ionization at the base of the magnetosphere. On this basis it has been shown by Booker (1962) that at frequencies close to 10 c/s and above, both the R and the L wave are likely to be guided along the direction of the earth's magnetic field. The generation and amplification processes in general, as will be discussed in section 5, involve propagation parallel to the magnetic field lines. We therefore assume propagation parallel to the direction of the magnetic field.

The refractive indices as a function of height in the ionosphere, for parallel propagation, were calculated for the R wave at 8 c/s using the ionospheric data (Prince et. al., 1964; Akasofu, 1965), for sunspot minimum. The profiles for the real and imaginary part of the square of the refractive index have been plotted in Fig. (3.2) for various times of day. To calculate the transmission coefficients applying Epstein's theory, the constants in equation (3.13) have to be chosen. With appropriate constants, the profiles calculated from equation (3.13) for both the real and imaginary part of $n^2(z)$ should correspond to the profiles calculated from the dispersion relation.

A sample set of profiles for real and imaginary part of $n^2(z)$ corresponding to different times of day and calculated from equation (3.13) is given in Figs. (3.3 - 3.4). The profiles calculated directly from the dispersion relation for each case are also plotted. The variable constants and the origin z_o used for each profile are shown on each figure.

The power transmission coefficients calculated for these profiles are plotted in Fig. (3.5). It is to be noted that the maximum transmission coefficient occurs at about local midnight and the minimum at about local noon. This fact, easily explained from the higher imaginary part of $n^2(z)$ at noon due to higher electron densities, is in agreement with the results given by Akasofu (1965). His results, however, show much higher values of transmission coefficient because they are based only on attenuation due to the dissipative part of the propagation constant, and reflections due to inhomogeneities in the ionosphere are neglected.

The procedure used for the choice of constants which are required in obtaining the results discussed above may be indicated as follows: The constant K_3 was chosen to provide the known value of refractive index at some point within the ionosphere. This point, also used as the origin, was chosen in the vicinity of the height where maximum $Im(n^2)$ occurs. Such a choice ensures that the profiles in the region of maximum dissipation closely approximate the desired profiles. The slopes of the profiles for $Re(n^2)$ and $Im(n^2)$ are then mainly determined by the constants a and b. These were chosen to provide the desired refractive index below and above the ionosphere. The value of $Re(n^2)$ below the ionosphere was assumed to be unity at a height of about 40 km (where $Im(n^2)$ was taken to be zero). The variation in the slopes of the profiles corresponding to various times of day was obtained by variation of the constant a and b.

The procedure indicated above provides profiles with refractive indices closely approximating the desired values in three regions, namely, below and above the ionosphere, and in the region of maximum dissipation somewhere within the ionosphere. The constants a and b may be chosen fairly accurately to meet the above conditions. The order of magnitude of the effect of an inaccurate choice of the constants a and b, however, may be seen from the following example given as an illustration: For the Hour-18 profile shown in Fig. 3.3, an alternative choice of the constants a=625, b=615 (instead of a=670, b=660) lowers the point of unity refractive index from a height of about 40 km to about 30 km. The corresponding value for the transmission coefficient changes from .119 to .122. The curves for both choices of the constants a, b are shown on Fig. (3.4).

An estimate of the effects which changes of constants have upon the resulting attenuation can also be obtained by comparing the values of attenuation for day and night (for example hours 0 and 18 on Fig. 3.5) and the corresponding $Re(n^2)$ and $Im(n^2)$ profiles. Certainly the analytical approximations by hypergeometric functions (Figs. 3.3 - 3.4) for the "experimental" index of refraction profiles (that is profiles calculated from the ionospheric data, Fig. 3.2) for the same hour do not deviate more than the analytical approximations for the day profiles differ from the analytical approximation for the night profiles. Yet the resulting maximum difference in the calculated attenuation between day and night is ~ 6.2 db. This compares with a difference of ~ 0.4 db between our attenuation values (daylight hours, for example) and the attenuation values obtained by Akasofu (1965) neglecting reflections due to inhomogeneities in the ionosphere.

IV. EXPERIMENTAL RESULTS ON EXTREMELY LOW FREQUENCY NOISE ON THE EARTH'S SURFACE

As seen from the analysis given in the last chapter, hydromagnetic waves incident on the upper ionosphere from above, may be propagated through the ionosphere and reach the earth as pure electromagnetic waves. Excitation of the earth-ionosphere cavity could thus result from extra-terrestrial sources through these waves. In this chapter we shall examine the possibilities of excitation of the earth-ionosphere cavity by hydromagnetic waves on the basis of extremely low frequency measurements reported in the literature. Some of the discrepancies between the experimental results and the predicted noise characteristics deduced from thunderstorm activity will be discussed.

4.1 Earth-Ionosphere Cavity

The concentric spherical shells formed by the earth and the lower boundary of the ionosphere, form a cavity for extremely low frequency waves. That such a cavity exists, and is excited by sources of natural origin, was first suggested by Schumann (1952). Following an analysis based on a simplified model, and assuming infinite conductivities for the earth and the ionosphere, the resonant frequencies for such a cavity were shown to be

$$f_n = \frac{c}{2\pi R}\sqrt{n(n+1)} \qquad (4.1)$$

where f_n is the resonant frequency for the nth mode, c is the velocity of light in vacuum and R is the radius of the earth. This idealized model gives the resonant frequencies for the first few modes as

f_1 = 10.6 c/s, f_2 = 18.4 c/s, f_3 = 26.0 c/s, etc. Due to the finite conductivities of the ionosphere and the earth the actual resonant frequencies, however, are somewhat lower.

The first experimental evidence for the existence of these resonances was provided by Schumann and König (1954). Since then, a large number of papers, both theoretical and experimental, have appeared on this subject. More detailed theories of the earth-ionosphere cavity have been developed, in which the inhomogeneity of the ionosphere and the effects of the earth's magnetic field have been considered. Galejs (1963) considered an isotropic inhomgeneous ionosphere in which the conductivity is assumed to vary exponentially with height. The effect of the earth's magnetic field in a spherically stratified ionosphere has been considered by Thompson (1963), and Galejs (1965), in which the magnetic field is assumed to be in the radial direction. An anlysis for dipolar magnetic field has been given by Wait (1966). Several excellent review articles are now available, in particular those by Kleimenova (1963), Galejs (1965), Madden and Thompson (1965) and Wait (1965). For a detailed study of the theory of Schumann resonances, reference is made to the above papers and to the original references listed therein. Here, we shall only consider some of the important characteristics of the earth-ionosphere cavity pertinent to the present study.

4.2 Electromagnetic Fields in the Cavity

The theoretical analyses of the Schumann resonance phenomenon usually consider excitation by vertical dipole sources on the assumption that the cavity is excited by the vertical component of lightning discharges. The field due to an excitation by a horizontal dipole is believed to be small, being of the order of $10^{-5}/\sqrt{\sigma_e}$ of the field due to the vertical discharges

(Wait, 1960) where σ_e is the earth's conductivity. The fields due to a vertical dipole moment for any of the TM modes are of the form

$$E_r \sim P_n(\cos\theta) \tag{4.2}$$

$$H_\phi \sim \frac{d}{d\theta} P_n(\cos\theta) \tag{4.3}$$

where $P_n(\cos\theta)$ is the Legendre polynomial of order n and argument cos θ. For the first resonance mode, the Legendre polynomial of order one is $P_1(\cos\theta) = \cos\theta$ and is zero for $\theta = 90^\circ$. The radial electric field is thus zero at an angular distance of 90° from the dipole, and the associated horizontal magnetic field has a maximum at that point. Similarly, for an excitation in the 2nd mode, the radial electric field has zeroes for $\theta = 55^\circ$ and $\theta = 125^\circ$, with the corresponding maxima for the magnetic field at those points. Many attempts have been made to explain the variations of ELF noise in the earth-ionosphere cavity in terms of the above characteristics along with the seasonal and geographical variation of the noise sources (Balser and Wagner, 1962; Galejs, 1965; Madden and Thompson, 1965; Ryeroft, 1965).

4.3 Sources of Excitation of the Earth-Ionosphere Cavity

The sources of excitation of the earth-ionosphere cavity may in general be divided into two different classes:

(a) Lightning discharges due to the world wide thunderstorm activity.

(b) Processes in the magnetosphere and the ionosphere exciting waves which are propagated to the earth. Such processes will be examined in the last two chapters of this thesis (V and VI).

The electromagnetic waves generated by lightning discharges are capable of exciting earth-ionosphere cavity resonances. The frequency spectrum of

electromagnetic waves generated in lightning flashes has been discussed by Pierce (1963) and it has been shown that the various processes accompanying cloud to cloud and cloud to ground discharges are of comparable effectiveness in generating low frequency waves. The world wide thunderstorm activity has frequently been believed to be mainly limited to the continental land mass areas, in particular close to the equatorial belt (Balser and Wagner, 1962). Curves showing the diurnal variation of thunderstorm activity over the continents, are available (Handbook of Geophysics, 1960); they are based on the average number of days of thunderstorms as reported by observation posts in various regions, and indicate the period of maximum and minimum activity only over those regions. Various explanations of the variation of ELF noise in the earth-ionosphere cavity have been heavily based on these curves, which neglect thunderstorm activity over the oceans.

Thunderstorm activity over the oceans, generally ignored in explaining the variation of noise in the earth-ionosphere cavity, must, however, be included. The average thunderstorm activity over the oceans, as estimated by Pierce (1958), is larger than the total activity over all the continents.

The characteristics of measured ELF noise in the earth-ionosphere cavity and the relation of these characteristics to those expected due to excitation by hydromagnetic waves or thunderstorm activity is discussed in the next section.

4.4 Experimental Results on ELF Noise

Measurements of electromagnetic fields in the ELF band (1-3000 c/s) have been made by various investigators in different parts of the world.

These measurements have been reported for narrow as well as for wide frequency bands. The data are given in the form of electric field or magnetic field intensities or as power densities computed from either of the two.

The intensity of measured electromagnetic fields in the earth-ionosphere cavity depends upon generation as well as propagation characteristics and power spectra of both, measured electric and magnetic fields clearly show peaks at frequencies close to the predicted resonant frequencies of the cavity (Balser and Wagner, 1962).

The various characteristics of these resonances, such as resonant frequency variation, diurnal and seasonal variation of the power densities in the various modes, and their relation to some of the known characteristics of world wide thunderstorm activity, have been a subject of several investigations. There appear to be, however, some contradictions between some of the measured characteristics of the resonances, as reported by various investigators, and the theoretical predictions.

Most theoretical analyses of Schumann resonances assume thunderstorm activity as the almost exclusive source of excitation. As noted before, the world wide thunderstorm activity is assumed to be mainly limited to the land areas. The two land mass areas which are believed to be most effective in exciting the cavity are Central Africa and the Amazon Valley in South America. One of the most important characteristics of the measured fields, such as the diurnal variations of the cavity fields, are thus usually explained in terms of "storm maxima" corresponding to the time of maximum storm activity in any of the source areas, and "mode zeros" corresponding to the regions where the fields due to the sources have minima.

The diurnal variations of the fields in the cavity due to the thunderstorm activity in accordance with these theories are thus expected to depend upon the distance from the thunderstorm centers, and the diurnal variation at two widely separated locations should not be the same in terms of local time.

From the available published data, the following characteristics may be observed which do not seem to be consistent with the expected results of the theories, such as the one discussed above:

(1) In general, the diurnal variation of ELF measurements show higher signal during the day than at night, and the maximum occurs around local noon. This characteristic may be observed from both narrow and wide frequency band measurements.

In the narrow frequency band close to the first resonant frequency of the earth-ionosphere cavity, the measurements reported by Keefe and Polk (1964) at Kingston, R.I., and König at Brannenburg, Germany, and Ryeroft (1965) at Cambridge, England, all show maximum fields during the day close to the local noon or afternoon. Measurements conducted by Balser and Wagner (1961) in California at the end of July and in Massachusetts during the middle of August, show maxima for both places occurring during local afternoons.

From the measurements made over relatively wide frequency bands, the same characteristic may be observed. Measurements by Holzer and Deal (1956) in California, over the frequency range 25-130 c/s show maximum signals occurring before local noon for measurements in March and April, and at about local afternoon in August. Horizontal magnetic field measurements over the frequency range 1-150 c/s by Goldberg (1956), in Oregon during

the months of July and August show maximum signal during local afternoon.

(2) In general, the characteristics of diurnal variations of ELF noise measured at different longitudes, display time shifts similar to the time difference between universal and local times.

The most suggestive evidence for this is provided by the measurements conducted by Keefe, Polk and König (1964), simultaneously in U.S.A. and Germany. The maxima and minima of the diurnal variation of the horizontal magnetic field in the first resonance, as reported by them, seem to be shifted in time which is almost equal to the time difference between the universal and local times. The German and American curves for both, October-November and May measurements appear strikingly similar, when viewed against local time.

It is interesting to note, that even from the measurements made at similar times, a tendency towards this characteristic may be observed. For instance, the horizontal magnetic field measurements at 8 c/s by Gendrin and Stefant (1962) near Paris, and at Tromso, Norway, made during the months of July 1962 and April 1962 respectively, show very similar diurnal variations. The variation near Paris, however, appears to display a distinct time lag with respect to that in Norway (about 1½ hour) which is somewhat larger than the time difference corresponding to the difference in the longitudes of the two places (about 1 hour and one quarter). It should be noted that the above measurements are not only for different months but the two sites are also situated at different latitudes. These two differences may be significant factors in the larger time shifts observable from the curves.

Another example of this characteristic may be observed from the

horizontal magnetic field measurements reported by Aarons and Henissart (1953), over the frequency range .5-20 c/s, made for 15 days in August 1952, in Massachusetts and New Mexico. The three peaks in their diurnal variation curves display a distinct time shift which is slightly less than the time difference between universal and local time. Here, the measurements are for the same days but the two sites are at different latitudes.

Conclusions in contradiction to the above considerations have been drawn by Shand (1966), based on simultaneous ELF measurements at several widely separated sites in the frequency range of the resonant frequencies of the earth-ionosphere cavity. According to his observations, the diurnal variation of average ELF activity at all sites closely follows the occurrence of the world wide lightning as outlined in the Handbook of Geophysics (1960). The worldwide thunderstorm activity curves in this reference, however, as stated before, are based on the continental land mass areas centered around the equatorial belt. Excitation of the earth-ionosphere cavity by thunderstorm activity occurring in accordance with the Handbook of Geophysics would thus lead to variations in field intensity as described in section (4.2). The observations reported by Shand, however, indicate that the average field intensities were approximately equal at all measurement sites, which are widely separated both, with respect to latitude and longitude. This is inconsistent with the postulated distribution of thunderstorm sources. Furthermore, Shand does not show in his paper any curves of diurnal amplitude variations and it is therefore difficult to evaluate how justified his conclusion is that ELF amplitude variations agree with the Handbook of Geophysics curves for thunderstorm activity.

4.5 Discussion

The measured characteristics discussed in the preceding section, suggest a source of excitation in addition to thunderstorm activity. In particular, the processes in the magnetosphere which could generate extremely low frequency waves at the appropriate frequencies, and which could propagate to the earth and excite the earth-ionosphere cavity.

It will be seen in the following two chapters, that the conditions for generation and amplification processes at frequencies close to 10 c/s exist in various regions of the magnetosphere. The hydromagnetic waves thus generated, as seen from the results discussed in chapter 3, could propagate through the ionosphere and reach the earth as electromagnetic waves with reasonably high transmission coefficients. The transmission coefficients, however, were found to be minimum during the day and maximum at night. To explain higher field intensity measurements during the day due to hydromagnetic waves, ELF generation mechanisms on the day side of the hemisphere will have to be sufficiently higher than on the night side, in order to offset the lower transmission coefficients. Furthermore, it is possible that the earth-ionosphere cavity acts as a "half-cavity", i.e., the day ionosphere and the earth form an independent cavity which has much lower losses (by radiation through the ionosphere) than the night cavity. This is of particular importance if excitation takes place by hydromagnetic waves propagating along the magnetic field lines, with excitation centers being near the magnetic poles.

To compare some of the differences in excitation from the two sources, the following characteristics may be expected: Due to the guiding effects and the generation and amplification mechanisms being in general along the

earth's magnetic field lines, the incident circularly polarized waves from the ionosphere are probably of maximum intensity in the higher latitude regions. For excitation of the cavity, however, the angle of incidence of these waves has to deviate at least slightly from the normal. The field distribution in the first resonant mode due to the excitation of the cavity by hydromagnetic waves may thus be expected to have higher vertical electric field intensities in the mid or high latitude regions than in the equatorial regions or at the poles. Lower vertical electric field intensities will be expected in the equatorial regions due to the lower intensity of the incident waves.

On the other hand, if the worldwide thunderstorm activity is assumed to be mainly around the equatorial belt, including the oceans, as is usually believed, the electric fields in the first resonant mode should show higher values in the equatorial regions and lower in the higher latitude regions.

Since the fields due to both sources are probably superimposed, and since amplitude measurements at different latitudes reported in the literature, may not be compared accurately, it is difficult to identify these effects separately. Simultaneous measurements at different latitudes may, however, shed some light on this problem.

V. GENERATION OF ELF WAVES IN THE MAGNETOSPHERE

Extremely low frequency waves may be generated in the magnetosphere due to a variety of processes within the magnetosphere (and the ionosphere) or at the boundary between the magnetosphere and the solar plasma wind. The various processes may, in general, be separated into two different classes. The first involves single charged particle mechanisms and the resulting coherent radiation due to a large number of such particles. The second is based on instabilities and growing waves due to the interaction of charged particle beams with plasmas in a magnetic field. The radiation flux from the first type of mechanisms is believed to be an order of magnitude smaller than that from the second type. Since the coherent radiation from the single particle mechanisms may be amplified in some regions of the magnetosphere (Hultqvist, 1965), we shall also consider this type of generation.

The various single particle and instability mechanisms arising from charged particle beams have been classified by Brice (1964), according to the type of charged particle (electron or proton), type of resonance (longitudinal or transverse), and the type of emission mechanism (single particle or instability). The various combinations of these conditions give rise to eight different types of mechanisms. With the exception of two, all have been suggested as the possible sources for either VLF or hydromagnetic emissions. We shall consider here the mechanisms which may possibly give rise to extremely low frequency waves close to the resonant frequencies of the earth-ionosphere cavity at its first few modes.

5.1 Doppler Shifted Cyclotron Radiation

A charged particle gyrating about the magnetic field lines emits radiation at the local gyro-frequency (and its harmonics). For a particle moving at non-relativistic velocities, the Doppler shifted radiated frequency is given by

$$\omega = \frac{\Omega}{1 \pm \frac{u}{c} n} \qquad (5.1)$$

where Ω is the local gyrofrequency of the particle, u_r is the radial component of velocity of the particle relative to the observer, and n is the refractive index of the medium at the Doppler shifted frequency. The negative or positive signs are taken depending upon whether the particle is moving towards the observer or away from him.

The Doppler shifted cyclotron radiation from electrons as a possible source for VLF emissions was suggested and considered by Dowden (1962). The frequency band for the Doppler shifted cyclotron radiation of the electrons trapped in the earth's magnetic field is estimated to be in the VLF range for all heights in the magnetosphere and therefore is not likely to contribute to radiation at about 10 c/s.

The Doppler shifted cyclotron radiation from protons was considered by MacArthur and others (MacArthur, 1959; Murcray and Pope, 1960), as a possible source for VLF emissions. The proton cyclotron frequency on the earth's surface is about 10^3 c/s and decreases with height h as $\frac{1}{(R+h)^3}$, where R is the earth's radius. The Doppler shifted proton cyclotron radiation can therefore be expected in the frequency range of interest (7-30 c/s), from proton clouds at heights of about 3 or 4 earth radii or higher depending

upon the particle velocities. It has been pointed out (Murcray and Pope, 1961), however, that a large number of protons must radiate coherently if this radiation is to be detectable on the ground. Nevertheless, amplification processes in regions of the magnetosphere below the proton clouds may greatly enhance this radiation.

5.2 Cerenkov Radiation

A charged particle moving along the direction of a magnetic field with velocity u in a plasma of refractive index n will emit electromagnetic waves if the following coherent radiation condition is satisfied.

$$n \cos \theta = \frac{c}{u} \tag{5.2}$$

where c is the velocity of light, and θ is the angle between the wave normal of the radiated electromagnetic wave and the magnetic field.

Of all the single particle mechanisms which may generate low frequency waves in the magnetosphere, Cerenkov radiation is believed to be the strongest, and has been suggested as a source for VLF emissions (Ondoh, 1961). McKenzie (1963) has considered the problem of Cerenkov radiation from charged particles moving along the direction of the magnetic field in a magneto-ionic medium. On assumptions valid for the magnetospheric conditions, it has been shown that low frequency waves may be emitted over two bands. The lower frequency band, over which the extraordinary wave is emitted, extends from zero to an upper frequency ω_1 given by

$$\omega_1 \simeq \frac{u^2\omega_e^2}{c^2\Omega_e} \left(1 + \frac{u^2\omega_e^2}{c^2\Omega_e^2} \right) \tag{5.3}$$

where ω_e and Ω_e are the electron plasma and gyro-frequencies respectively. The maximum power radiated is at a frequency:

$$\omega_{1,max} = \frac{1}{\sqrt{3}}\ \omega_1 \qquad (5.4)$$

For particles with velocities of the order of those in the solar plasma wind, Cerenkov radiation in this mode is estimated to be in the frequency range of 10 c/s and above, for heights in the magnetosphere of about 6 to 2 earth radii. (McKenzie, 1963).

5.3 Instability Mechanisms from Plasma Beam Interactions

Electron or ion beam interactions with a plasma in a magnetic field can give rise to excitation and amplification of electromagnetic waves in a wide frequency range. A charged particle beam in a plasma, under appropriate conditions can either lead to an instability and a growing wave by transferring its own energy to the wave, or under different conditions, may absorb energy from the wave. The question of amplification or absorption under a given set of conditions for the plasma beam system may be decided from the direction of transfer of energy (Stix, 1962; Hultqvist, 1965). To determine, however, the type of instability (convective or non-convective), it is necessary to examine the plot of the dispersion relation in the real ω-k plane, or to examine the roots of the dispersion equation of the system.

In general, both an electron and an ion beam may excite electromagnetic waves of right or left hand polarization when certain conditions are satisfied (Neufeld and Wright, 1963). Under these conditions, the requirements are that the beam must move in the same direction as the wave, the beam must have a "superluminous" velocity, (i.e., the beam velocity must be

greater than the phase velocity of the wave) and the wave frequency is in resonance with the gyrofrequency of electrons or ions in the beam. The instability conditions for the various plasma-beam interactions have been the subject of a large number of recent papers.

An electron beam streaming parallel to the magnetic field lines can excite an R and L wave at one frequency under appropriate conditions. Electron beam and R wave interactions have been suggested to be a possible mechanism for VLF emissions (Cornwall, 1965; Gendrin, 1965), in the 1-100 kc/s range in which the electrons are believed to be the high energy electrons trapped in the radiation belts. For R wave excitations in the 7-30 c/s range, very high energy electrons with energies in the relativistic range are required (Neufeld and Wright, 1963; Cornwall, 1965). Whether such high energy electrons do exist in higher regions of the magnetosphere in large enough numbers is not known.

A proton beam instability with an R wave can take place either for one frequency or for three different frequencies, depending upon the beam velocity and the plasma parameters (Neufeld and Wright, 1963; Gendrin, 1965). For a "dense" plasma, for which the ratio $\frac{\omega_i}{\Omega_i} \gg 1$, (where ω_i is ion plasma frequency and Ω_i is the ion gyro-frequency) ion beams of relatively low velocities can excite hydromagnetic waves in a wide frequency range. In the limiting case, where the group velocity of the wave equals the beam velocity, two roots of the dispersion relation coalesce (Gendrin, 1965) for two values of u/V_a (where u is beam velocity and V_a is Alfvén velocity). The instability at the lower frequency in this case occurs at about twice the ion gyro-frequency, and at the higher frequency occurs at about half the electron gyro frequency. Proton beam and R wave interactions can take place

over longer distances in the equatorial regions since both the particle velocity as well as the plasma parameters remain essentially constant over relatively long distances. Calculations by Gendrin show that for the magnetospheric parameters and the instability corresponding to the lower frequency $2\,\Omega_i$, the excited frequencies are in the range 5-30 c/s for the L-parameter varying from 6-3 in the equatorial regions. The required proton energies for this frequency band are in the range 50-500 kev for trapped particles in the radiation belts, which are assumed to have mirror points at an altitude of 500 km. Emissions from such trapped particles satisfying the instability conditions, however, are expected to have a periodicity corresponding to the bounce period of the charged particles between successive reflections from the magnetic mirror points.

The two interaction frequencies $2\,\Omega_i$ and $\Omega_e/2$ discussed above are for the cases when the particle velocity is about equal to wave group velocity. For sufficiently large values of the ratio $\frac{\omega_i}{\Omega_i}$, curves given by Neufeld and Wright (1963) predict, however, excitation of hydromagnetic waves for "almost any velocity" of the beam. The quantity $\frac{\omega_i}{\Omega_i}$, which increases with height due to rapidly decreasing B_o, is very large in the magnetosphere for heights of about 5 or 6 earth radii and above in the equatorial regions. In these regions, untrapped particles directly from the solar wind may excite right hand polarized hydromagnetic waves in the frequency range 7-30 c/s. The conditions for excitation and amplification of R wave are therefore readily available in the magnetosphere.

5.4 ELF Waves from Electrostatic Instability Mechanisms

In addition to the plasma-beam interactions which give rise to growing transverse waves, it is also possible for an electrostatic instability to

generate such waves as has been pointed out by Lepechinsky (Lepechinsky and Rolland, 1964). When electrostatic oscillations created by charged particle beams grow into non-linear regions, the oscillations do not remain purely electrostatic in nature but acquire radiation properties and generate electromagnetic waves. The waves generated from this mechanism, however, must conform to the solutions of the dispersion equation for oscillations in the beam-plasma system. The instability band for such a system extends from zero to an upper frequency equal to the electron or ion plasma frequency depending upon the beam. The low-frequency waves generated by this mechanism may propagate to the earth in the whistler mode as guided by the field lines of the earth's magnetic field. This mechanism of generation for ELF waves is thus basically different from those discussed in Section (5.3) in connection with plasma beam interactions. Mechanisms of this type have been suggested to explain the electromagnetic radiation from the sun (Haeff, 1949).

VI. HYDROMAGNETIC WAVES IN A CURRENT CARRYING MEDIUM

6.1 Introduction

In this chapter we wish to investigate the propagation of hydromagnetic waves in current carrying regions of the ionosphere and the magnetosphere. The effects due to the existence of currents in the medium are usually ignored in discussions of wave propagation mainly to simplify the analysis and also because the data describing such currents is very incomplete. Constant currents in the ionosphere or the magnetosphere, however, may have significant effects at certain frequencies and for certain current densities.

The existence of electrostatic fields and a system of currents in the ionosphere is well established both on theoretical considerations and experimental observations (Maeda and Kato, 1966). The electrostatic fields arise due to the motion of atmospheric gases in the earth's magnetic field in the E-region of the ionosphere. These dynamo-induced electrostatic fields and the resulting currents, form a basis of the electrodynamics of the ionosphere. It has been suggested (Akasofu and Dewitt, 1964) that these electrostatic fields extend far beyond the ionosphere and cause large scale wind motions of the magnetospheric plasma. A strong coupling between the ionosphere and the magnetosphere is thus expected to exist through the dynamo-induced electrostatic fields.

A similar system of currents is produced by the solar plasma wind which is incident on the outer boundary of the magnetosphere. It has been suggested (Alfvén et al., 1964), that the electric fields and the currents

caused by the solar plasma wind, also penetrate deep into the magnetosphere and have an important role in the structure of the magnetosphere. Although a quantitative knowledge of these currents, either in the ionosphere or in the magnetosphere is not yet accurate, their existence is now well established.

In the present study we investigate explicitly the behavior of hydromagnetic waves as they propagate through regions carrying a constant current density $\overline{J}_o$. This constant current density $\overline{J}_o$ may arise due to any of the various processes capable of producing currents in the system.

It is of interest to study the conditions under which the refractive index of hydromagnetic waves in the ionosphere or the magnetosphere is significantly modified due to the presence of $\overline{J}_o$ in the medium, and its interaction with the wave fields. We investigate the frequencies which are most affected by the currents in various regions of the magnetosphere, and study the conditions under which the existence of currents may give rise to instabilities and to amplification or evanescence of waves.

An analogous problem, which has received considerable interest in the literature is wave propagation in a medium traversed by energetic charged particle beams. These beams give rise, under appropriate conditions, to instabilities and to growing or evanescent waves. A large number of papers have appeared in recent years on the instabilities arising from the plasma-beam interactions; some of these were discussed in particular in Chapter V. In the plasma-beam analysis, it is usually assumed that a very small fraction of one of the plasma constituents (electrons or ions) is moving with relatively high velocity in a particular direction (usually along the magnetic field). The streaming particles are assumed to

be an integral part of the total collection of charges which make up the neutral plasma. The modified dispersion relation for a system consisting of plasma and a single beam, thus, has a perturbation term added to the usual dispersion relation for the unperturbed plasma. The new resonances introduced due to the existence of the beam then appear as instabilities in the system. The analysis for a system with both electrons and ion beams is much more complicated.

To investigate the effects of constant currents in the medium, we use macroscopic equations for a fully ionized plasma involving additional terms due to the existence of a current density $\overline{J}_o$. The current density $\overline{J}_o$ arises as a result of the macroscopic motion of electron and ion fluids. A derivation of the macroscopic equations is given in Section (6.2). In Section (6.3) we use these equations to derive a general dispersion relation for small amplitude waves. Simplified forms of this dispersion equation are then used for studying the characteristics of these waves. In Section (6.4) we discuss the criteria for distinguishing between instabilities and evanescent waves.

In Sections (6.5) to (6.8) we study the simplified forms of the general dispersion equation for three special cases. In case (1), we consider transverse propagation and the currents also transverse to both the direction of propagation and the static magnetic field. In case (2) we assume longitudinal propagation and the currents in the transverse plane. In case (3) we consider longitudinal propagation again, but with currents also in the direction of the static magnetic field. The effects of the existence of $\overline{J}_o$ in the medium on the propagation constants of [illegible]dromagnetic waves and the current induced instabilities are investigated for the above three cases.

6.2 Basic Equations

The equation of motion for the jth species of particles may be written as:

$$N_j m_j \left[\frac{\partial \bar{V}_j}{\partial t} + \bar{V}_j \cdot \nabla \bar{V}_j \right] = N_j q_j \left[\bar{E}' + \bar{V}_j \times \bar{B}' \right] \qquad (6.1)$$

where N_j and $\bar{V}_j$ are the total particle density and the macroscopic velocity of the jth gas; $\bar{E}'$ and $\bar{B}'$ are the total electric and magnetic field intensities. The equation of continuity for the jth gas may be written as:

$$\frac{\partial N_j}{\partial t} + \nabla \cdot (N_j \bar{V}_j) = 0 \qquad (6.2)$$

In addition to the plasma equations, we have Maxwell's equations

$$\nabla \times \bar{E}' = - \frac{\partial \bar{B}'}{\partial t} \qquad (6.3)$$

$$\frac{1}{\mu_o} \nabla \times \bar{B}' = \bar{J}' + \epsilon_o \frac{\partial \bar{E}'}{\partial t} \qquad (6.4)$$

where the total current density $\bar{J}'$ is given by

$$\bar{J}' = \sum q_j N_j \bar{V}_j \qquad (6.5)$$

6.2.1 Linearized Equations

The set of Equations (6.1) to (6.5) completely determine the plasma field variations as a function of space and time. These equations are

non-linear, and in general have not been solved. The non-linear equations may, however, be linearized by assuming that the total fields are composed of perturbed fields superimposed on static fields which are assumed to be independent of space and time. Thus we set:

$$\bar{V}_j = \bar{v}_{oj} + \bar{v}_j$$

$$\bar{B}' = \bar{B}_o + \bar{B}$$

$$\bar{E}' = \bar{E}_o + \bar{E}$$

$$\bar{J}' = \bar{J}_o + \bar{J}$$

$$N_j = n_{oj} + n_j \qquad (6.6)$$

The streaming velocities $\bar{v}_{oj}$ are allowed for in each species of particles. The perturbed fields $\bar{v}_j$, $\bar{B}$ etc., are assumed to be small as compared to the static fields. Substituting Equation (6.6) in (6.1), and neglecting second order terms of perturbed quantities, the equation of motion may be written as:

$$n_{oj}\, m_j \left[\frac{\partial \bar{v}_j}{\partial t} + \bar{v}_{oj} \cdot \nabla \bar{v}_j \right] = q_j\, n_{oj} \left[\bar{E} + \bar{v}_{oj} \times \bar{B} + \bar{v}_j \times \bar{B}_o \right] \qquad (6.7)$$

In obtaining Equation (6.7) it has been assumed that the perturbed quantities are small as compared to the static quantities (with the exception of streaming velocities). Similarly, the linearized continuity equation may be written as:

$$\frac{\partial n_j}{\partial t} + n_{oj} \nabla \cdot \bar{v}_j + \nabla n_j \cdot \bar{v}_{oj} = 0 \qquad (6.8)$$

Substituting for $\bar{J}'$ from Equation (6.6) and neglecting second order terms, $\bar{J}'$ can be written as

$$\bar{J}' = \sum q_j n_{oj} \bar{v}_{oj} + \sum (q_j n_{oj} \bar{v}_j + q_j n_j \bar{v}_{oj}) \tag{6.9}$$

If the streaming velocities $\bar{v}_{oj}$ are assumed to be small, being of the order of $\bar{v}_j$ or less, the second term in the second summation may be neglected. This is valid due to the assumption that $n_j \ll n_{oj}$. Thus we may write:

$$\bar{J}_o = \sum q_j \; n_{oj} \; \bar{v}_{oj} \tag{6.10}$$

$$\bar{J} = \sum q_j \; n_{oj} \; \bar{v}_j \tag{6.11}$$

Using Equation (6.6), (6.10) and (6.11), Maxwell's equations may be written as

$$\nabla \times \bar{E} = -\frac{\partial \bar{B}}{\partial t}$$

$$\frac{1}{\mu_o} \nabla \times \bar{B} = \bar{J} + \epsilon_o \frac{\partial \bar{E}}{\partial t}$$

6.2.2 Generalized Ohm's law and momentum transfer equation

The linearized plasma equations given above involve fluid velocities of each species of particles. Assuming a plasma consisting of electrons and ions only, macroscopic equations may be derived involving a single fluid velocity $\bar{v}$. We define the perturbed velocity of the center of mass:

$$\bar{v} = \frac{\rho_i \bar{v}_i + \rho_e \bar{v}_e}{\rho_i + \rho_e} \tag{6.12}$$

where ρ is the mass density and the subscripts e and i now refer to electrons and ions. Similarly for the zero order velocity, we define

$$\bar{v}_o = \frac{\rho_i \bar{v}_{oi} + \rho_e \bar{v}_{oe}}{\rho_i + \rho_e} \tag{6.13}$$

Assuming a perfectly neutral plasma such that $n_{oe} = n_{oi} = n$, the currents $\bar{J}_o$ and $\bar{J}$ may then be written from (6.10) and (6.11) as:

$$\bar{J}_o = ne\,(\bar{v}_{oi} - \bar{v}_{oe}) \tag{6.14}$$

and

$$\bar{J} = ne\,(\bar{v}_i - \bar{v}_e) \tag{6.15}$$

Adding Equations (6.7) for electrons to that for ions, and making use of Equations (6.10-6.13), we obtain the momentum transfer equation expressed in the macroscopic plasma variables as:

$$\rho_o \frac{\partial \bar{v}}{\partial t} = \bar{J} \times \bar{B}_o + \left[\bar{J}_o \times \bar{B} - \frac{1}{\epsilon_o \omega_e^2} \bar{J}_o \cdot \nabla \bar{J} - \rho_o \bar{v}_o \cdot \nabla \bar{v} \right] \tag{6.16}$$

where $\rho_o = n(m_i + m_e) \simeq n\, m_i$ and ω_e is the electron plasma frequency. In deriving Equation (6.16), the approximation $1 + \frac{m_e}{m_i} \simeq 1$ was made. The three terms appearing in the bracket on the right hand side are introduced explicitly due to the presence of electron and ion streaming velocities.

In a similar way, by subtracting Equation (6.7) for electrons from that for ions, the generalized Ohm's law for a plasma with electron and ion streaming velocities and a resulting current density $\bar{J}_o$ may be derived as

$$\frac{1}{\epsilon_o \omega_e^2} \frac{\partial \bar{J}}{\partial t} - \bar{E} + \bar{v} \times \bar{B}_o - \frac{1}{ne} \bar{J} \times \bar{B}_o + \left[\bar{v}_o \times \bar{B} - \frac{1}{ne} \bar{J}_o \times \bar{B} \right.$$

$$\left. - \frac{1}{\epsilon_o \omega_e^2} (\bar{J}_o \cdot \nabla) \bar{v} - \frac{1}{\epsilon_o \omega_e^2} (\bar{v}_o \cdot \nabla) \bar{J} + \frac{1}{\epsilon_o \omega_e^2} \frac{1}{ne} (\bar{J}_o \cdot \nabla) \bar{J} \right] \qquad (6.17)$$

The last five terms in the bracket on the right hand side of the above equation arise as a result of the streaming velocities of electrons and ions in the plasma; only the first three terms remain in the absence of streaming velocities and the constant current density $\bar{J}_o$ in the system.

Equations (6.16) and (6.17) involve the zero order center of mass velocity vector $\bar{v}_o$ defined by Equation (6.13). This velocity is independent of space and time. A simplification of the equations may be achieved by choosing a moving reference system in which $\bar{v}_o$ vanishes. The current density $\bar{J}_o$ in the moving system, however, remains the same. This may be easily seen as follows: In the stationary system, $\bar{J}_o$ is given by

$$\bar{J}_o = ne (\bar{v}_{oi} - \bar{v}_{oe})$$

and in the reference system moving with a velocity $\bar{v}_o$, the current density $\bar{J}_o'$ is

$$\bar{J}_o' = ne \left[(\bar{v}_{oi} + \bar{v}_o) - (\bar{v}_{oe} + \bar{v}_o) \right] = \bar{J}_o$$

The results valid in the stationary frame of reference may be obtained by a transformation from the results in the moving reference system.

If, however, it is assumed that the particle streaming velocities are

small, being much less than the phase velocities of the waves, then the effect of the terms involving $\bar{v}_o$ may be considered to be negligible. This, in fact, is the case under consideration for currents in the ionosphere and the magnetosphere. Thus, after dropping the terms involving the zero order center of mass velocity $\bar{v}_o$, the macroscopic equations along with Maxwell's equations may be rewritten as

$$\rho_o \frac{\partial \bar{v}}{\partial t} = \bar{J} \times \bar{B}_o + \bar{J}_o \times \bar{B} - \frac{1}{\epsilon_o \omega_e^2} (\bar{J}_o \cdot \nabla) \bar{J} \tag{6.18}$$

$$\frac{1}{\epsilon_o \omega_e^2} \frac{\partial \bar{J}}{\partial t} = \bar{E} + \bar{v} \times \bar{B}_o - \frac{1}{ne} \bar{J} \times \bar{B}_o - \frac{1}{ne} \bar{J}_o \times \bar{B}$$

$$- \frac{1}{\epsilon_o \omega_e^2} (\bar{J}_o \cdot \nabla) \bar{v} + \frac{1}{ne(\epsilon_o \omega_e^2)} (\bar{J}_o \cdot \nabla) \bar{J} \tag{6.19}$$

$$\nabla \times \bar{E} = - \frac{\partial \bar{B}}{\partial t} \tag{6.20}$$

$$\frac{1}{\mu_o} \nabla \times \bar{B} = \bar{J} + \epsilon_o \frac{\partial \bar{E}}{\partial t} \tag{6.21}$$

The analysis to be given in the following sections will be based on the above equations.

6.3 Dispersion equation

The basic equations derived in the last section describe the propagation of waves in a plasma in which the effect of streaming particles is expressed explicitly in terms of a constant current density $\bar{J}_o$. An analysis of waves

based on these equations in the general case is complicated. Assuming a homogeneous medium, however, and field variations of the form $e^{j(\omega t - \bar{k}.\bar{r})}$, the dispersion equation for waves in a homogeneous current carrying plasma in a magnetic field may be derived.

The velocity vector $\bar{v}$ may be eliminated from Equations (6.18) and (6.19) to obtain an equation in $\bar{J}$, $\bar{E}$ and $\bar{B}$ as

$$b\bar{J} = \bar{E} + \frac{1}{j\omega\rho_o}\bar{B}_o(\bar{J}.\bar{B}_o) + \frac{(\bar{J}_o.\bar{B}_o)\bar{B}}{j\omega\rho_o} - \frac{\bar{J}_o}{j\omega\rho_o}(\bar{B}.\bar{B}_o)$$

$$+ (\bar{J}x\bar{B}_o)\left[\frac{2(\bar{J}_o.\bar{k})}{\omega\omega_e^2\rho_o\epsilon_o} - \frac{1}{ne}\right] + (\bar{J}_o x\bar{B})\left[\frac{(\bar{J}_o.\bar{k})}{\omega\omega_e^2\rho_o\epsilon_o} - \frac{1}{ne}\right] \qquad (6.22)$$

where $b = \frac{Z}{j\omega\epsilon_o}$

and $Z = x + Y$, $x = \left(\frac{\Omega_i^2}{\omega_i^2} - \frac{\omega^2}{\omega_e^2}\right)$

$$Y = \left[\frac{(\bar{J}_o.\bar{k})^2}{\omega^4\rho_o\epsilon_o} - \frac{\omega}{\omega_e^2}\frac{(\bar{J}_o.\bar{k})}{ne}\right]$$

The wave magnetic field $\bar{B}$ in Equation (6.22) may be eliminated by substitution from Maxwell's equation

$$\bar{B} = \frac{1}{\omega}(\bar{k} \times \bar{E}) \qquad (6.23$$

Taking the scalar and cross product of the above equation with $\bar{J}$, and substituting in Equation (6.22), we obtain an expression for $\bar{J}$ as follows:

$$b_1\bar{J} = \bar{E} + b_2\bar{B}_o\,(\bar{E}\cdot\bar{B}_o) + b_3\,(\bar{E}\times\bar{B}_o)$$

$$+ b_4\left[\,(\bar{J}_o\cdot\bar{B}_o)\,[(\bar{k}\times\bar{E})\times\bar{B}_o] - [(\bar{k}\times\bar{E})\cdot\bar{B}_o]\,(\bar{J}_o\times\bar{B}_o)\right]$$

$$+ b_5\left[\,[\bar{J}_o\times(\bar{k}\times\bar{E})]\cdot\bar{B}_o\right]\bar{B}_o - b_6\left[\,[\bar{J}_o\times(\bar{k}\times\bar{E})]\times\bar{B}_o\right]$$

$$+ b_7\left[\,[\bar{B}_o\cdot(\bar{k}\times\bar{E})]\;\bar{J}_o - (\bar{J}_o\cdot\bar{B}_o)(\bar{k}\times\bar{E})\right]$$

$$+ b_8\left[\,\bar{J}_o\times(\bar{k}\times\bar{E})\right] \qquad (6.24)$$

Defining $a_1 = \left(\dfrac{2\bar{J}_o\cdot\bar{k}}{\omega\omega_e^2\,\rho_o\epsilon_o} - \dfrac{1}{ne}\right)$

and $a_2 = \left(\dfrac{\bar{J}_o\cdot\bar{k}}{\omega\omega_e^2\,\rho_o\epsilon_o} - \dfrac{1}{ne}\right)$

The coefficients b_1 through b_8 in the above equation are given by:

$$b_1 = b + \frac{a_1^2 B_o^2}{b}$$

$$b_2 = \frac{\left(\dfrac{2\epsilon_o}{\rho_o} - a_1^2\omega^2\epsilon_o^2\right)}{z\left(z - \dfrac{\Omega_i^2}{\omega_i^2}\right)}$$

$$b_3 = \frac{j\omega\epsilon_o a_1}{z}$$

$$b_4 = \frac{\epsilon_o a_1}{\rho_o \omega Z}$$

$$b_5 = \frac{(\epsilon_o Z - \omega^2 \rho_o \epsilon_o^2 a_1^2)}{\omega \rho_o Z \left(Z - \frac{\Omega_i^2}{\omega_i^2}\right)}$$

$$b_6 = -\frac{j\epsilon_o a_1 a_2}{Z}$$

$$b_7 = \frac{j}{\omega^2 \rho_o}$$

$$b_8 = \frac{a_2}{\omega}$$

An expression relating $\bar{J}$ and $\bar{E}$ may also be obtained from Maxwell's Equations (6.20) and (6.21) as

$$\bar{J} = \frac{1}{j\omega\mu_o} \left[\bar{k} \times \bar{k} \times \bar{E} + \mu_o \epsilon_o \omega^2 \bar{E} \right] \qquad (6.25)$$

Combining Equations (6.24) and (6.25) and eliminating $\bar{J}$, an equation involving only the electric field $\bar{E}$ may now be obtained:

$$k^2 \bar{E} - \bar{k}(\bar{k}\cdot\bar{E}) + \alpha_1 \bar{E} + \alpha_2 (\bar{E}\cdot\bar{B}_o)\bar{B}_o + \alpha_3 (\bar{E}\times\bar{B}_o)$$

$$+ \alpha_4 \left[[\bar{B}_o \cdot (\bar{k}\times\bar{E})]\, \bar{J}_o - (\bar{J}_o \cdot \bar{B}_o)\, [\bar{k}\times\bar{E}] \right]$$

$$+ \alpha_5 \left[(\bar{J}_o \cdot \bar{B}_o)(\bar{k}\times\bar{E}\times\bar{B}_o) - [\bar{B}_o \cdot (\bar{k}\times\bar{E})]\, (\bar{J}_o \times \bar{B}_o) \right]$$

$$+ \alpha_6 \left[[\bar{J}_o x (\bar{k} x \bar{E})] \cdot \bar{B}_o \right] \bar{B}_o + \alpha_7 \left[\bar{J}_o x (\bar{k} x \bar{E}) x \bar{B}_o \right]$$

$$+ \alpha_8 \left[\bar{J}_o \times (\bar{k} x \bar{E}) \right] = 0 \qquad (6.26)$$

where, defining the denominator D as $D = (Z^2 - \omega^2 \epsilon_o^2 a_1^2 B_o^2)$, the coefficients α_1 through α_8 are now given by:

$$\alpha_1 = - \frac{\frac{\omega^2}{c^2} Z}{D} - \frac{\omega^2}{c^2}$$

$$\alpha_2 = - \frac{\frac{\omega^2}{c^2} \left(\frac{Z \epsilon_o}{\rho_o} - \omega^2 \epsilon_o^2 a_1^2 \right)}{D \left(Z - \frac{\Omega_i^2}{\omega_i^2} \right)}$$

$$\alpha_3 = - \frac{\frac{\omega^2}{c^2} (j \omega \epsilon_o a_1)}{D}$$

$$\alpha_4 = - \frac{jZ}{\rho_o c^2 D}$$

$$\alpha_5 = - \frac{a_1 \epsilon_o \omega}{\rho_o c^2 D}$$

$$\alpha_6 = - \frac{\omega a_2 (\epsilon_o Z - a_1^2 \omega^2 \epsilon_o^2 \rho_o)}{\rho_o c^2 D \left(Z - \frac{\Omega_i^2}{\omega_i^2} \right)}$$

$$\alpha_7 = - \frac{j \frac{\omega^2}{c^2} (a_1 a_2 \epsilon_o)}{D}$$

$$\alpha_B = -\frac{a_2 \omega Z}{c^2 D} \tag{6.27}$$

In deriving Equation (6.26), no assumptions have yet been made about the directions of propagation, the static magnetic field or the currents. Equation (6.26) is too complicated to be considered in general. To simplify this equation we shall first assume that (y-z) is the plane of incidence and that the static magnetic field is along the z-axis, i.e., $\bar{k} = (0, k_y, k_z)$, and $\bar{B}_o = (0, 0, B_o)$. With these simplifying assumptions, Equation (6.26) may now be conveniently written in the form

$$R \cdot \bar{E} = 0 \tag{6.28}$$

where R is a 3 x 3 matrix. A necessary and sufficient condition that Equation (6.28) have non-trivial solutions is that the determinant of the matrix R vanish, i.e.,

$$\| R \| = 0 \tag{6.29}$$

An equation in ω and k resulting from (6.26) to (6.29) gives the dispersion relation $D(\omega,k) = 0$. With the simplifying assumptions stated above, the elements of the 3 x 3 matrix R may be written as follows:

$$R = \begin{bmatrix} R_{11} & R_{12} & R_{13} \\ R_{21} & R_{22} & R_{23} \\ R_{31} & R_{32} & R_{33} \end{bmatrix}$$

where the elements R_{ij} are given by:

$$R_{11} = k_y^2 + k_z^2 + \alpha_1 - \alpha_4 J_{ox} B_o k_y + \alpha_5 B_o^2 (J_{oy} k_y + J_{oz} k_z)$$

$$+ \alpha_7 J_{ox} B_o k_y - \alpha_8 (J_{oy} k_y + J_{oz} k_z)$$

$$R_{12} = \alpha_3 B_o + J_{oz} B_o k_z (\alpha_4 - \alpha_7)$$

$$R_{13} = J_{oz} B_o k_y (\alpha_7 - \alpha_4)$$

$$R_{21} = -\alpha_3 B_o - \alpha_4 B_o (J_{oy} k_y + J_{oz} k_z) - \alpha_5 J_{ox} B_o^2 k_y$$

$$+ \alpha_7 B_o (J_{oy} k_y + J_{oz} k_z) + \alpha_8 J_{ox} k_y$$

$$R_{22} = k_z^2 + \alpha_1 + \alpha_5 J_{oz} B_o^2 k_z - \alpha_8 J_{oz} k_z$$

$$R_{23} = -k_y k_z - \alpha_5 J_{oz} B_o^2 k_y + \alpha_8 J_{oz} k_y$$

$$R_{31} = \alpha_6 J_{ox} B_o^2 k_z + \alpha_8 J_{ox} k_z$$

$$R_{32} = -k_y k_z + \alpha_6 J_{oy} B_o^2 k_z + \alpha_8 J_{oy} k_z$$

$$R_{33} = k_y^2 + \alpha_1 + \alpha_2 B_o^2 - \alpha_6 J_{oy} B_o^2 k_y - \alpha_8 J_{oy} k_y \qquad (6.30)$$

Equation (6.28) with the matrix elements given by Equations (6.30) is too involved to be analyzed in the general form. Further simplifications in the matrix elements may, however, be made by considering special cases

which will be discussed in Section (6.5).

The solutions of Equation (6.29) for k give the possible modes of propagation. The characteristics of a particular mode depend upon the nature of k and its variation with frequency. Since constant current densities in the medium have been assumed, it may be expected that at certain frequencies and parameters of the medium, the existence of currents will give rise to instabilities. A brief discussion on the criteria for instabilities, based on an examination of the dispersion relation, is given in the following section.

6.4 Criteria for Instabilities

The dispersion relation $D(\omega,k) = 0$ gives a relation between ω and k. For wave functions of the form $e^{j(\omega t-kz)}$ to exist, ω and k must be solutions of the dispersion relation. The dispersion relation may be solved either for k or for ω and may be written as

$$k = K(\omega) \tag{6.31}$$

or $$\omega = \Omega(k) \tag{6.32}$$

where K and Ω are functions of k and ω respectively. The solutions for the propagation constant k and the frequency ω, in general, are complex quantities which may be expressed as:

$$k = k_r + j\, k_i \tag{6.33}$$

$$\omega = \omega_r + j\, \omega_i \tag{6.34}$$

where k_r, k_i, ω_r and ω_i are real quantities. The existence of a positive

imaginary part of k for real ω appears to indicate a wave growing in space. The presence of a growing wave, however, has to be consistent with physical considerations. A wave in certain cases may only be an evanescent wave although both signs for the propagation constant are permissible. This is so, in particular, in systems where there is no physical process for a transfer of energy to the wave.

The question of whether a particular solution indicates a growing or an evanescent wave may, however, be decided from a more detailed examination of the dispersion relation. The precise criteria for this which not only indicate the existence of an instability but also the type of instability, were put forward by Sturrock (1958).

According to Sturrock's analysis, instabilities may be classified into two classes; convective and nonconvective. A convective instability, which is synonymous with an amplifying wave, is excited and propagated away from the point of origin. For a convective instability, the wave grows as it propagates, and at some point away from the source, the wave amplitude gets larger than at the source. A nonconvective instability, on the other hand, grows indefinitely with time at all points in the neighborhood of the point of origin.

The criteria for the existence of instabilities and a distinction between the two types of instabilities are very clearly provided by plotting Sturrock's Λ and Γ diagrams. The Λ diagram is the locus of $k = K(\omega)$ in the complex k plane for real values of ω and the Γ diagram is the locus of $\omega = \Omega(k)$ in the complex ω plane for real values of k.

If $K(\omega)$ is real for real values of ω, and $\Omega(k)$ is real for real values of k, then there is no instability and the wave is a simple propagating wave,

The contours for ω and k as shown in Figures (6.1a) are both along the real axis. If for a certain range of values of ω, k is complex, but ω is real for all real values of k, then the wave is evanescent. The Λ and Γ diagrams have the configuration as shown in Figures (6.1b).

For a convective instability to exist, the Λ and Γ diagrams must have the configuration shown in Figures (6.1c). The Λ contour bridges the gap between k_1 and k_2 and has complex k over this range. The contour Γ bridges the gap between ω_1 and ω_2. For a convective instability, k is complex for real values of ω and ω is complex for a certain range of real values of k.

On the other hand, if k is real for all real ω, then any complex ω for real values of k indicates a nonconvective instability. The Λ and Γ diagrams for a nonconvective instability must have the configuration shown in Figure (6.1d). In this case the contour Γ bridges the gap between ω_1 and ω_2; the contour Λ, however, lies along the real axis.

A distinction between convective and nonconvective instabilities is also provided by simply examining a plot of the dispersion relation in the real ω real k plane. The ω-k plots for a simply propagating wave, a convective instability and a nonconvective instability are shown in Figure (6.2). The corresponding plots of frequency versus refractive index (f-n) are shown in Figure (6.3).

6.5 Special Cases of Propagation

The special cases of interest for which the equations are relatively simple are for the transverse and longitudinal propagations (perpendicular and parallel to the magnetic field). In this investigation we shall consider

the following three cases.

(1) Transverse propagation: The constant currents are perpendicular to both the direction of propagation and the static magnetic field. For this case, the static magnetic field, the propagation vector, and the constant currents are thus all mutually perpendicular. This case is of interest for its application to the propagation in the ionosphere and the magnetosphere in the equatorial regions.

(2) Longitudinal propagation with constant currents transverse to the direction of propagation. This case is of interest for its application to the waves in the ionosphere in the high latitude regions.

(3) Longitudinal propagation with constant currents also along the direction of propagation. For this case, the static magnetic field, the propagation vector and the constant currents are all in the same direction. This case is also of interest for its application to propagation in the high latitude regions in the ionosphere and the magnetosphere.

We shall investigate the above three cases in more detail in the following sections. It will be our objective to derive the simplified forms of the dispersion relations for each case and to study the characteristics of the waves by examining solutions of the dispersion relations.

6.6 Case (1): Transverse Propagation

For transverse propagation in a plasma with a magnetic field in the absence of constant currents, it is known that two modes of propagation are possible. The extraordinary mode, which has electric field components in the transverse plane, and the ordinary mode, which has the electric field along the direction of the static magnetic field.

In the present case, we assume that $\bar{J}_o$ is transverse to both the direction of propagation and the magnetic field, thus:

$$\bar{B}_o = (0, 0, B_o) \qquad \bar{k} = (0, k, 0)$$

and $\bar{J}_o = (J_o, 0, 0)$

With this choice, both $(\bar{J}_o \cdot \bar{k})$ and $(\bar{J}_o \cdot \bar{B}_o)$ are now equal to zero, and the coefficients α given by Equations (6.27) are independent of J_o and k. Equation (6.28) can now be written as

$$\begin{bmatrix} R_{11} & R_{12} & 0 \\ R_{21} & R_{22} & 0 \\ 0 & 0 & R_{33} \end{bmatrix} \begin{bmatrix} E_x \\ E_y \\ E_z \end{bmatrix} = 0 \qquad (6.35)$$

where

$$R_{11} = k^2 + \alpha_1 + B_o J_o k (\alpha_7 - \alpha_4), \qquad R_{12} = \alpha_3 B_o$$

$$R_{21} = -\alpha_3 B_o + J_o k (\alpha_8 - B_o^2 \alpha_5), \qquad R_{22} = \alpha_1$$

and

$$R_{33} = k^2 + \alpha_1 + \alpha_2 B_o^2$$

The dispersion relations for the two modes may be obtained in the usual way by setting the determinant of the matrix in Equation (6.35) equal to zero. The ordinary mode, which has an electric field component along the magnetic field is given by $R_{33}=0$

and is independent of J_o. The ordinary mode is therefore not affected by the presence of constant currents. Substituting for the coefficients in R_{33}, the dispersion relation for this mode may be shown to reduce to the usual expression given by

$$k_o^2 = \frac{\omega^2}{c^2}\left(1 - \frac{\omega_e^2}{\omega^2}\right) \tag{6.36}$$

The extraordinary mode for which the electric field components are in the transverse plane is, however, modified by the presence of constant currents. The dispersion relation for this mode is given by

$$k^2 + J_o B_o k\left(-\alpha_4 + \alpha_7 + \frac{\alpha_3\alpha_5}{\alpha_1} B_o^2 - \frac{\alpha_3\alpha_8}{\alpha_1}\right) + \left(\alpha_1 + \frac{\alpha_3^2 B_o^2}{\alpha_1}\right) = 0 \tag{6.37}$$

For $J_o = 0$, the second term in the above equation vanishes, and the last term may be shown to give the propagation constant k_x for the extraordinary mode in an unperturbed plasma (no currents). Equation (6.37) may thus be written conveniently in the form

$$k^2 + (jP)\, k - k_x^2 = 0 \tag{6.38}$$

Where P and k_x^2 may be shown to be given by

$$P = \frac{\omega^2}{c^2}\left(\frac{J_o B_o}{\rho_o}\right)\left\{\left(\frac{x}{\omega^2} - \frac{1}{\omega_i^2}\right) + \frac{1}{(D_1 + x)}\left(\frac{x}{\omega_i^2} - \frac{\Omega_e^2}{\omega^4}\right)\right\} \tag{6.39}$$

$$k_x^2 = \frac{\omega^2}{c^2} + \frac{\omega^2}{c^2} x / D_1 - \frac{\omega^2}{c^2}\left(\frac{\omega^2\Omega_i^2}{\omega_i^4}\right) \Big/ [D_1(D_1 + x)] \tag{6.40}$$

The denominator D_1 in Equations (6.39) and (6.40) is now given by

$$D_1 = x^2 - \frac{\omega^2 \Omega_i^2}{\omega_i^4} \quad \text{and} \quad x = \left(\frac{\Omega_i^2}{\omega_i^2} - \frac{\omega^2}{\omega_e^2} \right) \tag{6.41}$$

The dispersion Equation (6.38) is a quadratic equation in k, in which the coefficient of the first power of k is imaginary. This term, which arises only due to the presence of J_o, indicates wave characteristics which do not exist in unperturbed plasmas. The solution of this equation may be written as

$$k = -\frac{jP}{2} \pm \frac{1}{2} \left(4 k_x^2 - P^2\right)^{1/2} \tag{6.42}$$

Equation (6.42) indicates that k has an imaginary part which may be negative or positive depending upon whether J_o is positive or negative; k becomes completely imaginary if

$$| P | \geq 2 \quad | k_x | \tag{6.43}$$

The existence of a positive imaginary part of the propagation constant indicates evanescence or amplification of the wave. A positive imaginary part of k occurs for negative values of J_o. Which of the two processes actually does take place in a given situation may be determined on the basis of the instability criteria discussed in Section (6.6).

To find the conditions under which evanescence or instability is indicated, we solve Equation (6.38) for frequency. For this, we first simplify

the expression for P for the special case when the wave frequency is less than or of the order of the ion cyclotron frequency. For this case the expressions for P and k_x given by Equation (6.39) and Equation (6.40) are very much simplified and may be approximated by

$$P \simeq \frac{J_o B_o}{\rho_o V_a^2} \tag{6.44}$$

$$k_x \simeq \frac{\omega}{V_a} \tag{6.45}$$

where V_a is the Alfvén velocity. For frequencies less than or of the order of the ion-cyclotron frequency, Equation (6.38) can then be written as

$$k^2 + \left(j \frac{J_o B_o}{\rho_o V_a^2} \right) k - \frac{\omega^2}{V_a^2} = 0 \tag{6.46}$$

Equation (6.46) may now be easily solved for ω to give

$$\omega = \omega_r \pm j\omega_i \tag{6.47}$$

where

$$\omega_r = |\omega| \cos\theta$$

$$\omega_i = |\omega| \sin\theta$$

$$|\omega| = k V_a \left(1 + \frac{P^2}{k^2}\right)^{1/4}$$

$$\theta = 1/2 \tan^{-1} \left(\frac{P}{k} \right)$$

Since time variations of the form $e^{j\omega t}$ have been assumed, a negative imaginary part of ω indicates an instability. The real part ω_r of the frequency gives the amplified or excited frequency, and the imaginary part ω_i indicates the growth rate of the wave.

The solution of the dispersion equation for real values of ω indicates a positive imaginary part of k for negative values of J_o. As shown above, these currents also give complex roots with respect to frequency for real values of k. Thus, as may be seen from the criteria discussed in Section (6.4) these roots correspond to a convective instability and the wave propagates as it grows.

The case discussed above is applicable to the propagation conditions in the equatorial regions of the ionosphere and the magnetosphere. Hydromagnetic waves propagating transverse to the magnetic field may thus be excited and amplified in regions where currents exist which are transverse to both the magnetic field and the direction of propagation.

6.7 Case (2): Longitudinal Propagation, Transverse Currents

We assume that the magnetic field and the direction of propagation are along the z-axis, so that

$$\bar{B}_o = (0, 0, B_o) \text{ and } \bar{k} = (0, 0, k)$$

In this case of longitudinal propagation, we assume that $\bar{J}_o$ is in the transverse plane so that

$$\bar{J}_o = (J_{ox}, J_{oy}, 0)$$

With the above restrictions we have

$$(\bar{J}_o \cdot \bar{k}) = 0 \text{ and } (\bar{J}_o \cdot \bar{B}_o) = 0$$

Equation (6.28) can thus be written as

$$\begin{bmatrix} k^2 + \alpha_1 & \alpha_3 B_o & 0 \\ -\alpha_3 B_o & k_2 + \alpha_1 & 0 \\ J_{ox} k(\alpha_6 B_o^2 + \alpha_8) & J_{oy} k(\alpha_6 B_o^2 + \alpha_8) & (\alpha_1 + \alpha_2 B_o^2) \end{bmatrix} \begin{bmatrix} E_x \\ E_y \\ E_z \end{bmatrix} = 0 \qquad (6.48)$$

Since $(\bar{J}_o \cdot \bar{k}) = 0$, the coefficients α_1 to α_8 are now independent of $\bar{J}_o$ and k, and α_1 to α_3 are the same as for the plasma without constant currents. It may be seen by setting the determinant of the matrix in Equation (6.48) equal to zero, that the propagation constant for the two transverse waves turns out to be the same as for the two circularly polarized waves in a plasma without constant currents, and is given by (see for expl. Bostick, 1964)

$$k^2 = \frac{\omega^2}{c^2} \mp \frac{\frac{\omega^2}{c^2} \frac{\Omega_e}{\omega} \omega_e^2}{\left[\Omega_e^2 - \omega^2 \left(1 - \frac{\Omega_i \Omega_e}{\omega^2}\right)^2\right]} + \frac{\frac{\omega^2}{c^2} \omega_e^2 \left(1 - \frac{\Omega_i \Omega_e}{\omega^2}\right)}{\left[\Omega_e^2 - \omega^2 \left(1 - \frac{\Omega_i \Omega_e}{\omega^2}\right)^2\right]} \qquad (6.49)$$

The propagation constant thus remains unaffected by the introduction of

a current density $\bar{J}_o$ in the transverse plane. It is interesting to note from Equation (6.48), however, that an electric field component along the direction of the static magnetic field has now been introduced which vanishes in the absence of $\bar{J}_o$. This introduction of an electric field component along the wave normal causes a change in the direction of the ray path. In the absence of $\bar{J}_o$ the ray path is along the direction of the wave normal. With the presence of transverse currents, the direction of ray path deviates from the direction of the wave normal, and the wave is continuously refracted as it propagates through transverse current sheets.

6.8 Case (3): Longitudinal Propagation, Longitudinal Currents.

In this case of longitudinal propagation we assume that the magnetic field, propagation vector and the constant currents are all along the same direction. Thus we set:

$$\bar{B}_o = (0, 0, B_o) \quad , \quad \bar{k} = (0, 0, k)$$

and $\bar{J}_o = (0, 0, J_o)$

Equation (6.28) then reduces to

$$\begin{bmatrix} R_{11} & R_{12} & 0 \\ R_{21} & R_{22} & 0 \\ 0 & 0 & R_{33} \end{bmatrix} \begin{bmatrix} E_x \\ E_y \\ E_z \end{bmatrix} = 0 \qquad (6.50)$$

where

$$R_{11} = R_{22} = k^2 + \alpha_1 + J_o k (\alpha_5 B_o^2 - \alpha_8)$$

$$R_{12} = -R_{21} = \alpha_3 B_o + J_o B_o k(\alpha_4 - \alpha_7)$$

and $$R_{33} = \alpha_1 + \alpha_2 B_o^2$$

As seen from the symmetry of the coefficients in the above equations, the two transverse waves in this case may be decoupled into circularly polarized waves by substituting in Equation (6.50).

$$E_{\pm} = E_x \pm j E_y$$

Substituting for the coefficients α's from Equations (6.27) we obtain, after some algebra and simplifications, the dispersion relations for the two polarizations as:

$$k^2 - \frac{\omega^2}{c^2} - \frac{\omega^2}{c^2}\left\{ \pm \frac{\omega\Omega_i}{\omega_i^2} + \left[\left(\frac{\Omega_i^2}{\omega_i^2} - \frac{\omega^2}{\omega_e^2}\right) + y\left(y - \frac{\omega}{\omega_i}\right)\right]\left[1 \pm \frac{\Omega_e \omega y}{\omega^2} - \frac{\omega_e^2}{\omega\omega_i} y \left(\frac{\omega_i}{\omega} y - 1\right)\right]\right.$$

$$\left. + y\left(\frac{2\omega_i}{\omega} y - 1\right)\left[\frac{\Omega_e \Omega_i}{\omega\omega_i} \pm \frac{\Omega_e}{\omega}\left(\frac{\omega_i}{\omega} y - 1\right)\right]\right\} / D_2 = 0 \qquad (6.51)$$

where the denominator D_2 is given by

$$D_2 = \left[\left(\frac{\Omega_i^2}{\omega_i^2} - \frac{\omega^2}{\omega_e^2}\right) + y\left(y - \frac{\omega}{\omega_i}\right)\right]^2 - \frac{\omega^2\Omega_i^2}{\omega_i^4}\left[\frac{2\omega_i}{\omega} y - 1\right]^2 \qquad (6.52)$$

The dimensionless parameter y in the above equations has been defined as $y = \frac{J_o k}{\omega_{e,i}^2 (\rho_o \epsilon_o)^{\frac{1}{2}}}$; $\omega_{e,i}$ are the electron and ion plasma frequencies and $\Omega_{e,i}$ are the electron and ion cyclotron frequencies. The upper sign in the bracket in Equation (6.51) applies to the left hand polarized waves and the lower sign to the right hand polarized waves.

It may be noticed that in the absence of constant currents, Equation (6.51) reduces to the usual dispersion relation for the two circularly polarized waves given by Equation (6.49).

6.8.1 Roots of the denominator D_2

The presence of constant currents in the plasma will have drastic effects in the neighborhood of frequencies or for currents such that the denominator of the dispersion Equation (6.51) becomes very small. The frequencies or currents at which the denominator vanishes may be determined by obtaining the roots of the denominator D_2 which may be rewritten by defining

$$\alpha = \frac{\omega}{\omega_i} \quad , \quad \beta = \frac{\Omega_i}{\omega_i} \quad , \quad \epsilon = \frac{m_e}{m_i}$$

$$D_2 = \left[(\beta^2 - \epsilon\alpha^2) + y(y-\alpha)\right]^2 - \alpha^2\beta^2 \left[\frac{2y}{\alpha} - 1\right]^2 \qquad (6.53)$$

The four roots of Equation (6.53) with respect to α, at which the denominator of the dispersion equation vanishes, are approximated by

$$\alpha_1 = (y+\beta) \quad , \quad \alpha_2 = (y-\beta)$$

$$\alpha_3 = -\frac{1}{\epsilon}(y+\beta) \quad , \quad \alpha_4 = -\frac{1}{\epsilon}(y-\beta) \qquad (6.54)$$

In the absence of constant currents, when $y = 0$, these four roots reduce to $\pm \Omega_i$ and $\pm \Omega_e$ corresponding to ion and electron cyclotron resonances which may be seen from Equation (6.49). In the presence of currents, these roots are modified in accordance with Equations (6.54).

Conversely, the values of constant currents at some particular frequency, such that the denominator becomes very small may be obtained by solving for the roots of Equation (6.53) with respect to y. The four roots of (6.53) may be shown to be approximated by

$$y \simeq \pm \beta$$

$$y \simeq (\alpha \pm \beta) \qquad (6.55)$$

As may be seen from Equations (6.54) or (6.55), the roots of the denominator are modified significantly for the current densities and plasma parameters for which $y \sim \beta$. For hydromagnetic waves in the ionosphere and the magnetosphere, this occurs only for relatively large values of currents.

For current densities which may be normally expected in the ionosphere and the magnetosphere, y is small as compared to β ($\beta \ll 1$). In Section (6.8.2) y is assumed to be less than β. The assumption $y \ll \beta$ has been made in the derivation of approximate results in Sections (6.8.3) and (6.8.4).

6.8.2 Numerical Solution of the Dispersion Equation

The dispersion Equation (6.51) is rather involved in the general form. If the constant current density J_o is assumed to be relatively small, such that $y < \beta$ for $\beta \ll 1$, and α is less than or of the order

of 1, the dispersion equation for longitudinal propagation and currents may be written as a fourth order algebraic equation in k

$$a_4 k^4 + a_3 k^3 + a_2 k^2 + a_1 k + a_o = 0 \tag{6.56}$$

where

$$a_4 = z^2(\alpha^2 - 2\beta^2) - x_4 z^4(\alpha^2 - \frac{1}{\epsilon})$$

$$a_3 = 2\alpha z(\beta^2 + \epsilon\alpha^2) + x_4 z^3 (2\alpha^3 - \frac{2\alpha}{\epsilon} \mp \frac{2x_3}{\alpha} \mp x_1)$$

$$a_2 = [(\beta^2 - \epsilon\alpha^2)^2 - \alpha^2\beta^2] - x_4 z^2 [\alpha^4 + \alpha^2(2 - \frac{1}{\epsilon}) \mp \alpha x_1 + (2x_2 \pm 3x_3 - \frac{\beta^2}{\epsilon})]$$

$$a_1 = -x_4 z[-2\alpha^3 + \alpha^2(\mp \epsilon x_1) + \alpha(-x_2 \mp x_3 + \frac{\beta^2}{\epsilon}) \pm (x_1\beta^2)]$$

$$a_o = -x_4\alpha^2[(\beta^2 - \epsilon\alpha^2)^2 - \alpha^2\beta^2 \pm \alpha\beta + \beta^2 - \epsilon\alpha^2]$$

In the above coefficients the upper and lower signs refer to the left and right hand polarized waves respectively. The constants x and z have been defined as

$$x_1 = \frac{\Omega_e \omega_e}{\omega_i^2} \qquad x_2 = \frac{\Omega_e \Omega_i}{\omega_i^2} \qquad x_3 = \frac{\Omega_e}{\omega_i}$$

$$x_4 = \frac{\omega_i^2}{c^2} \qquad z = \frac{J_o}{\omega_e^2 (\rho_o \epsilon_o)^{\frac{1}{2}}} = \frac{y}{k} \tag{6.57}$$

Equation (6.56) has four roots for k corresponding to four waves; two for each direction of propagation. It is expected, however, that the two additional waves will be significant only for relatively stronger currents. For extremely small values of J_o, the two original waves are only expected to be modified due to the existence of currents. Equation (6.56) will be solved numerically for data corresponding to the ionosphere and the magnetosphere. The numerical results are given in Section (6.8.5).

To investigate the existence of any instabilities due to the presence of currents, the dispersion equation has to be solved for the frequency. Assuming frequencies less than or of the order of the ion-cyclotron frequency, such that $\epsilon\omega^2 \ll \Omega_i^2$, Equation (6.51) may also be written as a fourth order algebraic equation in frequency. Thus, assuming $\epsilon\omega^2 \ll \Omega_i^2$, and letting $X = \frac{\omega}{\Omega_i}$, where Ω_i is the ion cyclotron frequency, the dispersion relation (6.51) may be written as

$$A_4 X^4 + A_3 X^3 + A_2 X^2 + A_1 X + A_o = 0 \qquad (6.58)$$

where

$$A_4 = \beta^4 x_4 \ (\pm \beta - 2y)$$

$$A_3 = \beta^3 \left[x_4(\beta^2 + 2y^2 - \frac{y^2}{\epsilon}) - k^2(y^2 - \beta^2) \right]$$

$$A_2 = \beta^2 \left[x_4 \left(\frac{\beta^2 y}{\epsilon} + \frac{2y^3}{\epsilon} - x_2 y \mp (x_1 y^2 + x_3 y) \right) - k^2(2y\beta^2 - 2y^3) \right]$$

$$A_1 = \beta \left[x_4 \left(2x_2 y^2 - \frac{\beta^2 y^2}{\epsilon} - \frac{y^4}{\epsilon} \pm (x_1 \beta^2 y \pm x_1 y^3 + 3x_3 y^2) \right) - k^2(\beta^2 - y^2)^2 \right]$$

$$A_o = x_4 \ (\mp 2x_3 y^3)$$

To investigate any instabilities introduced due to the presence of currents, Equation (6.58) will be solved numerically for data corresponding to the ionosphere and the magnetosphere. The existence of any complex roots of the above equation will indicate an instability. The real part of X, denoted as $R_e(X)$, will indicate the excited or amplified frequencies and the imaginary part of X, denoted as Im (X), will indicate the growth rates. The type of instability is then decided on the basis of the criteria discussed in Section (6.4).

6.8.3 Approximate Solution for the Propagation Constant

The general fourth order equation in k may be reduced to a quadratic equation for extremely small currents such that the terms involving all powers of z (or of J_o) except the first are vanishingly small, and the frequencies are less than or of the order of ion cyclotron frequencies. With this approximation, the dispersion equation may be written as:

$$k^2 + a_1 k + a_o = 0 \qquad (6.59)$$

where the coefficients are now given by

$$a_1 = \frac{x_4 x (\pm \alpha x_3 \mp x_2 \beta^2)}{\beta^2(\beta^2 - \alpha^2)}$$

$$a_o = \frac{-k_o^2 (\beta \pm \alpha)}{\beta (\beta^2 - \alpha^2)}$$

The upper and lower signs in the brackets apply to the left and right hand polarized waves; k_o is the propagation constant for free space. The two solutions for k may be explicitly written as

$$k = \frac{1}{2(\beta^2-\alpha^2)}\left\{x_4 z(\pm x_1\beta^2 \mp \alpha x_3) \pm \left[x_4^2 z^2(\mp x_1\beta^2 \pm \alpha x_3)^2 + 4k_o^2\beta^3(\beta\pm\alpha)(\beta^2-\alpha^2)\right]^{\frac{1}{2}}\right\} \tag{6.60}$$

For very small current densities, and frequencies of the order of the ion-cyclotron frequency or less, the above formula gives results approximating those obtained numerically from the general fourth order equation. As may be seen, the propagation constant now has a resonance at ion-cyclotron frequency ($\alpha=\beta$) for both left and right hand polarized waves. In the absence of currents, this resonance occurs only for the left hand polarized wave.

It may be noted that Equation (6.60) gives real values of propagation constant for the right hand polarized wave for both positive and negative values of currents. For the left hand polarized wave, the propagation constant is also real for frequencies less than the ion-cyclotron frequency. On the basis of the criteria discussed in Section (6.4), any instability for such currents, indicated by the complex roots for frequency, must then be nonconvective. This conclusion is confirmed by the numerical results obtained from the general fourth order equation, as well as the configuration of the ω/k plots in the real ω and real k plane.

6.8.4 Approximate Solution for Frequency

To investigate the existence of instabilities due to the presence of currents in the system, we solve the dispersion equation for frequency. The dispersion equation in the general form, as given by Equation (6.58), is a fourth order algebraic equation. For very small current densities, such that $y \ll \beta$, retaining terms containing only the first power of y, the

dispersion equation may be reduced to a cubic equation in frequency which may be written in the form:

$$X^3 + a_2X^2 + a_1X + a_o = 0 \qquad (6.61)$$

where the coefficients are now given by

$$a_2 \simeq \pm \frac{1}{x_4} \left(k^2 + x_4\right)$$

$$a_1 \simeq - \left(\frac{x_3 y}{\beta^3} \right)$$

$$a_o \simeq \left(\frac{x_1 y}{\beta^2} \mp \frac{k^2}{x_4} \right)$$

The upper and the lower signs in the above coefficients apply to the left and right hand polarized waves respectively.

The cubic Equation (6.61) may be solved in the usual way by putting it in the "reduced" form by the transformation

$$X = Y - \frac{a_2}{3}$$

which gives

$$Y^3 + p\,Y + q = 0 \qquad (6.62)$$

where the coefficients p and q are now given by

$$p = a_1 - \frac{a_2^2}{3} \qquad (6.63)$$

$$q = a_o - \frac{a_1 a_2}{3} + \frac{2a_2^3}{27} \qquad (6.64)$$

The three solutions of the cubic equation are given by

$$Y_1 = A+B \text{ and } Y_{2,3} = -\frac{1}{2}(A+B) \pm j\frac{\sqrt{3}}{2}(A-B) \tag{6.65}$$

where

$$A = \left[-\frac{q}{2} + \sqrt{R}\right]^{1/3}, \qquad B = \left[-\frac{q}{2} - \sqrt{R}\right]^{1/3}$$

$$R = \left(\frac{p}{3}\right)^3 + \left(\frac{q}{2}\right)^2 \tag{6.66}$$

The three solutions of the original Equation (6.61) are then given by

$$X_1 = Y_1 - \frac{a_2}{3}, \quad X_2 = Y_2 - \frac{a_2}{3}, \quad X_3 = Y_3 - \frac{a_2}{3}$$

The existence of any complex roots of the cubic equation may be ascertained without solving for the roots by making use of the following theorem: A cubic equation with real coefficients has either three distinct real roots, a single real and two complex conjugate roots, or three real roots of which at least two are identical, depending upon whether its discriminant is positive, negative, or zero. The discriminant for the cubic equation is given by

$$\Delta = -108\,R = -4\,p^3 - 27\,q^2 \tag{6.67}$$

Complex roots with respect to frequency exist if the discriminant $\Delta < 0$, or if

$$p > \left(-\frac{27}{4}\,q^2\right)^{1/3} \tag{6.68}$$

The currents and real values of propagation constants for which the above inequality is satisfied will give rise to instabilities in the medium. Since the propagation constants for small values of currents and

real frequencies were found to be real in Section (6.8.3), any complex roots, if they exist, must correspond to a nonconvective instability.

6.8.5 Numerical Results

Numerical results have been obtained by solving the fourth order equations for propagation constant and frequency for two different sets of data. In the first case, representative of the conditions in the upper ionosphere, data corresponding to a height of 500 km was used. In the second case, representative of the conditions in the magnetosphere, data corresponding to a height of 50,000 km (below the magnetospheric boundary) was used.

The Figures (6.4 - 6.7) show the plots of frequency (f) versus refractive index (n) for the right hand polarized wave for 500 km data for various values of current density. The plot for zero current density is shown in Figure (6.4). The refractive index for the right hand polarized wave decreases monotonically with frequency over the frequency range shown and has no resonance at the ion-cyclotron frequency.

With the presence of currents, the f-n plots are modified as illustrated in Figures (6.5-6.7). It may be seen that the right hand polarized wave now has a resonance at the ion-cyclotron frequency as is indicated by the approximate solution for propagation constant given by Equation (6.60). The plots for various values of currents show significant modifications at frequencies much below and in the neighborhood of the ion-cyclotron frequency. Over the frequency range shown, the refractive index, however, is real at all frequencies. It may be seen from the configuration of the f-n plots that the frequencies at which the refractive index is most affected correspond to a nonconvective instability. This is verified by solving for

the roots of dispersion equation with respect to frequency or the fourth order equation in frequency (6.58). For certain current densities and real values of propagation constants, this equation gives complex roots with respect to frequency indicating the existence of an instability. Since the refractive index is real over the entire frequency range shown, this instability must be nonconvective. The real part of the complex root for frequency, denoted by Re(x), gives the excited or amplified frequency; the imaginary part of frequency, denoted by Im(x) gives the growth rate.

The complex roots of the dispersion equation with respect to frequency, for the right hand polarized wave for 500 km data, are illustrated in Figures (6.8-6.9) for various current densities. It may be noted, that for the right hand polarized wave, the complex roots appear only for negative values of currents (opposite to the direction of propagation). For positive currents, the roots of the dispersion equation with respect to frequency are all real and there is no instability.

The f-n plots and the complex roots of the dispersion equation with respect to frequency, for the left hand polarized wave for 500 km data are shown in Figures (6.10-6.13). In the absence of currents, the left hand polarized wave has a resonance at the ion-cyclotron as shown in Figure (6.10). With the presence of currents the f-n plots are modified as shown in Figures (6.11-6.12). For the left hand polarized wave, the complex roots of the dispersion equation with respect to frequency for real k, appear only for positive values of J_o and are shown in Figure (6.13). For negative current densities, the dispersion equation has only real roots and there is no instability.

The curves for data corresponding to a height of 50,000 km in the magnetosphere, for the right hand polarized wave, are shown in Figures (6.14-6.19). With the presence of currents, as before, an instability occurs in the neighborhood of the ion-cyclotron frequency. It may be noticed, that for the 50,000 km height data, the current densities which may give rise to complex roots with respect to frequency, producing an instability, are much smaller than for lower altitudes. This is consistent with the results predicted by the charged particle beam analysis, which indicates excitation of hydromagnetic waves for lower beam velocities at higher altitudes (Neufeld and Wright, 1963).

As seen from the solution of the denominator of the dispersion equation, the existence of currents has drastic effects for current densities for which the parameter $y = \frac{J_o k}{\omega_e^2 (\rho_o \epsilon_o)^{\frac{1}{2}}}$ is of the order of $\beta = \frac{\Omega_i}{\omega_i}$. With increasing altitudes, the quantity β gets smaller due to the rapidly decreasing magnetic field. The parameter y thus approaches β for smaller current densities at higher altitudes.

The numerical results presented for longitudinal propagation for two different altitudes and for various current densities indicate excitation and amplification of hydromagnetic waves in the neighborhood of the local (average ion) ion-cyclotron frequency. The ion-cyclotron frequency varies from an order of 40 c/s in the upper ionosphere to about 1 c/s in the upper parts of the magnetosphere. Hydromagnetic waves in this frequency range may thus be excited in the various parts of the ionosphere and magnetosphere due to the presence of longitudinal components of current densities. This excitation arises from the existence of a nonconvective instability produced by the currents. The waves excited by this process may be propagated to the earth.

VII. SUMMARY AND CONCLUSIONS

Hydromagnetic waves which are generated in various regions of the magnetosphere through a variety of mechanisms and are propagated to the earth in the extremely low frequency spectrum, were investigated. Basically, two different aspects of the problem were studied:

(1) Propagation through inhomogeneous regions of the ionosphere at frequencies close to the resonant frequency of the earth-ionosphere cavity.

(2) Propagation through current carrying regions of the ionosphere and the magnetosphere, and the resulting instabilities and amplifying processes.

For propagation through inhomogeneous media, two different methods were employed. In the first method, a relatively simple approach was used by assuming that the square of the propagation constant k in the inhomogeneous medium is linearly varying with distance. Power transmission coefficients for the transition from hydromagnetic waves in a homogeneous plasma to electromagnetic waves in vacuum through an inhomogeneous transition were obtained. This model provides relatively simple expressions for the transmission coefficients.

The second method for the study of wave propagation through an inhomogeneous ionosphere involved an application of "Epstein's theory". The theory is based upon transformation of the wave equation into a hypergeometric differential equation. By using various transformation equations and by making a proper choice of the constants involved, it is possible to study a wide range of index of refraction profiles. The ionosphere was assumed to be described by the macroscopic equations for a partially

ionized inhomogeneous plasma embedded in the earth's magnetic field. Considering a hydromagnetic wave incident from above and propagating parallel to the earth's magnetic field at a frequency close to the resonant frequency of the earth-ionosphere cavity, power transmission coefficients were calculated. Complex refractive index profiles were used in these calculations which approximate those which are obtained from the dispersion relations and published ionospheric data. The transmission coefficients calculated for various times of day indicated maximum transmission at about local midnight and minimum transmission at about local noon.

Hydromagnetic waves are generated and amplified in various parts of the magnetosphere by a variety of single particle and instability processes. These processes were examined in particular for frequencies close to the resonant frequency of the earth-ionosphere cavity. Waves generated by any of the various processes may be propagated to the earth along the earth's magnetic field lines. Earth-ionosphere cavity resonances could thus be excited through these waves in high latitude regions. The angle of incidence of the waves for excitation of the cavity has to deviate, however, at least slightly from the radial direction. The field distribution in the first resonant mode of the cavity due to excitation by hydromagnetic waves may thus be expected to produce higher electric field intensities in the mid to high latitude regions than in the equatorial or polar regions. Lower electric field intensities will be expected in the equatorial regions due to the lower intensity of the incident waves. The generally accepted source of excitation, namely the worldwide thunderstorm activity, does not clearly explain some of the experimentally established characteristics of ELF electromagnetic noise in the cavity. Excitation of

the cavity by thunderstorm activity in the first resonant mode, should produce higher electric fields in the equatorial regions and lower intensities in the higher latitude regions. Simultaneous measurements at different latitudes may shed some light on this problem.

Following an analysis based on macroscopic equations, propagation of hydromagnetic waves through a current carrying plasma was investigated. The macroscopic equations involving additional terms due to the existence of a constant current density, were derived from the basic plasma equations in which streaming velocities for both electron and ion fluids were allowed. Assuming a homogeneous medium, a general dispersion relation for small amplitude waves was derived from these equations. Simplified forms of this dispersion relation were investigated by considering three special cases:

(1) Transverse propagation, with constant currents also transverse to both the direction of propagation and the static magnetic field.

(2) Longitudinal propagation, with constant currents transverse to the direction of propagation.

(3) Longitudinal propagation, with constant currents also along the direction of propagation.

For transverse propagation when the currents are also transverse to the direction of propagation and the static magnetic field, the waves were found to be amplifying. The dispersion relation admits complex solutions with respect to both the propagation constant and the frequency (for real values of frequency and propagation constant respectively). A convective instability was found to result from the existence of these currents. Approximate solutions for the propagation constant and the complex frequency were obtained.

For longitudinal propagation with transverse currents the propagation constant was found to remain unaffected by the existence of currents. It was found, however, that a component of electric field is now introduced along the wave normal which has the effect of changing the direction of the ray path.

For longitudinal propagation with currents also along the same direction, it was found that the propagation constant now has a resonance at the ion-cyclotron frequency for both right and left hand polarized waves. A nonconvective instability was found to exist in the neighborhood of this frequency for certain values of currents. Numerical results were obtained for data corresponding to heights of 500 km and 50,000 km, representative respectively of the conditions in the ionosphere and the magnetosphere. Existence of currents in the various parts of the ionosphere and the magnetosphere may have significant effects at frequencies much below and in the neighborhood of the ion-cyclotron frequencies. Hydromagnetic waves in the frequency range of 1-40 c/s may be excited due to currents along the static magnetic field in the various parts of the ionosphere and the magnetosphere.

APPENDIX

The "conductivities" σ_{11} and σ_{21} appearing in the dispersion relations (3.27) are defined by the following equation (Bostick et al., 1964).

$$\sigma_{11} = \frac{\epsilon_o \omega_e^2 \left[\nu_3 + j\omega\left(1 - \frac{\Omega_e \Omega_i}{\omega^2}\right) L \right]}{\left[\nu_3 + j\omega\left(1 - \frac{\Omega_e \Omega_i}{\omega^2}\right) L\right]^2 + [\Omega_e + M]^2}$$

$$\sigma_{21} = \frac{\epsilon_o \omega_e^2 [\Omega_e + M]}{\text{Denominator of } \sigma_{11}}$$

where

$$L = \frac{\left[\left(\frac{n}{n_n}\right)\left(\frac{\nu_2}{\omega}\right)^2 - \left(\frac{\nu_1}{\Omega_e}\right)^2 \right] \left(1 + \frac{n}{n_n}\right)}{XE} + \frac{j\left(\frac{\nu_2}{\omega}\right)\left[1 - \left(\frac{\nu_1}{\Omega_e}\right)^2 \left(1 + \frac{n}{n_n}\right)^2\right]}{XE}$$

$$M = -\frac{2\Omega_i \frac{\nu_1 \nu_2}{\omega^2} \left(1 + \frac{n}{n_n}\right) + j2\Omega_i \left(\frac{\nu_1}{\omega}\right)}{XE}$$

$$P = \frac{M}{2} \left(\frac{\nu_1}{\Omega_e}\right) \left(1 + \frac{n}{n_n}\right)$$

$$XE = 1 + \left(\frac{\nu_2}{\omega}\right)^2 \left(1 + \frac{n}{n_n}\right)^2$$

The frequencies ν_1, ν_2, and ν_3 are the linear combination of interparticle collision frequencies, and are given by

$$\nu_1 = \nu_{en} - \frac{\nu_{in}}{2}$$

$$\nu_2 = \frac{\nu_{in}}{2} + \frac{m_e}{m_i}\ \nu_{en}$$

$$\nu_3 = \nu_{ei} + \nu_{en} + \frac{m_e}{m_i}\ \frac{\nu_{in}}{2}$$

The various symbols appearing in the above equations are defined as follows:

ω = frequency in radians

$$\omega_e^2 = \frac{ne^2}{m_e \epsilon_o}$$

$$\Omega_{e,i} = \frac{eB_o}{m_{e,i}}$$

ν_{en} = electron-neutral collision frequency

ν_{ei} = electron-ion collision frequency

ν_{in} = ion-neutral collision frequency

n = electron or ion density

n_n = neutral particle density

μ_o = permeability of vacuum

ϵ_o = permittivity of vacuum

e = electron charge

$m_{e,i}$ = electron or ion mass

B_o = earth's magnetic field intensity

The interparticle collision frequencies are calculated by using the following formulas:

$$\nu_{en} = (5.4 \times 10^{-16})\ n_n\ T^{\frac{1}{2}}$$

$$\nu_{in} = (2.6 \times 10^{-15})\ \frac{(n+n_n)}{W^{\frac{1}{2}}}$$

$$\nu_{ei} = (34.0 + 4.18 \log_{10} \frac{T^3}{n \times 10^{-6}}) \frac{n \times 10^{-6}}{T^{3/2}}$$

where

T = Temperature in ^{o}Kelvin

W = ion or neutral particle molecular weight

The earth's magnetic field is calculated by using the formula

$$|\vec{B}_o| = \frac{M}{(z+R)^3} \sqrt{1 + 3\cos^2 \phi}$$

where

M = magnetic moment of the earth (8.06×10^6 Weber-m)

R = earth's radius in km

z = altitude above the earth in km

ϕ = magnetic colatitude

REFERENCES

Aarons, J., and M. Henissart, Low-frequency noise in the range .5-20 c/s, Nature, 172, 682-683, 1953.

Akasofu, Syun-Ichi, Attenuation of hydromagnetic waves in the ionosphere, J. Res., NBS 69 D, No. 3, 361-366, 1965.

Abramowitz, M., and I. A. Stegun, (Ed.) Handbook of Mathematical Functions, National Bureau of Standards, 1964.

Alfvén, H., and L. Danielsson, C-G. Fälthammer and L. Lindberg, On the penetration of interplanetary plasma into the magnetosphere, in Natural Electromagnetic Phenomena Below 30 kc/s, 33-48, Plenum Press, New York, 1964.

Balser, M., and C. A. Wagner, Diurnal power variations of the earth-ionosphere cavity modes and their relationship to worldwide thunderstorm activity, J. Geophys. Res. 67, No. 2, 619-625, 1962.

Balser, M. and C. A. Wagner, Thunderstorm excitation of the earth-ionosphere cavity, in Propagation of Radio Waves at Frequencies Below 300 kc/s, Ed. W. T. Blackband, Pergamon Press, 1964.

Bell, T. F., and O. Buneman, Plasma instability in the whistler mode caused by a gyrating electron stream, Phys. Rev., 133 (5A), A1300-A1302, 1964.

Booker, H. G., Guidance of radio and hydromagnetic waves in the magnetosphere, J. Geophys. Res., 67, 4135-4162, 1962.

Bostick, F.X., and C. E. Prince, Jr., and H. W. Smith, Propagation characteristics of small amplitude hydromagnetic disturbances in the earth's upper

atmosphere, Electrical Engineering Res. Lab., University of Texas, Report No. 135, 1964.

Brice, N., Fundamentals of very low frequency emission mechanisms, J. Geophy. Res. 69 (21), 4515-4522, 1964.

Budden, K. G., Radio waves in the ionosphere, Cambridge University Press, 1961.

Burman, R., and R. N. Gould, The reflection of waves in a generalized Epstein profile, Can. J. Phys., 43, 921-934, May 1965.

Cornwall, J. M., Cyclotron instabilities and electromagnetic emission in the ultra low frequency and very low frequency ranges, J. Geophys. Res., 70 (1), 61-69, 1965.

Dewitt, R. N. and S. I. Akasofu, Dynamo action in the ionosphere and motions of the magnetospheric plasma, Planet. Space. Sci., 12, 1147-1156, 1964.

Dowden, R. L., Theory of generation of exospheric very low frequency noise (hiss), J. Geophys. Res. 67 (6), 2223-2230, 1962.

Dowden, R. L., Doppler-shifted cyclotron radiation from electrons: A theory of very low frequency emissions from the exosphere, J. Geophys. Res. 67 (5), 1745-1750, 1962.

Dungey, J. W., The propagation of Alfvén waves through the ionosphere, Ionosph. Res. Lab. Sci. Rept. No. 57, Penn. State Univ., 1954.

Epstein, P.S., Reflection of waves in an inhomogeneous absorbing medium, Proc. Nat. Acad. Sci., Wash., 16, 627-637, 1930.

Erdelyi, A., Higher transcendental functions, vol. 1, McGraw-Hill Book Co., New York, 1953.

Fejer, J. A., Hydromagnetic wave propagation in the ionosphere, J. Atmospheric Terrest. Phys., 18, 135-146, 1960.

Field, E.C., and C. Greifinger, The transmission of geomagnetic micropulsations through the ionosphere and lower exosphere, J. Geophys. Res., 70, 4885-4899, 1965.

Francis, W. E., and R. Karplus, Hydromagnetic waves in the ionosphere, J. Geophys. Res., 65, 3593-3600, 1960.

Galejs, J., On the terrestrial propagation of ELF and VLF waves in the presence of a radial magnetic field, Radio Sci., J. Res., NBS 69 D, No. 5, 705-720, 1965.

Galejs, J., Terrestrial extremely-low-frequency propagation, Proc. NATO Advanced Study Institute on Natural Electromagnetic Phenomena Below 30 kc/s, Bad Homburg, West Germany, 205-258, 1963, (Plenum Press, New York).

Galejs, J., Schumann resonances, J. Res., NBS 69 D, No. 8, 1043-1055, 1965.

Gendrin, R., and R. Stefant, Magnetic records between 0.2 and 30 c/s, AGARD Conference on Propagation of Radio Frequencies Below 300 kc/s, Munich, Germany, 1962.

Gendrin, R., Gyroresonance radiation produced by proton and electron beams in different regions of the magnetosphere, J. Geophys. Res., 70 (21), 5369-5383, 1965.

Goldberg, P., Electromagnetic phenomena of natural origin in the 1-150 c/s band. Nature, 177, No. 4522, 1219-20, 1956.

Greifinger, Carl and Phyllis Greifinger, Transmission of micropulsations through the lower ionosphere, J. Geophys. Res., 70, 2217-2332, 1965.

Haeff, A. V., On the origin of solar radio noise, Phys. Rev. 75, 1546-1551, 1949.

Handbook of Geophysics, USAF Air Research and Development Command, Airforce Cambridge Research Center, Macmillan Co., New York, New York, 1960.

Hines, C. O., Generalized magnetohydrodynamic formula, Proc. Cambridge Phil. Soc., 49, 229-307, 1953.

Holzer, R. F., and O. E. Deal, Low audio-frequency electromagnetic signals of natural origin, Nature, 177, 536-537, 1956.

Hultqvist, Bengt, On the amplification of ELF emissions by charged particles in the exosphere, with special reference to the frequency band around the proton cyclotron frequency, Planet. Space Sci., 13, 391-401, 1965.

Kahalas, S. L., Magneto-hydrodynamic wave propagation in the ionosphere, Phys. Fluids, 3, 372-378, 1960.

Karplus, R., W. E. Francis, and A. J. Dragt, The attenuation of hydromagnetic waves in the ionosphere, Planet. Space Sci. 9, 771-785, 1962.

Keefe, T. J., C. Polk, and H. L. König, Results of simultaneous ELF measurements at Brannenburg, Germany, and Kingston, R. I., ULF symposium, Boulder, Colorado, August 17-20, 1964.

Kleimenova, N. G., Present ideas regarding the nature of high-frequency variations in the electromagnetic field of the earth (1 cps-1 kcps), Bull. Acad. Sci. USSR, Geophys. No. 12, 1798-1813, A.G.U. Translation, No. 12, 1091-1100, 1963.

Lepechinsky, D., and P. Rolland, On plasma instabilities and their probable role in ionospheric phenomena, J. Atmospheric Terrest. Phys., 26 (1), 31-40, 1964.

MacArthur, J. W., Theory of the origin of the very low frequency radio emissions from the earth's exosphere, Phys. Rev. Letters, 2, 491-492, 1959.

Madden, T., and W. Thompson, Low-frequency electromagnetic oscillations of the earth-ionosphere cavity, Rev. Geophys., V3, No. 2, 211-254, 1965.

Maeda, K., and S. Kato, Electrodynamics of the ionosphere, Space, Sci. Rev., 5, 57-79, 1966.

McKenzie, J. F., Cerenkov radiation in a magnetoionic medium (with application to the generation of low-frequency electromagnetic radiation in the exosphere by the passage of charged corpuscular streams), Phil. Trans. Roy. Soc. London, A, 255, 585-606, July 11, 1963.

Murcray, W. B., and J. H. Pope, Energy fluxes from the cyclotron radiation model of the VLF radio emission, Proc. IRE, 49, 811-812, 1961.

Murcray, W. B. and J. H. Pope, Radiation from protons of auroral energy in the vicinity of the earth, J. Geophys. Res., 65, 3569-3574, 1960.

Neufeld, J. and H. Wright, Instabilities in a plasma-beam system immersed in a magnetic field, Phys. Rev., 129 (4), 1489-1507, 1963.

Ondoh, Tadanori, On the origin of VLF noise in the earth's exosphere, J. Geomag. Geoelect., 12, No. 2, 77-83, 1961.

Piddington, J. H., Geomagnetic storms, auroras and associated effects, Space Sci. Rev. 3, 724-780, 1964.

Pierce, E. T., Some topics in atmospheric electricity, in "Recent Advances in Atmospheric Electricity", 5-16, Pergamon Press, 1958.

Pierce, E. T., Excitation of earth-ionosphere cavity by lightning flashes, J. Geophys. Res., 68, No. 13, 4125-4127, 1963.

Prince, C. E., F. X. Bostick, Jr., and H. W. Smith, A study of the transmission of plane hydromagnetic waves through the upper atmosphere, Electrical Engineering Res. Lab., Univ. of Texas, Report No. 134, 1964.

Rawer, K., Electrische wellen in einem geshichteten medium, Ann. Phys. Lpz., 35, 385, 1939.

Rycroft, M. J., Resonances of the earth-ionosphere cavity observed at Cambridge, England, J. Res. NBS, 69 D, No. 8, 1071-1081, 1965.

Schumann, W. O., and H, Kŏnig, Uber die Beobachtung von atmospherics bei geringsten frequenzen, Z. Naturwiss, No. 41, 183-184, 1954.

Schumann, W. O., Uber die strahlunglosen eigen-schwingungen einer bitenden Kugel, die von einer Luftschiet und einer Ionospharenhulle umgebenist, Z. Naturforsch., 7a, 149-154, 1952.

Shand, J. A., Some quantitative characteristics of the Schumann-ELF natural electromagnetic background, Can. J. Phys., 44, 449-459, 1966.

Spitzer, L., Physics of fully ionized gases, Interscience, New York, 1963.

Stix, T. H., The Theory of Plasma Waves, McGraw-Hill Book Company, New York, 1962.

Sturrock, P. A., Kinematics of growing waves, Phys. Rev., 112 (5), 1488-1503, 1958.

Ti-Shu Li, C. E. Prince, Jr., and F. X. Bostick, Jr., Hydromagnetic wave propagation and theoretical power spectra, Electrical Engineering Res. Lab., Univ. of Texas, Report No. 136, 1964.

Thompson, W. B., A layered model approach to the earth-ionosphere cavity resonance problem, Ph.D. Thesis, Department of Geology and Geophysics, MIT, 1963.

Ullah, N., and S. L. Kahalas, Coupling of magneto-hydrodynamic to electromagnetic waves at a plasma discontinuity, I. Radiation field, Phys. Fluids, 6 (2), 284-289, 1963.

Wait, J. R., Terrestrial propagation of very-low-frequency radio waves: a theoretical investigation, J. Res. NBS 64D, No. 2, 153-204, 1960.

Wait, J. R., Earth-ionosphere cavity resonances and the propagation of ELF radio waves, J. Res. NBS 69D, No. 8, 1057-1070, 1965.

Wait, J. R., Analysis of Schumann resonances for dipolar magnetic field, paper presented in Seminar on Extremely Low Frequency Propagation, Univ. of Rhode Island, November 16, 1966.

Whittaker, E. T., and G. N. Watson, A Course of Modern Analysis, Cambridge University Press, 1935.

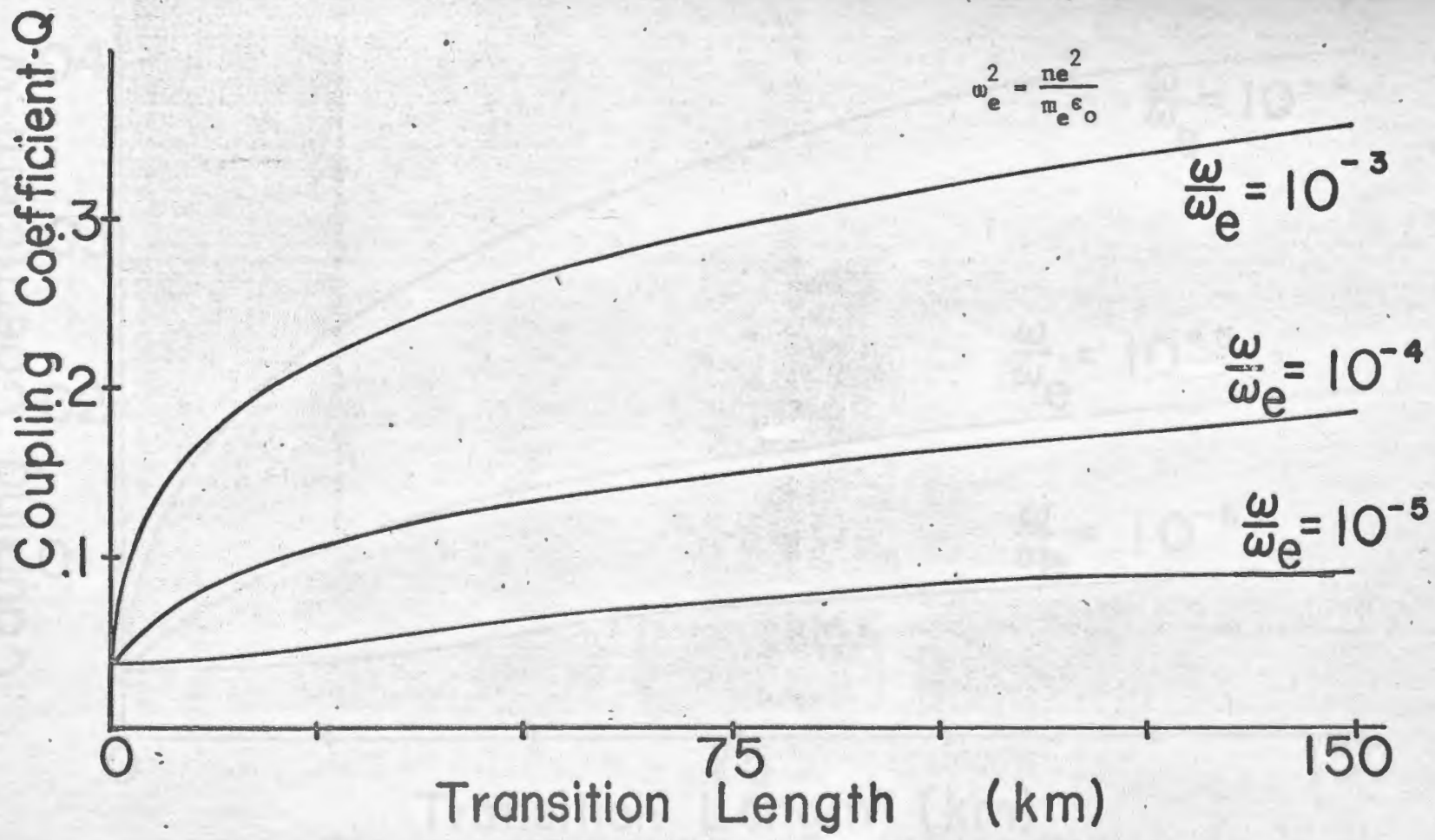

Figure 2.1 Coupling coefficient vs transition length for $\frac{V_a}{c} = 10^{-2}$.

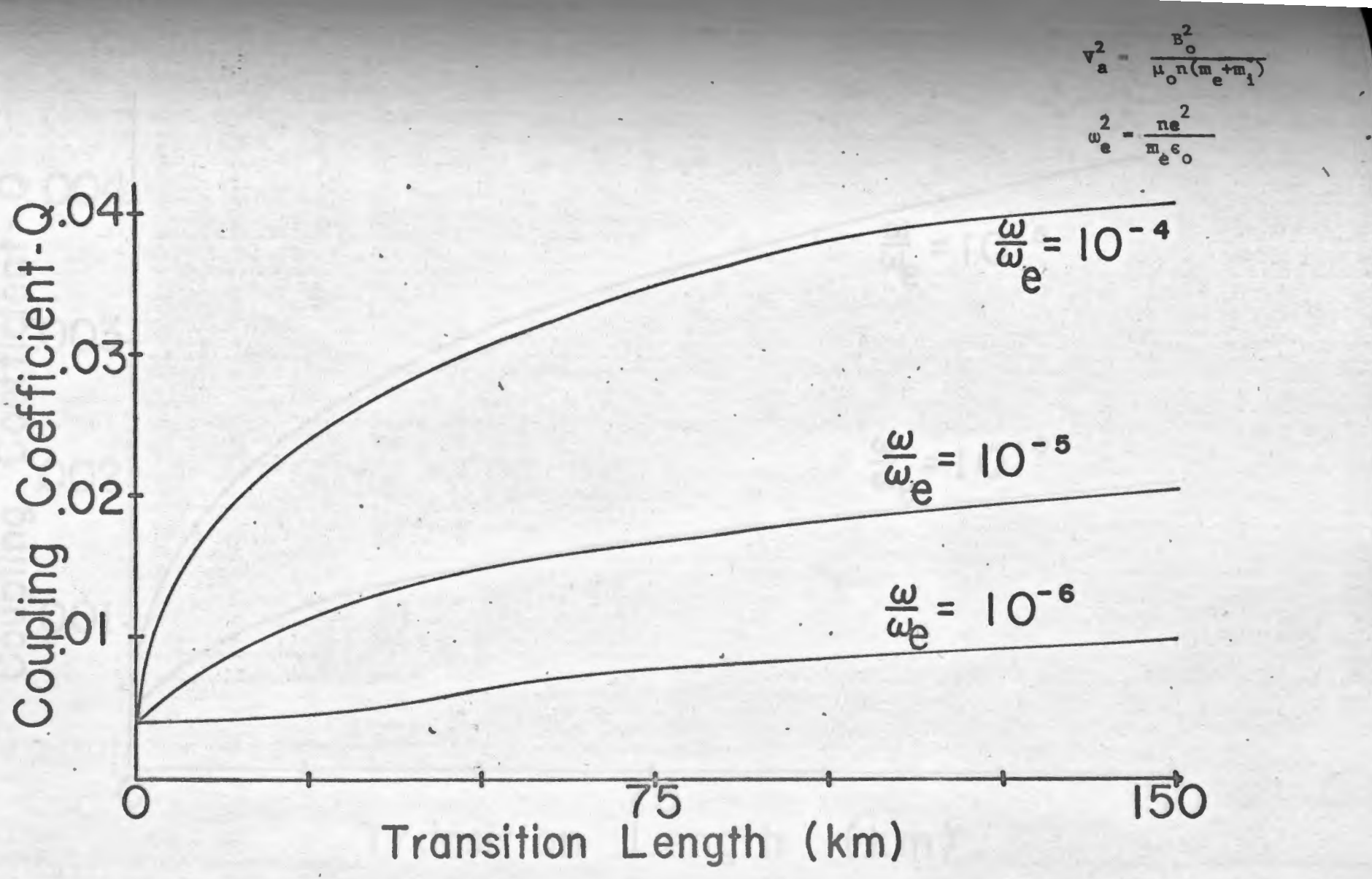

Figure 2.2 Coupling coefficient vs transition length for $\frac{V_a}{c} 10^{-3}$.

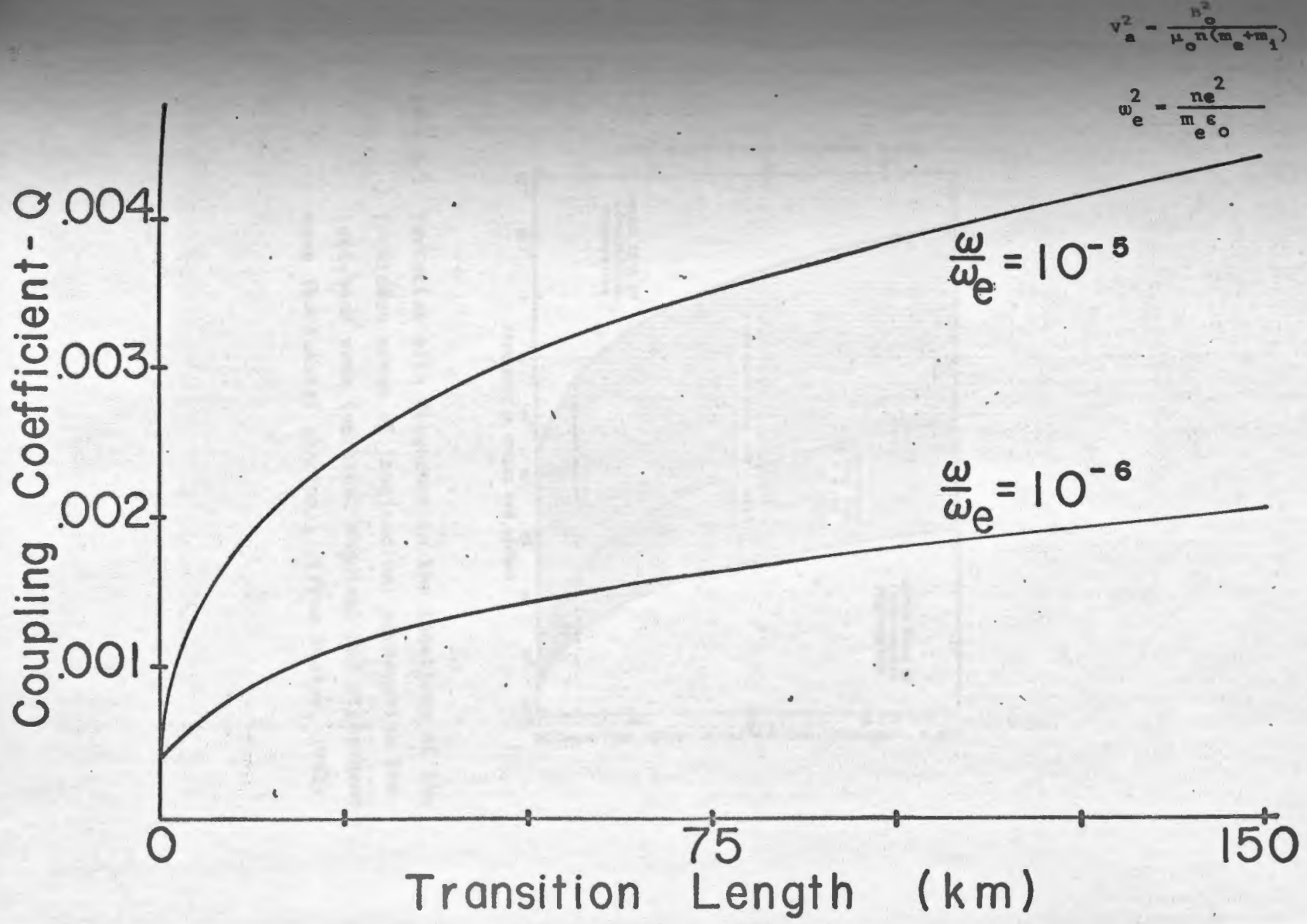

Figure 2.3 Coupling coefficient vs transition length for $\frac{V_a}{c} = 10^{-4}$.

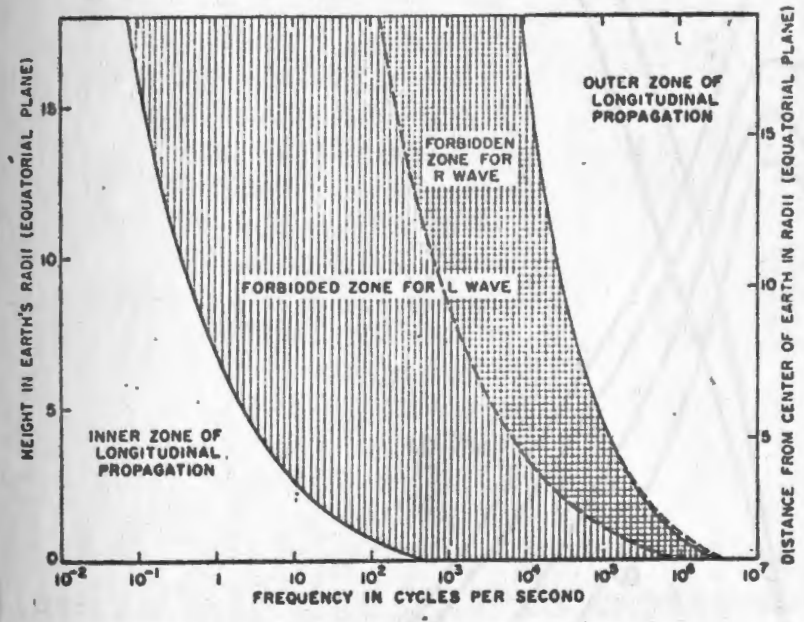

Figure 3.1 Variation with frequency in the locations of the forbidden zones of longitudinal propagation for left-hand wave (vertical shading) and right-hand wave (horizontal shading). (From Booker, 1962)

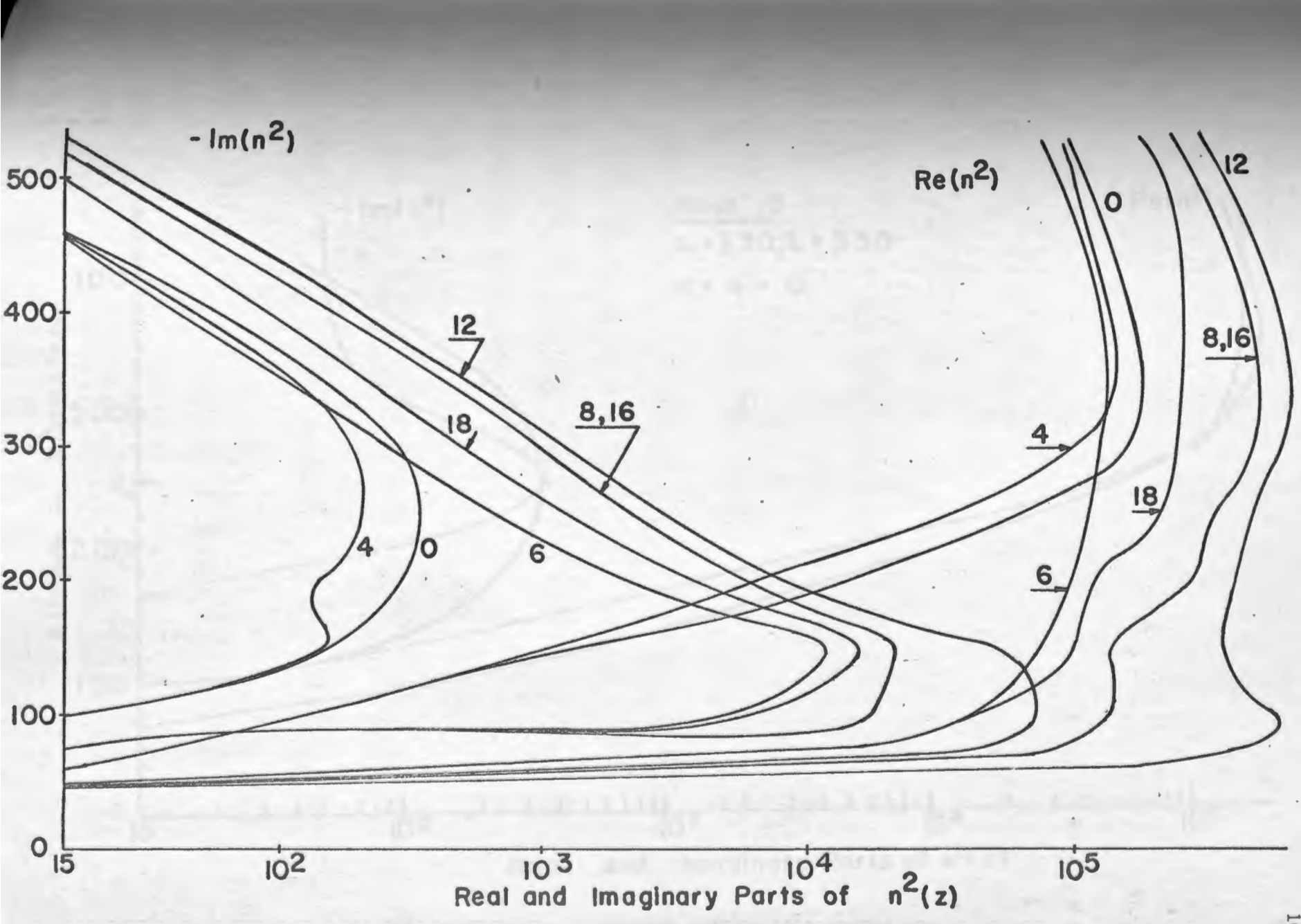

Figure 3.2 Complex $n^2(z)$ profiles for various times of day using dispersion equation (3.27).

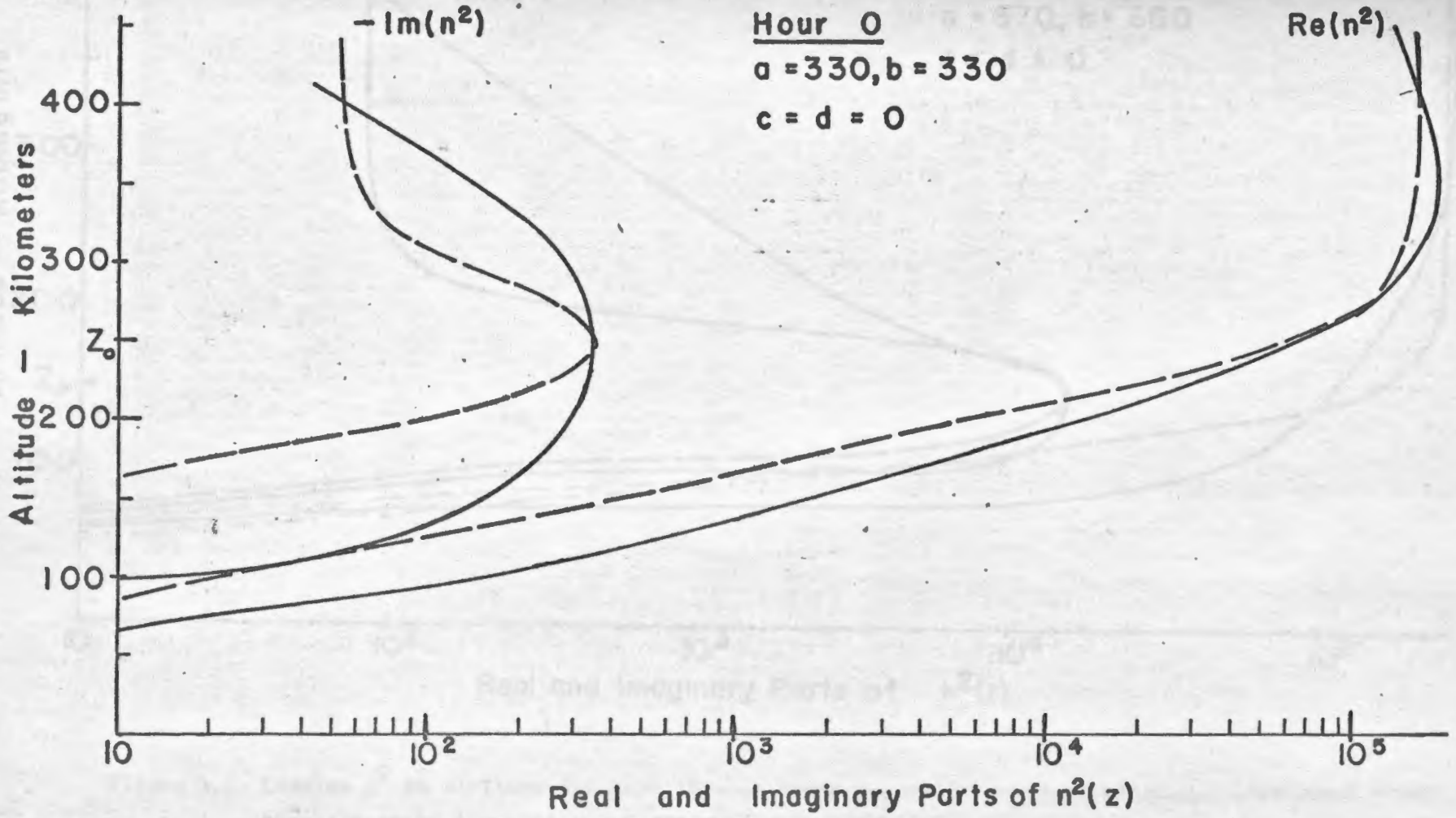

Figure 3.3 Complex n^2 vs altitude for hour 0. —— "experimental," ---- analytical.

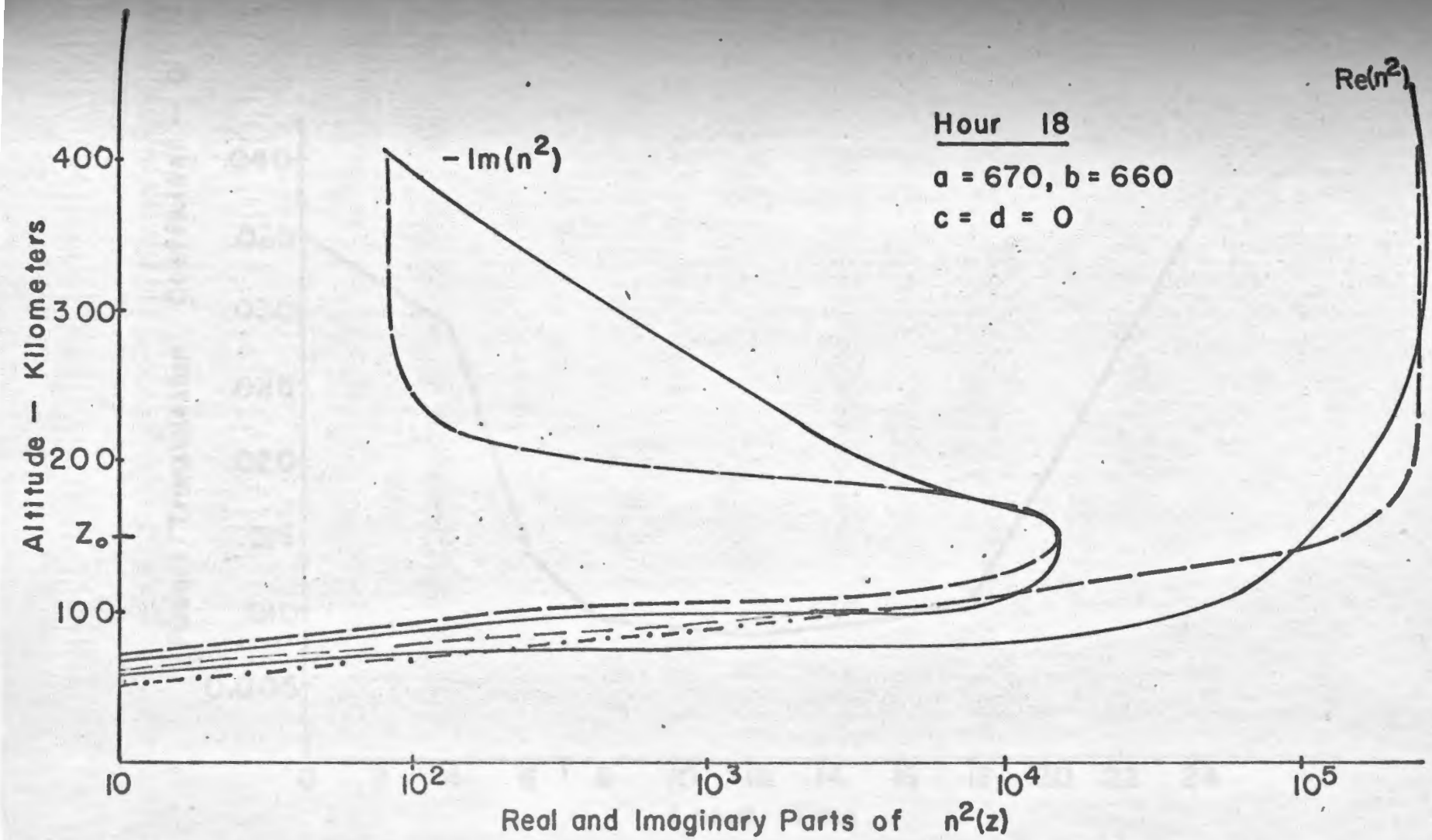

Figure 3.4 Complex n^2 vs altitude for hour 18. —— "experimental" ---- analytical _ _ _ deviation from the analytical curve with a = 625, b = 615.

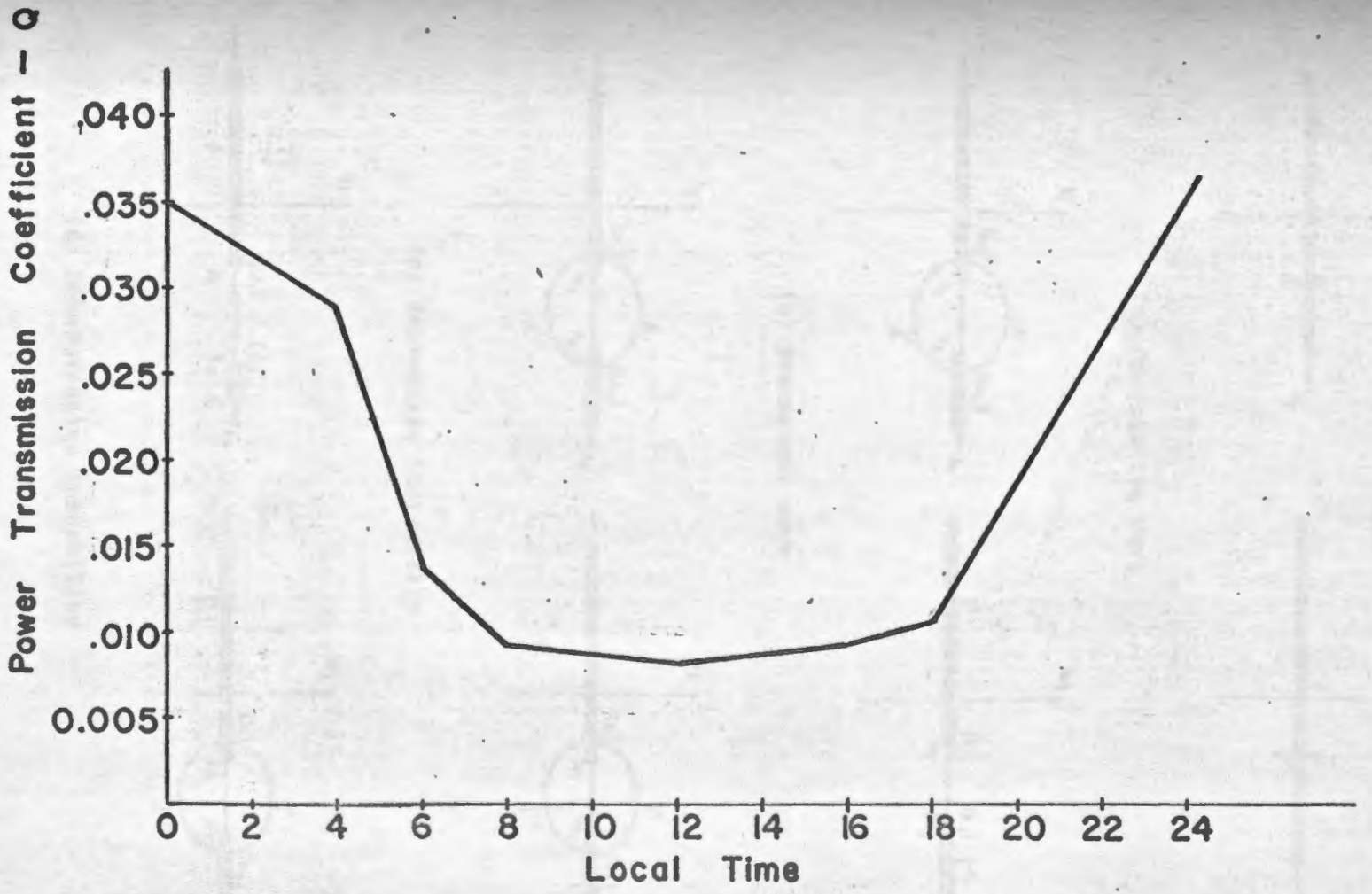

Figure 3.5 Diurnal variation of power transmission coefficient.
(For approximations to $n^2(z)$ of Fig. 3.2 frequency = 8 cps)

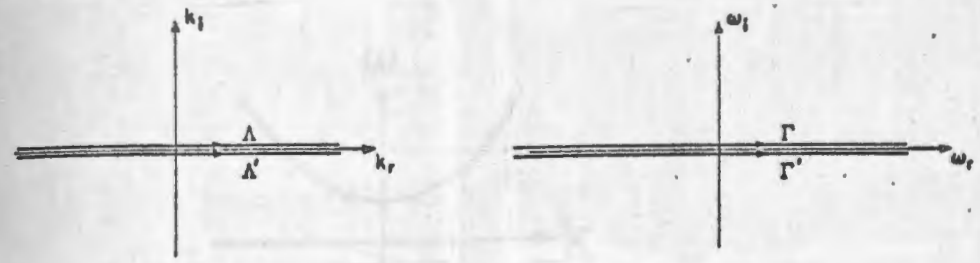

(a) Propagating wave

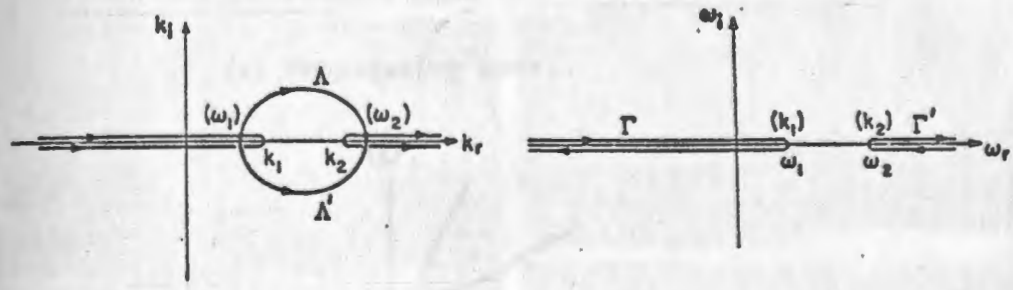

(b) Evanescent wave

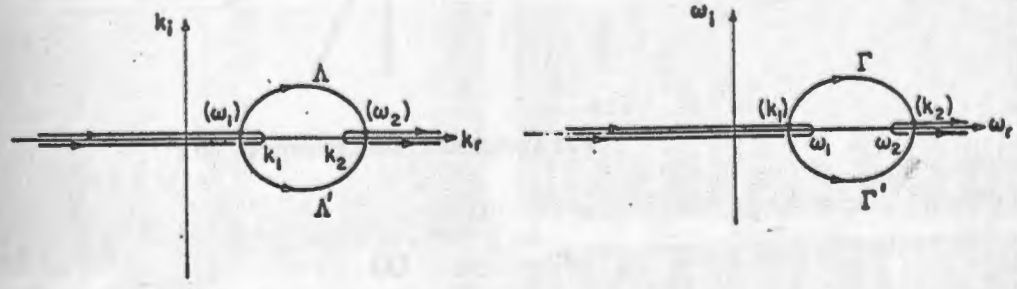

(c) Convective instability

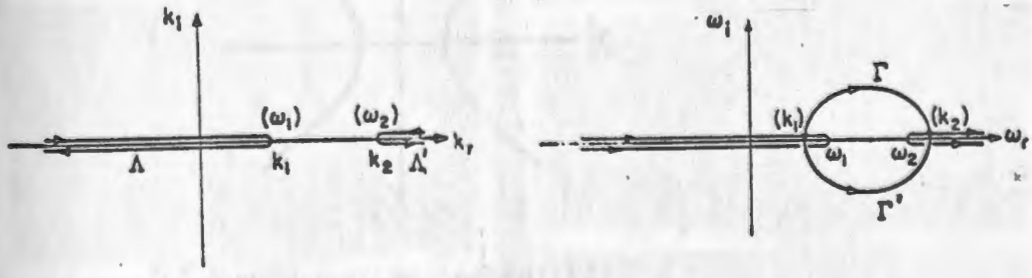

(d) Nonconvective instability

Figure 6.1 Instability criteria. (From Sturrock, 1958).

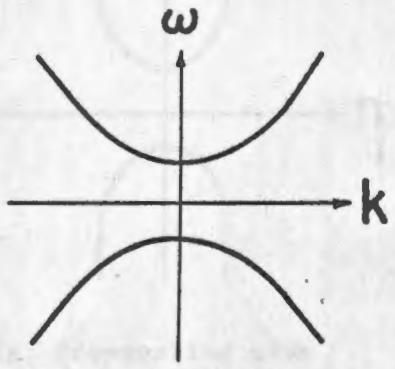

(a) Propagating wave

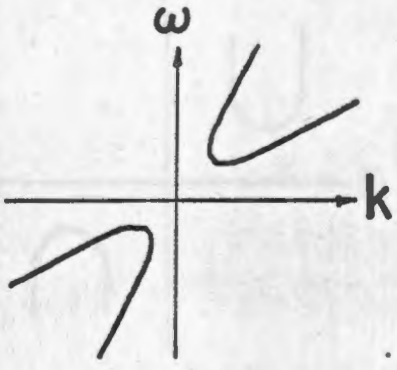

(b) Convective instability

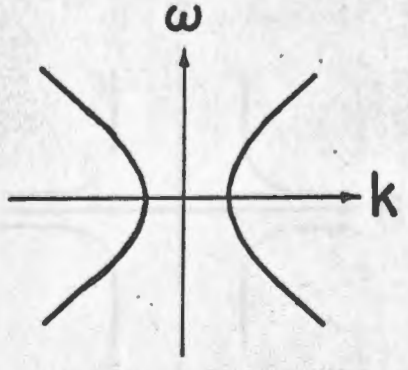

(c) Nonconvective instability

Figure 6.2 ω vs k plots of the dispersion relation

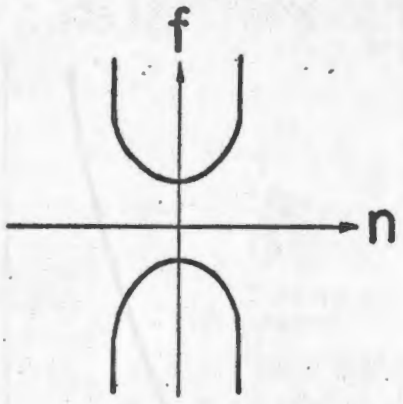

(a) Propagating wave

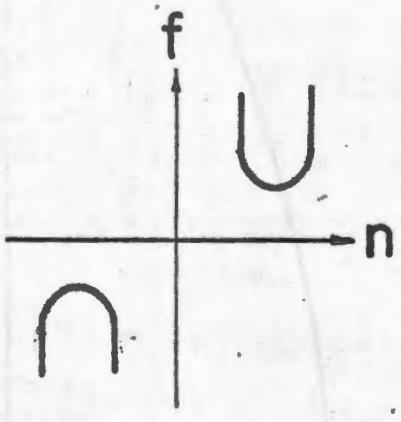

(b) Convective instability

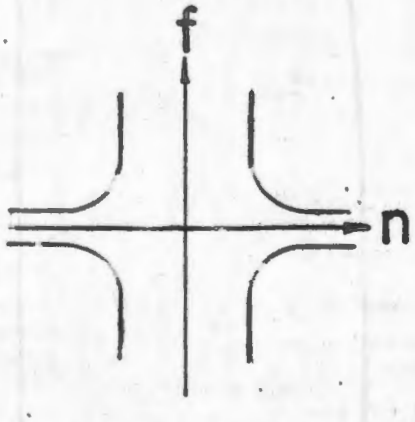

(c) Nonconvective instability

Figure 6.3 Frequency vs refractive index plots of the dispersion relation in the real f real n plane.

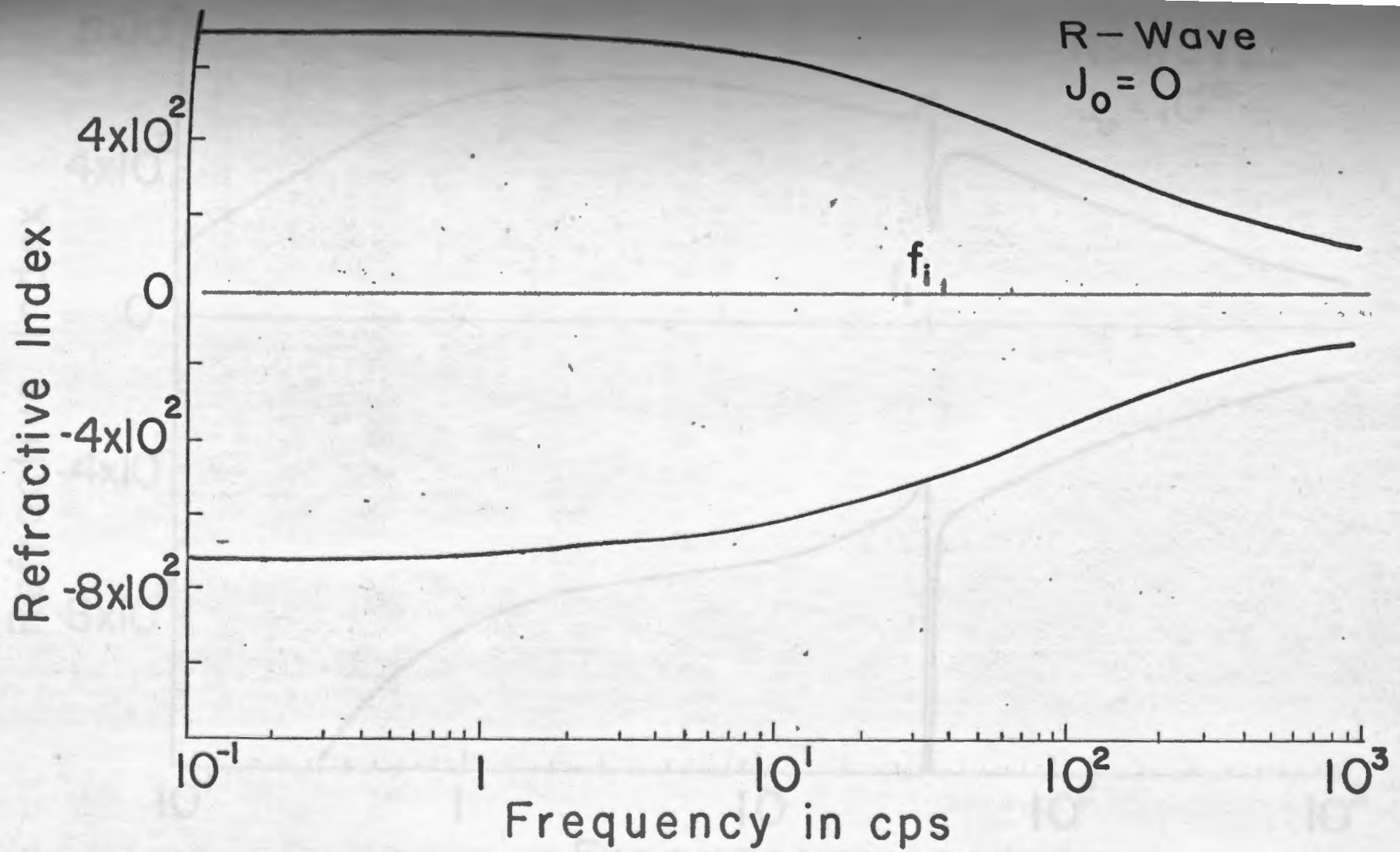

Figure 6.4 Refractive index vs frequency for the R-wave, at 500 km, $J_o = 0$. Ion cyclotron frequency $f_i \simeq 38$ cps.

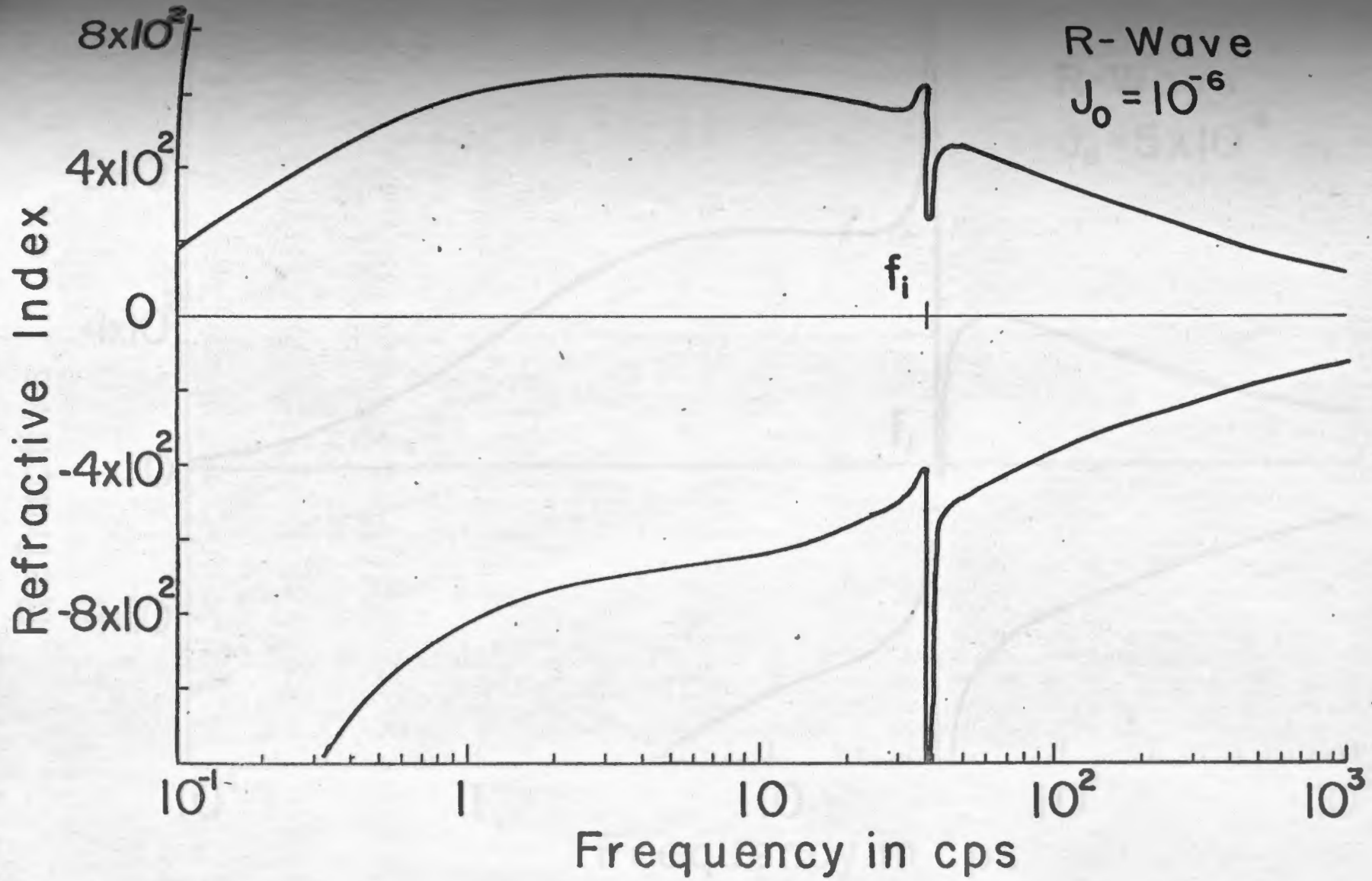

Figure 6.5 Refractive index vs frequency for the R-wave, at 500 km, $J_o = 10^{-6}$ A/m^2. Ion-cyclotron frequency $f_i \simeq 38$ cps.

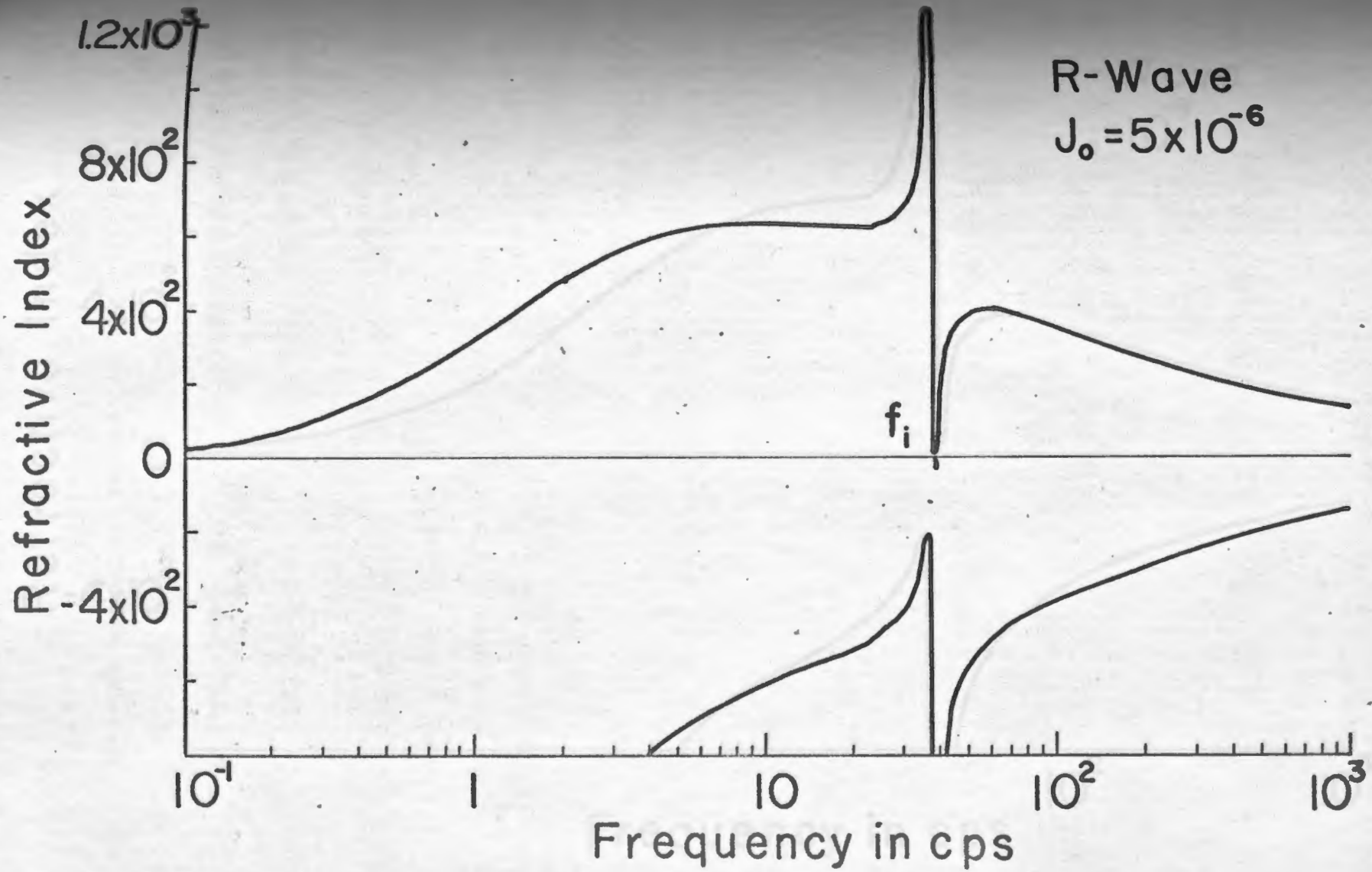

Figure 6.6 Refractive index vs frequency for the R-wave, at 500 km, $J_o = 5 \times 10^{-6}$ A/m^2. Ion-cyclotron frequency $f_i \simeq 38$ cps.

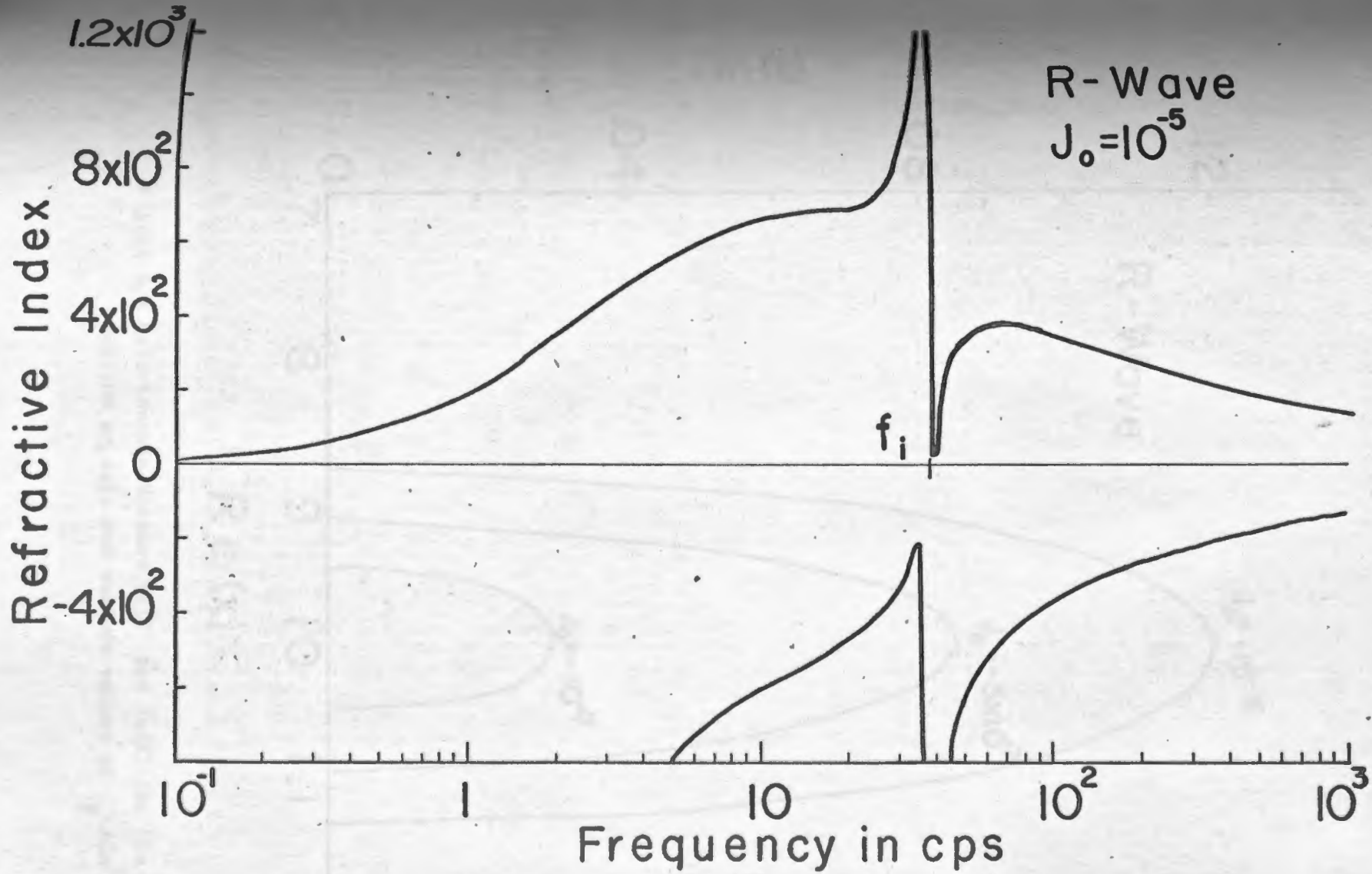

Figure 6.7 Refractive index vs frequency for the R-wave, at 500 km, $J_o=10^{-5}$ A/m^2. Ion-cyclotron frequency $f_i \simeq 38$ cps.

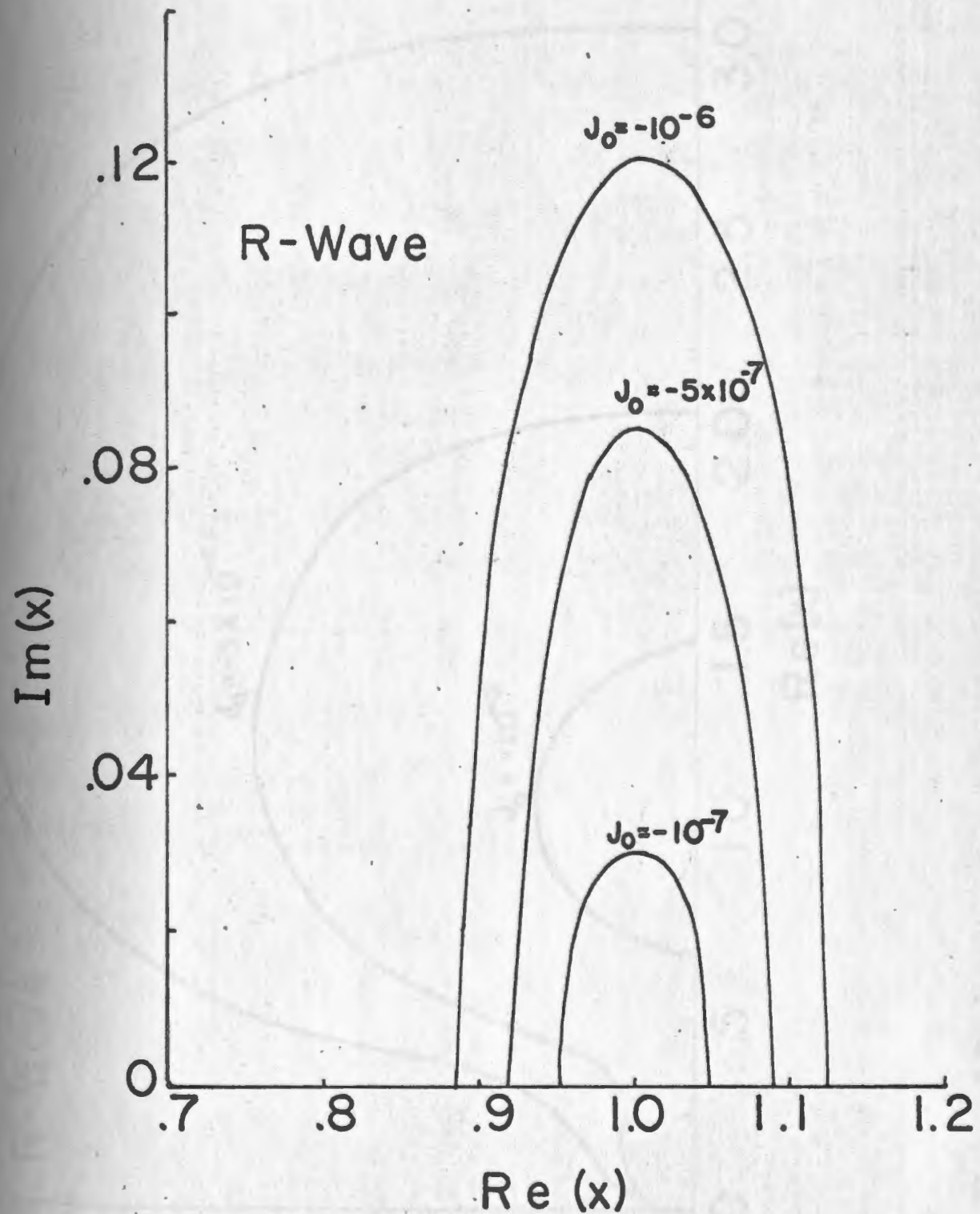

Figure 6.8 Relationship between Re(X) and Im(X) for the R-wave for 500 km, data and various values of J_o (A/m^2).

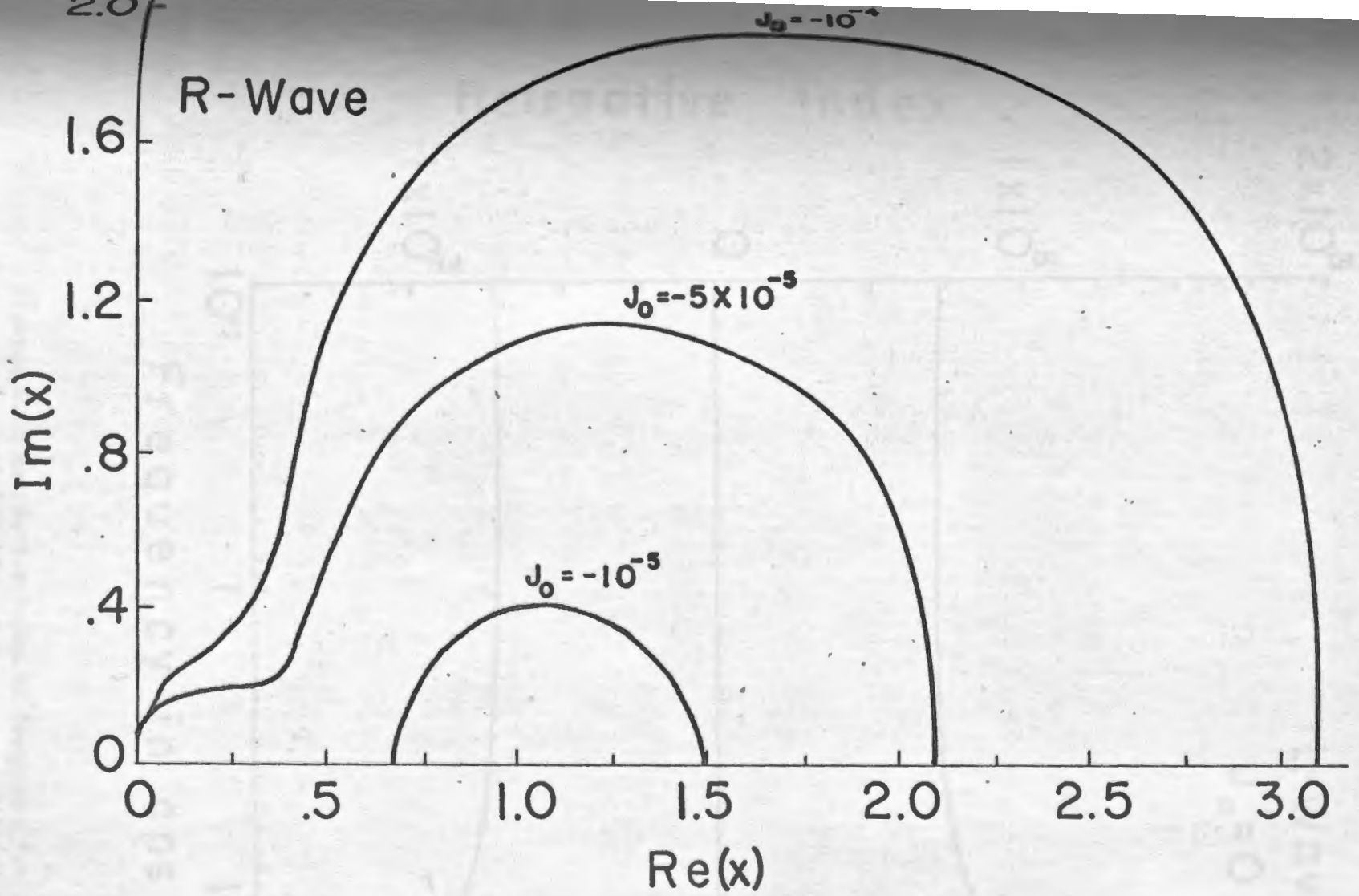

Figure 6.9 Relationship between Re(X) and Im(X) for the R-wave for 500 km data and various values of $J_o(A/m^2)$.

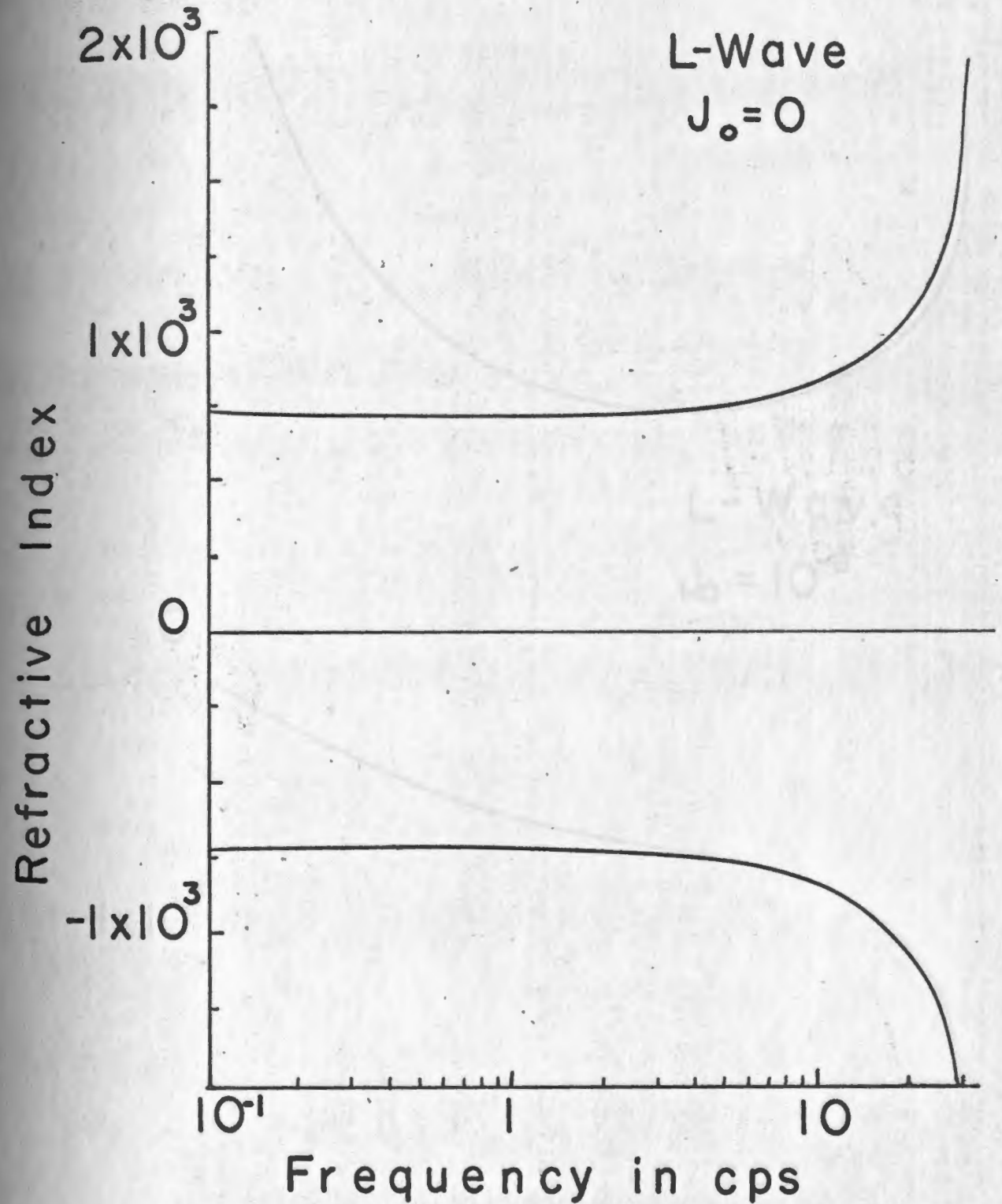

Figures 6.10 Refractive index vs frequency for the L-wave, at 500 km, $J_o = 0$. Ion-cyclotron frequency $f_i \simeq 38$ cps.

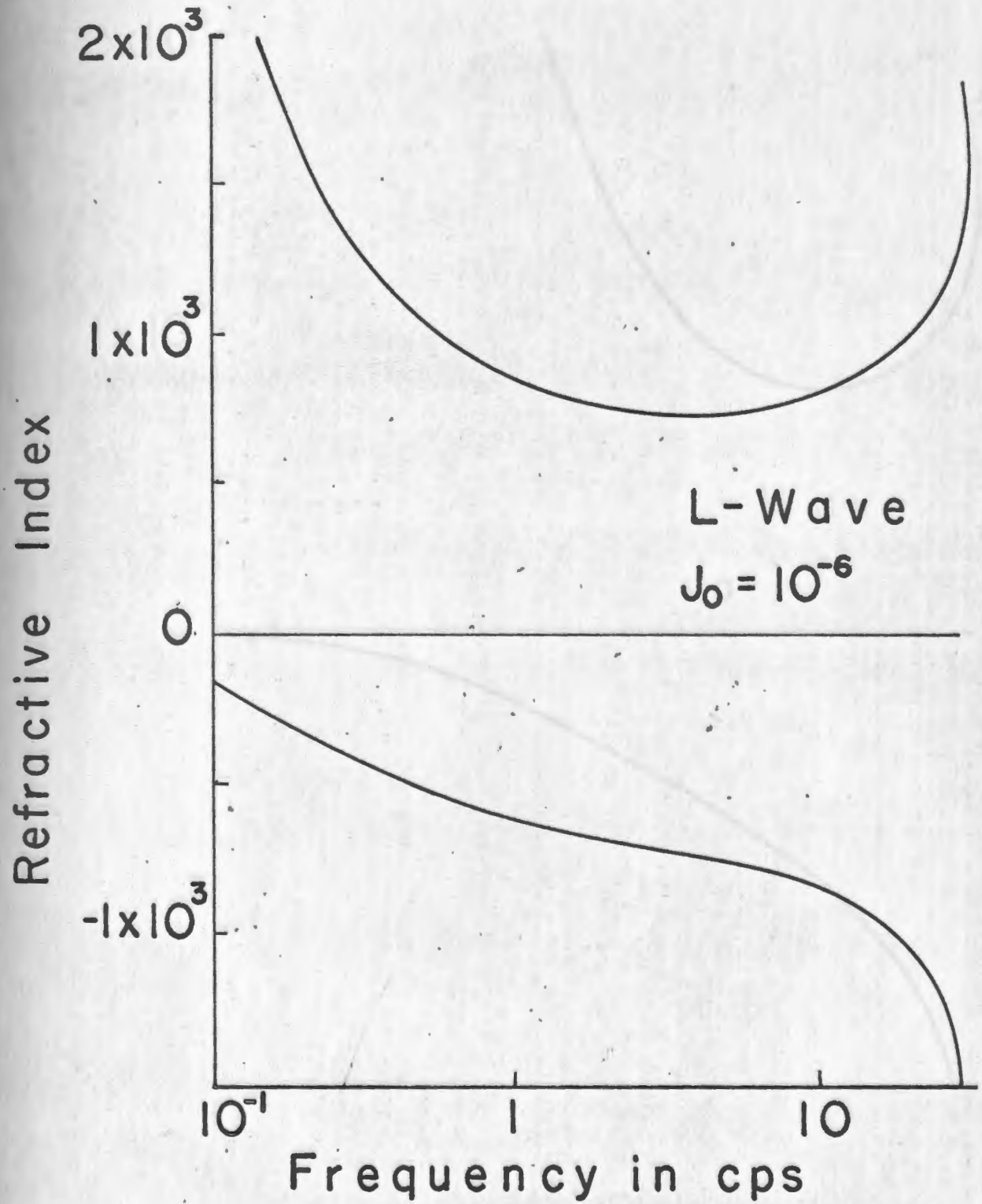

Figure 6.11 Refractive index vs frequency for the L-wave, at 500 km, $J_o = 10^{-6}$ A/m^2. Ion-cyclotron frequency $f_i \simeq 38$ cps.

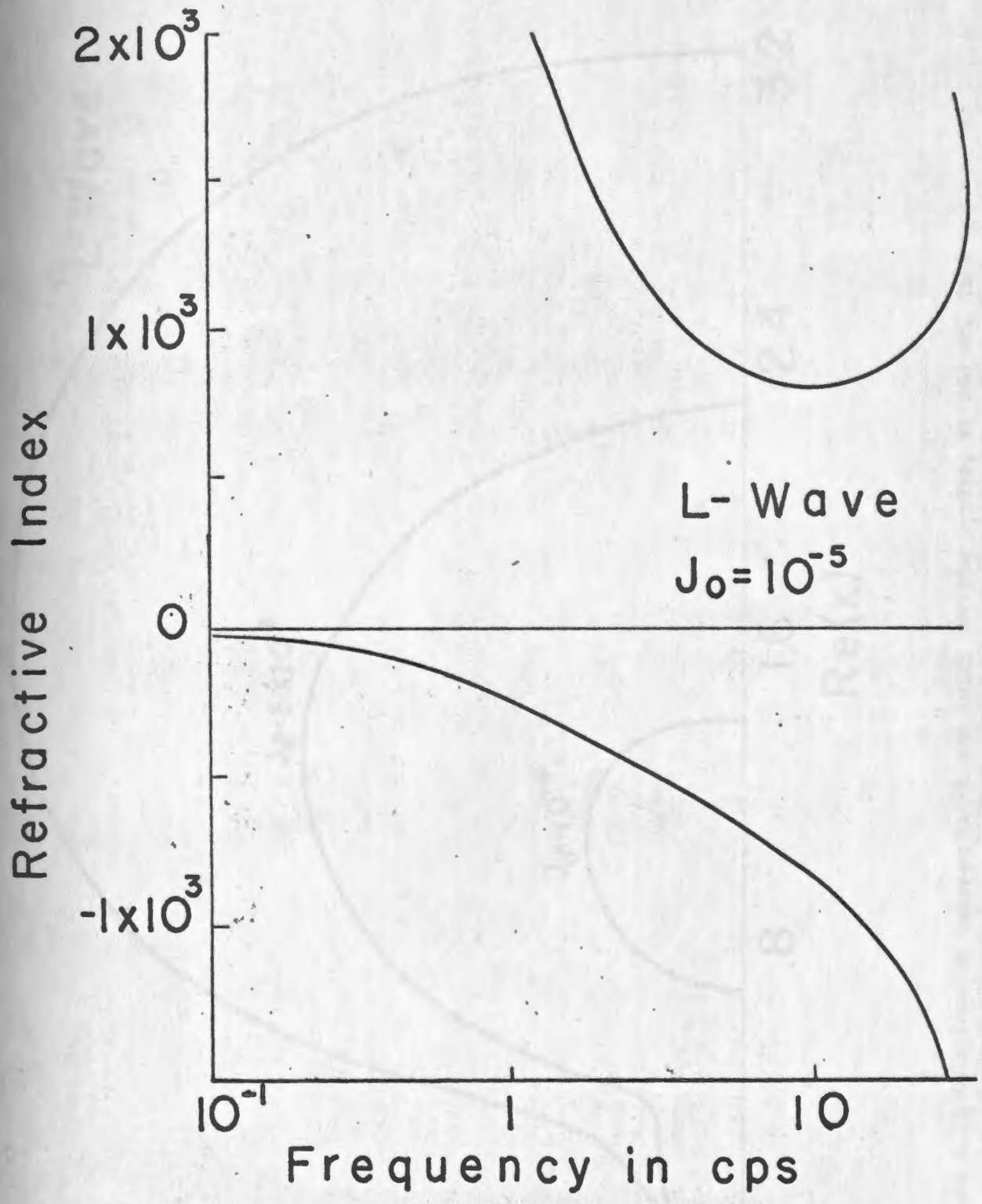

Figures 6.12 Refractive index vs frequency for the L-wave, at 500 km, $J_o = 10^{-5}$ A/m^2. Ion-cyclotron frequency $f_i \simeq 38$ cps.

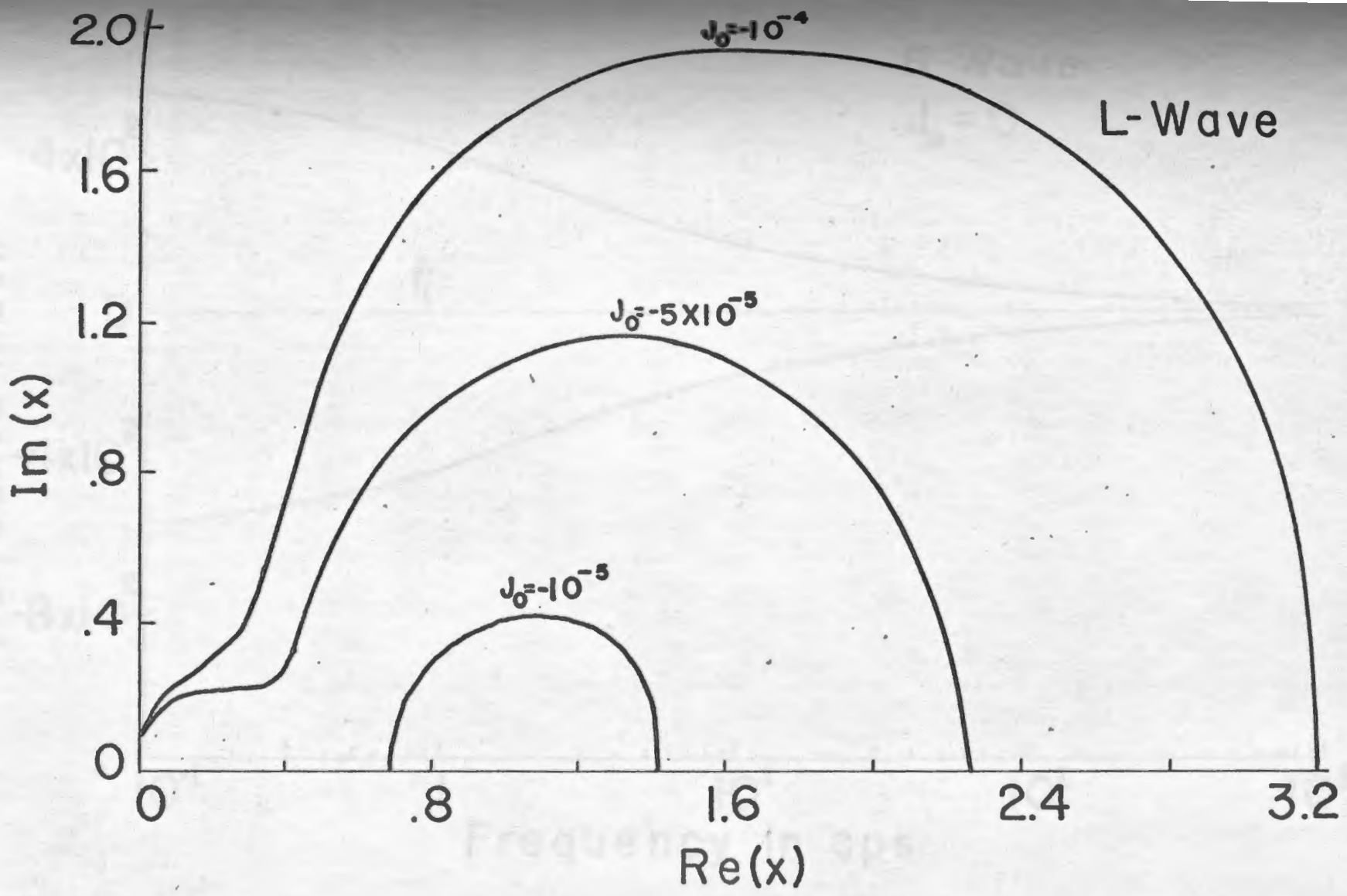

Figure 6.13 Relationship between Re(X) and Im(X) for the L-wave, at 500 km, data and various values of J_o(A/m^2).

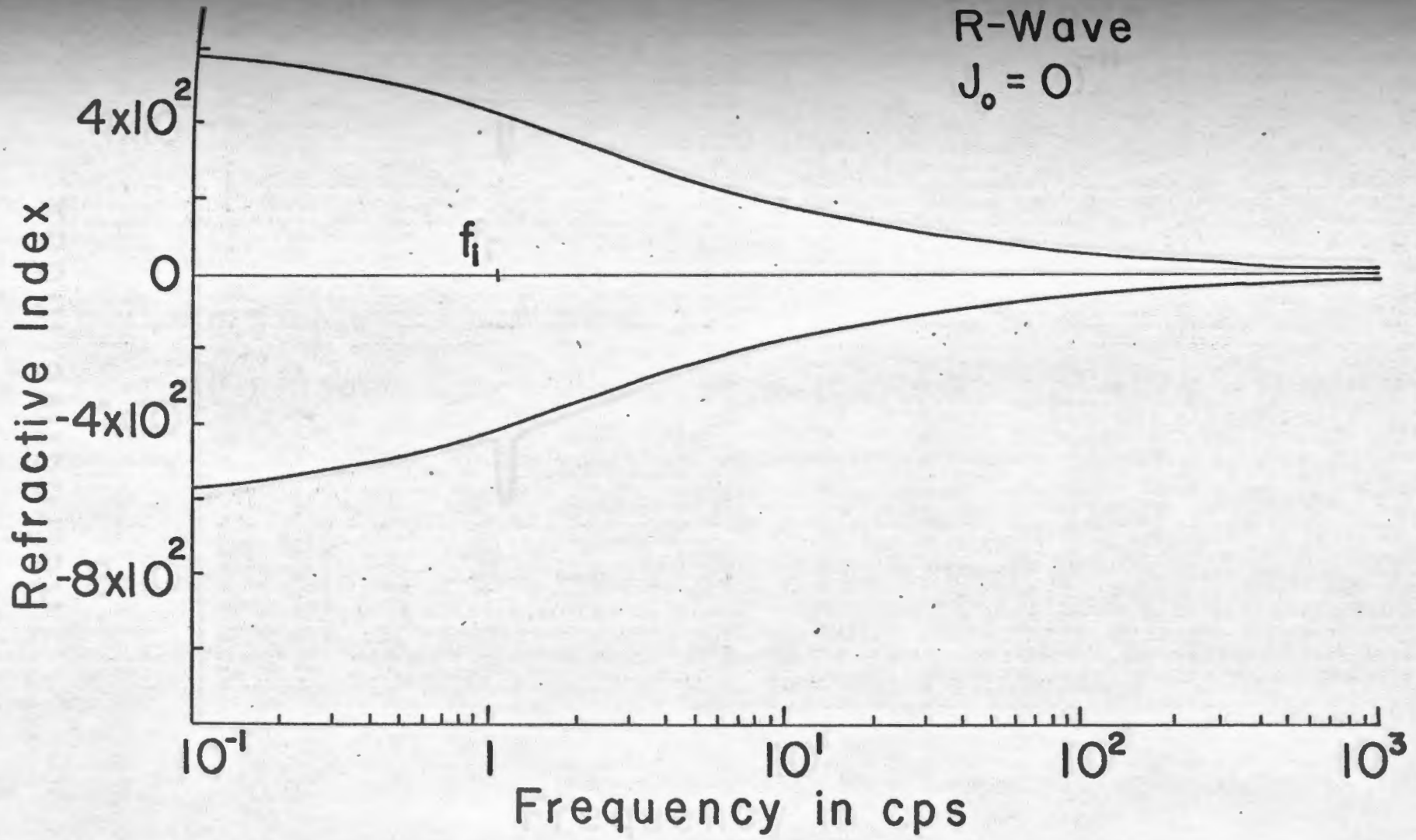

Figure 6.14 Refractive index vs frequency for the R-wave, at 50,000 km, $J_o=0$. Ion-cyclotron frequency $f_i \simeq 1.1$ cps.

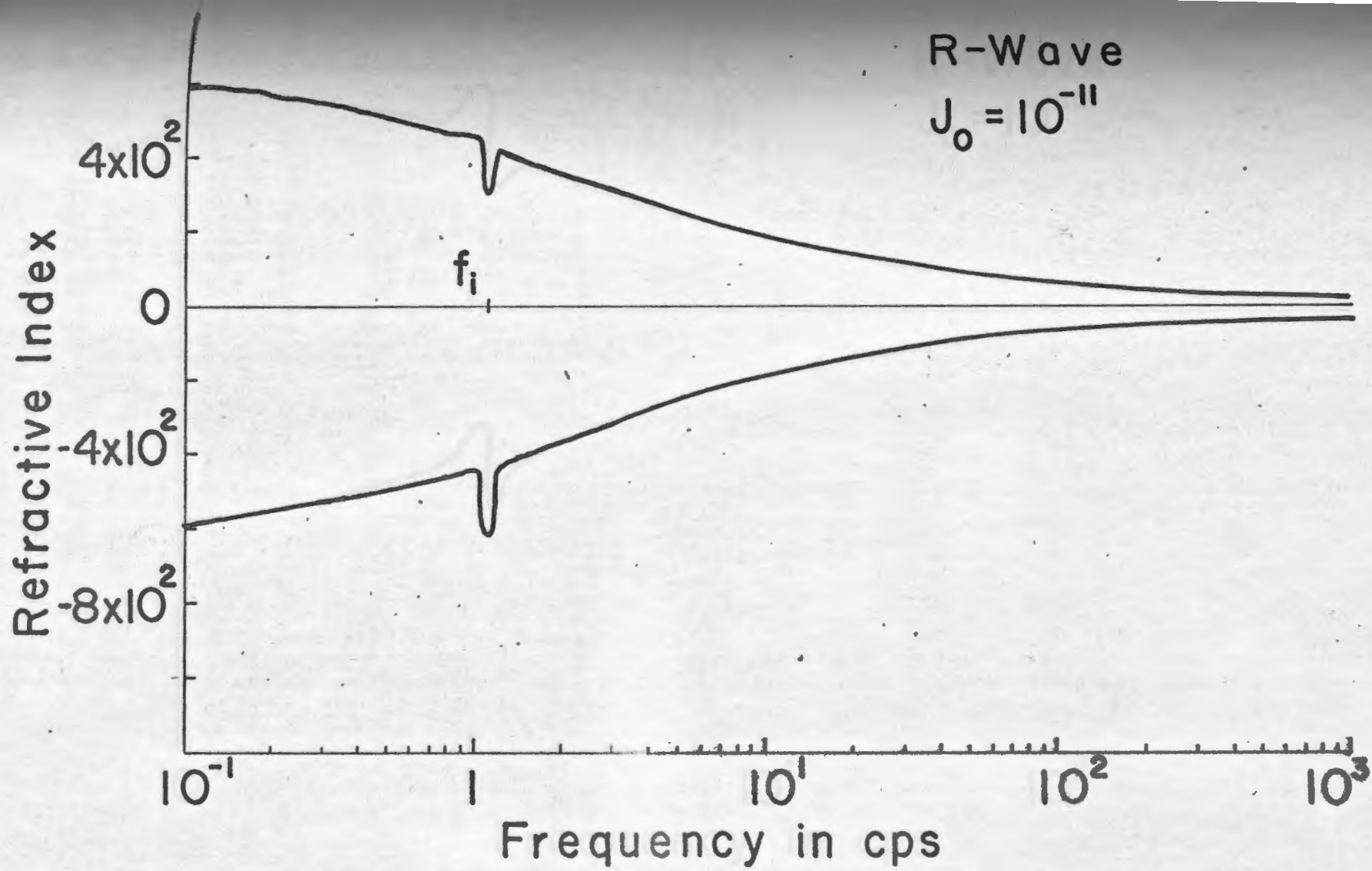

Figure 6.15 Refractive index vs frequency for R-wave, at 50,000 km, $J_o = 10^{-11}$ A/m^2.
Ion-cyclotron frequency $f_i \simeq 1.1$ cps.

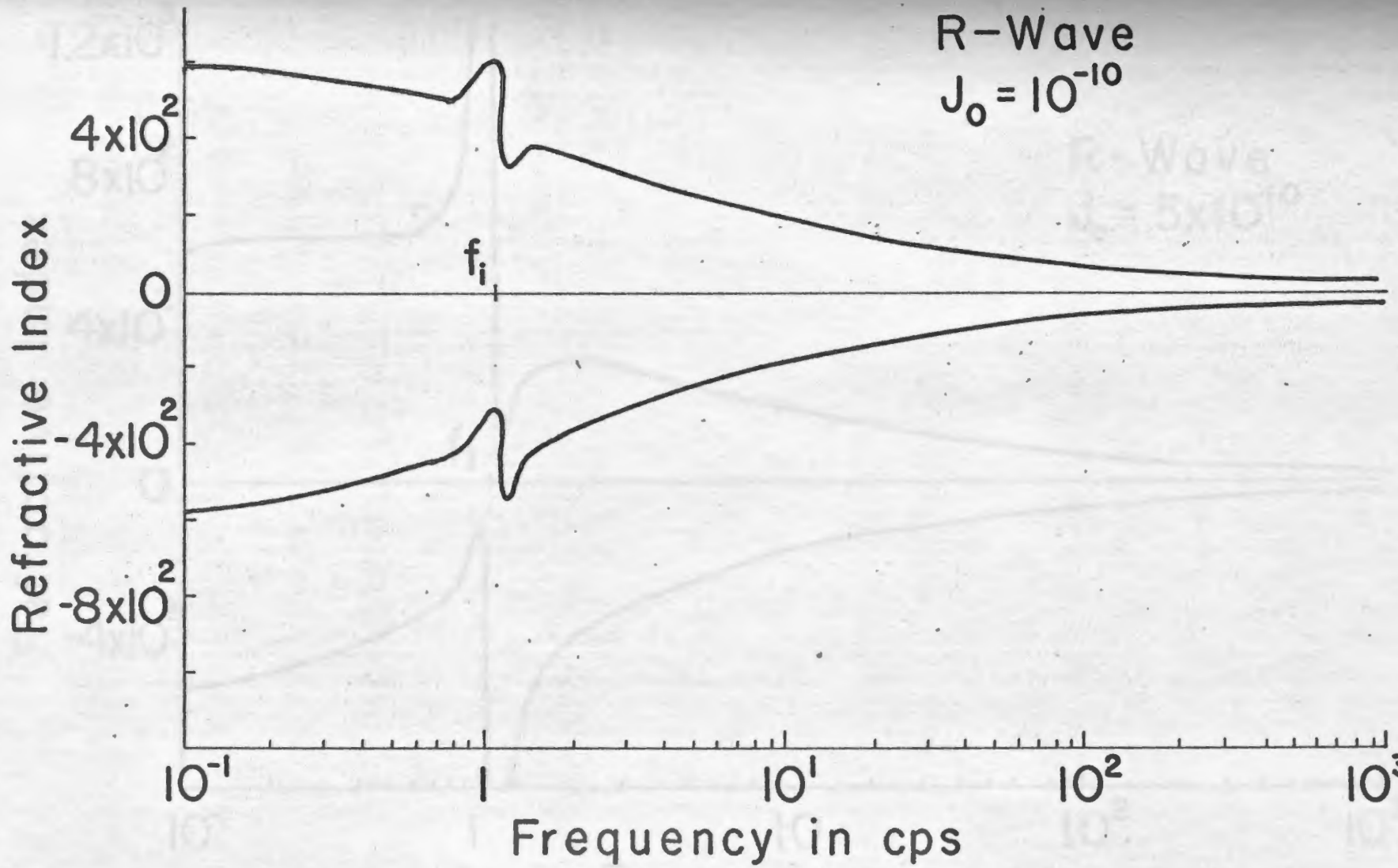

Figure 6.16 Refractive index vs frequency for the R-wave, at 50,000 km, $J_o = 10^{-10}$ A/m^2. Ion-cyclotron frequency $f_i \simeq$ 1.1 cps.

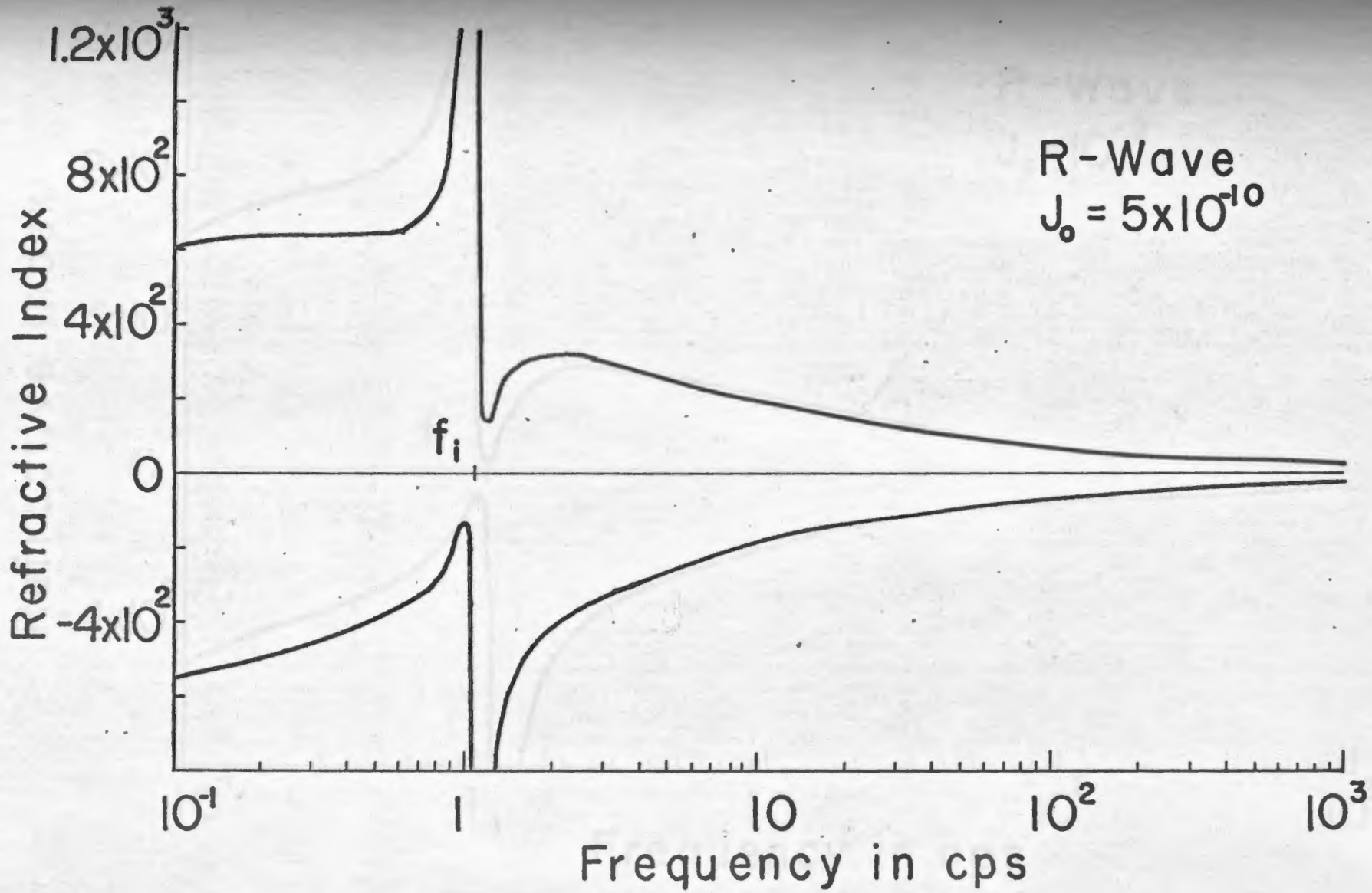

Figure 6.17 Refractive index vs frequency for the R-wave, at 50,000 km, $J_o = 5 \times 10^{-10}$ A/m^2. Ion-cyclotron frequency $f_i \simeq 1.1$ cps.

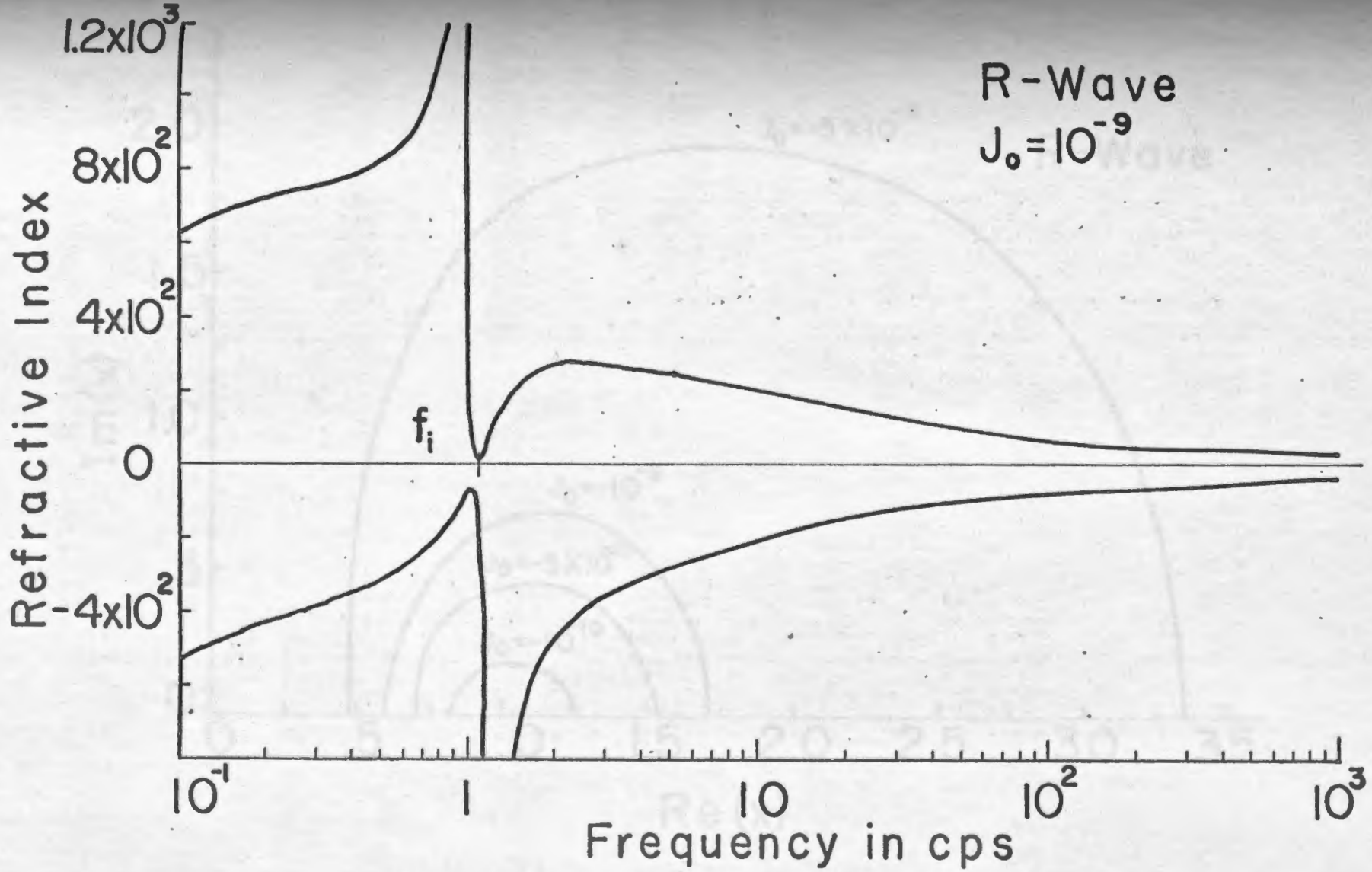

Figure 6.18 Refractive index vs frequency for the R-wave, at 50,000 km, $J_o = 10^{-9}$ A/m^2. Ion-cyclotron frequency $f_i \simeq 1.1$ cps.

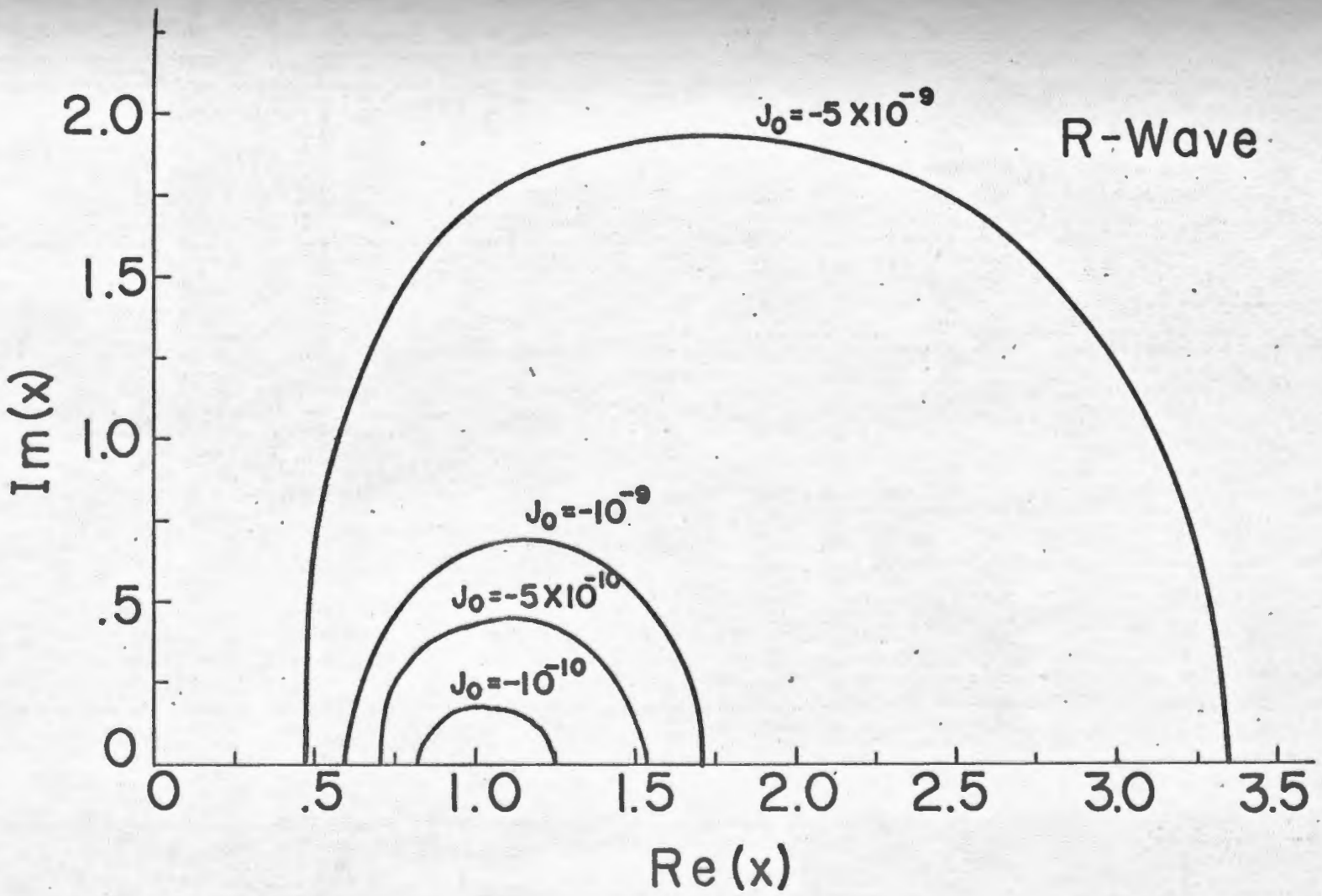

Figure 6.19 Relationship between Re(X) and Im(X) for the R-wave, for 50,000 km, data and various values of $J_o(A/m^2)$.